

UNCLASSIFIED

AD NUMBER

AD481395

LIMITATION CHANGES

TO:

Approved for public release; distribution is unlimited.

FROM:

Distribution authorized to U.S. Gov't. agencies and their contractors;  
Administrative/Operational Use; 28 NOV 1958.  
Other requests shall be referred to Bureau of Aeronautics, Navy Department, Washington, DC.

AUTHORITY

CFSTI per DDC-I DF, 15 Jul 1966

THIS PAGE IS UNCLASSIFIED

~~CONFIDENTIAL~~

A-D-481-395

AD 481 395

C.W.R. REPORT NO. 300-39

EXPERIMENTAL INVESTIGATION OF THE COOLING  
CHARACTERISTICS OF TRANSPIRATION AIR-COOLED  
TURBINE BLADES IN A HIGH TEMPERATURE GAS CASCADE  
FINAL REPORT

Department of the Navy  
Bureau of Aeronautics  
Power Plant Division

Contract NOas 56-495-c

Security Control No. RE 58-11-61  
CA 58-12-3

Copy No. 25

November 28, 1958

CLASSIFICATION CONTROL  
BY AUTHORITY OF DSC-4:  
HSA/683, dated 8-25-61  
by W. S. Holt  
9-21-61: Sel

~~CONFIDENTIAL~~

UNCLASSIFIED

~~CONFIDENTIAL~~

C.W.R. REPORT NO. 300-39

NOTICES

When Government drawings, specifications, or other data are used for any purpose other than in connection with a definitely related Government Procurement Operation, the United States Government thereby incurs no responsibility nor any obligation whatsoever; and the fact that the Government may have formulated, furnished, or in any way supplied the said drawings, specifications, or other data, is not to be regarded by implication or otherwise as in any manner licensing the holder or any other person or corporation, or conveying any rights or permission to manufacture, use, or sell any patented invention that may in any way be related thereto.

The information furnished herewith is made available for study upon the understanding that the Government's proprietary interests in and relating thereto shall not be impaired. It is desired the Legal Officer of the Bureau of Aeronautics be promptly notified of any apparent conflict between the Government's proprietary interests and those of others.

This document contains information affecting the National defense of the United States within the meaning of the Espionage Laws, Title 18, U.S.C., Sections 793 and 794. Its transmission or the revelation of its contents in any manner to an unauthorized person is prohibited by law.

~~CONFIDENTIAL~~

~~CONFIDENTIAL~~

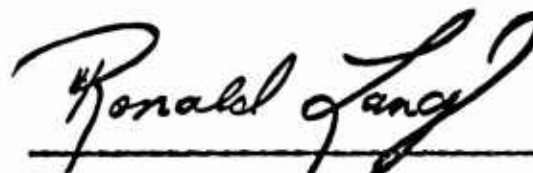
CURTISS-WRIGHT CORPORATION

RESEARCH DIVISION

C.W.R. REPORT NO. 300-39

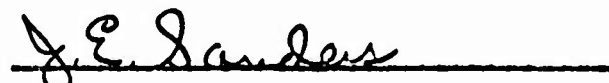
APPROVAL PAGE

Prepared by:

  
\_\_\_\_\_  
Ronald Lang  
Research Engineer

Approvals:

  
\_\_\_\_\_  
S. Lombardo  
Division Chief

  
\_\_\_\_\_  
J. E. Sanders  
Department Head

~~CONFIDENTIAL~~

UNCLASSIFIED

~~CONFIDENTIAL~~

C.W.R. REPORT NO. 300-39

TABLE OF CONTENTS

	<u>Page</u>
Notices	i
Approval Page	ii
Table of Contents	iii
List of Tables	v
List of Figures	vi
Forward	1
Object	2
Summary	3
Conclusions	4
Recommendations	5
Discussion	6
Introduction	6
Test Facility	8
Stand Equipment	8
Test Vehicle	8
Test Apparatus	
Air Cooled Porous Stator Blades	9
Water Cooled Non Porous Blades	9
Porous Tube and Wedge	9
Porous Rotor Blade	10

~~CONFIDENTIAL~~

UNCLASSIFIED

~~CONFIDENTIAL~~

C.W.R. REPORT NO. 300-39

	<u>Page</u>
<b>Instrumentation</b>	11
Test Vehicle	11
Porous Stator Blades	11
Water Cooled Blades	16
Porous Rotor Blades	16
Control Room	16
<b>Test Procedure</b>	17
Porous Stator Blades	17
Porous Rotor Blades	20
<b>Analysis</b>	21
Reduction of Data	21
Cascade Blade Design Procedure	29
<b>Results</b>	32
Pressure Profiles Around Permeable Airfoils	32
Correlation of Porous Metal Temperature	32
Experimentally Determined Cooling Characteristics of Transpiration Cooled Cascade Blade	33
Effects of Hot Gas Reynolds Number Variations	35
Transpiration-Cooled Rotor Blade	36
Permeability	39
Comparison of Calculated and Measured Gas Temperatures	40
Turbine Performance	41
<b>Appendix</b>	42
Nomenclature	42
References	45

LIST OF TABLES

		<u>Page</u>
Table 1 (a)	Instrumentation Schedule-Temperature Instrumented Cascade Blade, Type I	13
Table 1 (b)	Instrumented Schedule-Temperature Instrumented Cascade Blade, Type II	14
Table 1 (c)	Instrumented Schedule-Pressure Instrumented Cascade Blade	15
Table II	Tabulation of Running Test Schedule	19
Table III A	Tabulation of Coolant Flow Parameters for a Sample Point	25
Table III B	Tabulation of Coolant Flow Parameters for a Sample Point (Continued)	26
Table IV	Tabulation of Pressure, Temperature, Mach Number, Acoustic Velocity and Gas Velocity Profiles for a Sample Running Point	27
Table V	Tabulation of Hot Gas Reynolds Numbers	28

LIST OF FIGURES

<u>Figure Number</u>		<u>Page</u>
1	Cascade Rig Installed on Test Facility (Schematic)	46
2	Cooling Air Supply Flow Diagram	47
3	Control Room Equipment	48
4	Control Room Equipment	48
5	Sectional View of Transpiration Cooled Cascade Rig	49
6	Cascade Geometry	50
7	Exploded View of Cascade Rig	51
8	Downstream View of Cascade Housing	52
9	Over-all View of Temperature Instrumented Blade; Before Test and After Test Close-up Views	53
10	Pressure Instrumented Blade; Before Test and After Test Close-up Views	54
11	Exploded View of a Cascade Blade Assembly	55
12	Cooling Water Supply Flow Diagram	56
13	Water-Cooled Workhorse Cascade Blades	57
14	Flow Diagram of Porous Wedge Test Set-up	58
15	Porous Wedge Assembly	59
16	Porous Tube Assembly	59

C.W.R. REPORT NO. 300-39

<u>Figure Number</u>		<u>Page</u>
17	Over-all and Close-up of Open Tip Section, of Transpiration Cooled J-65 Turbine Rotor Blade, Before Test	60
18	Two Views of Transpiration Cooled Rotor Blade Installed in Rig	61
19	Section Showing Instrumentation Set-up at Cascade Inlet	62
20	Temperature Instrumented Porous Blade Assembly - Shop Blueprint	63
21	Pressure Instrumented Porous Blade Assembly - Shop Blueprint	64
22	Cross-Section of Constant Section Cascade Blade Showing Passage Designations	65
23	Test Stand Running Curves used for approximate Setting of Gas Velocity	66
24	Graphic Determination of Total Pressure at Cascade Inlet by Iteration	67
25	Pressure Distribution Around Transpiration Cooled Cascade Stator Blades at Various Gas Temperature and Flow Rates	68
26	Temperature Difference Ratio Versus Velocity Ratio for Various Gas Temperatures and Chordwise Stations	69
27	Temperature Difference Ratio Versus Mass Velocity Ratio for Various Gas Temperatures and Chordwise Stations	70

~~CONFIDENTIAL~~

C.W.R. REPORT NO. 300-39

<u>Figure Number</u>		<u>Page</u>
28	Temperature Difference Ratio Versus Mass Velocity Ratio for Various Gas Weight Flows and Chordwise Stations	71
29	Peripheral Cooling Air Flows, Temperature Difference Ratios and Absolute Temperature Distributions for Various Gas Weight Flows	72
30	Peripheral Cooling Air Flows, Temperature Difference Ratios, and Absolute Temperature Distributions for Various Gas Temperatures	73
31	Peripheral Variation of Hot Gas Reynolds Number at Several Gas Weight Flows and Inlet Gas Temperatures	74
32	Variation of Strut Temperature With Coolant Flow and Gas Temperature for an Uncapped Rotor Blade	75
33	Comparison of Transpiration and Convection Cooling Data	76
34	Variation of Leading Edge Temperature at Several Gas Temperatures and Coolant Mass Flows for Capped and Uncapped Rotor Tip Configurations	77
35	Correlation Curve-Comparison of Transpiration Cooled Turbine Rotor Blade with Tip Capped and Uncapped at Various Gas Temperatures and Coolant Air Flows	78
36	Comparison of Skin Permeability of Two Blades Before and After Test	79

~~CONFIDENTIAL~~

C.W.R. REPORT NO. 300-39

Figure Number

Page

37

Comparison of Temperatures Measured in  
Cascade Rig with Temperatures Predicted  
By Calculation Procedure

80

FOREWORD

Under BuAer Contract NOas 56-495-c, the Research Division of the Curtiss-Wright Corporation conducted analytical design and development work on a transpiration air-cooled turbine rotor blade concept. The following work statement is quoted, in part, from the contract under the heading of Articles or Services:

"Item 2 - Conduct a program of study, design, and rig testing to compile and report experimental and theoretical data on transpiration air-cooled turbine blades."

(Under this item reference is made to the statement of work as put forth in Curtiss-Wright Research letter dated 5 October 1955 which proposed a cascade rig program to obtain experimental heat transfer data in the range of 1600°F to above 2000°F gas temperature.)

This report is submitted in fulfillment of the requirement to summarize the work conducted on item 2, above, which culminated in the design, fabrication, and testing of a completely instrumented transpiration air-cooled turbine stator cascade.

OBJECT

1. To evaluate by means of cascade testing the performance of transpiration cooled turbine blades in a hot gas stream ranging from 1600°F to 2050°F.
  - . To measure the savings in coolant demand realized by chordwise metering in porous turbine blades.
3. To study the effects of capping the tip of a transpiration-cooled rotor blade (of the type used in the full-scale engine test) thereby forcing all the coolant through the blade wall.
4. To evaluate by experimental test the validity of the analytical design procedure as presented in Reference 7.
5. To apply advanced instrumentation techniques in an attempt to obtain dependable turbine data.

SUMMARY

An experimental investigation was conducted on a transpiration air cooled stator cascade to evaluate the heat transfer characteristics, to observe the temperature patterns, and to verify the existing transpiration-cooling theory for hot gas streams ranging in temperature from 1600°F to 2000°F.

A total of 49 hours and 55 minutes of cascade testing were logged. Hot gas Reynolds numbers computed at ten span-wise positions on the blade varied between 7800 on the pressure side near the leading edge and 280,000 at the convex side just upstream of the trailing edge. Hot gas weight flows of 2.46 lb/sec and 1.64 lb/sec were directed at the cascade section.

A comprehensive analysis of the data accumulated along with detailed descriptions of the test facility, the component test hardware, and the problems associated with instrumentation is presented.

In order to adequately prepare for this test two preliminary experimental configurations were designed, built, and tested. A porous tube was set up to provide a method of experimentally determining skin permeability. Another preliminary rig was built to evaluate the approximate local heat transfer coefficient in the laminar boundary layer around a porous wedge in high velocity streams. Based on the findings of these two investigations the material for the cascade test was procured.

In the final study, a J-65 transpiration-cooled turbine rotor blade was installed in the gas stream to compare its performance with the cascade blades. This blade was tested with the tip open and closed. The open tip configuration provided for a combination of convection and transpiration cooling. With the tip sealed, all the coolant was forced through the porous walls. In this way a comparison of the two methods was made at temperatures up to 2050°F.

CONCLUSIONS

1. The transpiration cooling method is extremely effective in high temperature turbine operation. Based on the test results reported herein, it is anticipated that the blades fabricated for full-scale engine testing will perform satisfactorily.
2. In order to minimize local over-cooling and total bleed requirement, it is necessary to employ chordwise metering of coolant. Considering coolant economy, chordwise metering accomplished by varying the coolant pressure level is, at best, second to metering by controlled variations in permeability.
3. In the hot gas temperature range up to 2000°F, a combination of transpiration and convection cooling (open tip - porous wall) is more effective than either method used independently.
4. The design procedure (Reference 7) predicts with good accuracy the wall temperature that will prevail under given conditions of coolant flow, hot gas temperature, pressure, and permeability.
5. Instrumentation in turbine blade applications should be arranged so that a reasonably complete set of related data could be obtained from a single blade.

RECOMMENDATIONS

1. Inasmuch as the transpiration cooled blade has been found to be a reasonable approach to solving the problems encountered in extreme temperature operation, continued efforts should be directed toward the development of the technique for operational use.
2. Refine the manufacture of porous material so that controlled variation in permeability is attainable.
3. Until such time as Recommendation No. 2 can be accomplished, a reappraisal of the strut cross-section as regards to the positioning of a partition in the trailing edge passage should be made. The difference in static hot gas pressure between the pressure and suction sides makes it unrealistic to use a single coolant supply to serve both surfaces.
4. Seek new methods of instrumentation for utilization in the high temperature - limited space applications encountered in turbines.

DISCUSSION

INTRODUCTION

To date, the two principle reasons given for cooling the blades of turbines are: (a) reduction in critical material content; and (b) increase in the turbine inlet temperature. Cooling is also desirable to permit an increase in the turbine stress level, i.e., higher allowable engine speeds resulting in increased mass flow and thrust per unit frontal area.

A program to reduce critical material content is not of first order priority at the present time. In the event of high level production, however, such a program undoubtedly would be emphasized.

In order to increase the operating temperature of the gas turbine above the limits possible with convectional solid turbine blades, various methods of convection cooling have been studied and developed over the past decade. Nearly all of these methods employ the passage of a coolant through the hollow interior of a blade.

Film cooling, which strives for the prevention of heat transfer from hot gas to blade, requires the passing of cooling air through longitudinal slots in the airfoil. This method is sensitive to external gas velocities and pressures, in addition to which the strength of the blade is seriously impaired by the slots.

The heat transfer rate from blade to coolant has limited the potential of convection cooling. For this reason, it was decided to investigate other blade cooling methods. Transpiration cooling, also called sweat or porous wall cooling appears to be a substantial improvement. In this cooling method air passes through the porous or screen walls of the component and insulates the surface. An inherent disadvantage to be overcome is the poor strength of most transpiration cooled materials. Therefore, designs minimizing the airfoil stress level were sought.

It has been shown that high pressure gradients around the periphery of gas turbine blades require the blade wall permeability to be varied in order for uniform cooling to be obtained over the entire blade surface. This condition can be verified in a static cascade rig. Moreover, feasibility studies of new porous blade designs are best evaluated on the cascade rig because of the relatively simple arrangement and the ease with which various configurations can be interchanged.

The series of tests reported herein were designed to evaluate commercially available porous material applicable to jet engine turbine blades. Initially it was hoped that these tests could compare blades of constant and variable chordwise permeability. In this way the coolant demands of the local areas of the skin profile could be satisfied, i.e., the hot section on the pressure side and leading edge could be more porous, thus allowing for more cooling air flow. Inasmuch as these blades are made from wire wound tubes which are formed into airfoil contours, the permeability is very difficult to keep constant, let alone controlled or varied precisely. Thus it was necessary to substitute an analagous system of chordwise metering; that of varying the inside coolant pressure around the skin periphery. By this system, flow of coolant, which depends on the difference between the squares of the coolant and hot gas static pressures, could be varied to fulfill the local needs. This was accomplished by using eight passages with separate air supplies. Tests were conducted to obtain a relative evaluation of the blades at high operating gas temperatures and to determine the savings in cooling air afforded by the use of a system of chordwise metering.

TEST FACILITY

STAND EQUIPMENT

The cascades tests reported herein were conducted in the air flow laboratory at the Wright Aeronautical Division of Curtiss-Wright in Wood-Ridge, New Jersey.

The air is supplied by two rotary Nash pumps working individually or in parallel. They are positive displacement type pumps with a combined capacity of 4000 standard CFM (approximately 5 lbs/sec at 20 psig). At airflows up to 8000 lb/hr only one pump is necessary. Above this flow both are used. The maximum obtainable discharge pressure is 22 psig. Airflow through the system is measured by a set of various sizes of calibrated orifices located at the inlet. These orifices vary in diameter from 1" to 1/4". The atmospheric and downstream orifice pressures are fed to the inputs of a sensitive 60" inclinometer. The discharge line of the pump incorporates a steam fed heat exchanger (maximum temperature 240°F) and water separator. For the purpose of this investigation, the heat exchanger was not used. To heat the air, a segment of a J-65 combustion chamber liner (See Figure 1) was installed in a burner housing, upstream of the cascade. A manually controlled Bosch pump supplied 40 to 300 lb/hr of JP-4 fuel. In order to maintain maximum cascade inlet gas temperature, the hot duct work and cascade section were insulated with four inches of asbestos. The maximum hot gas temperature recorded at the cascade inlet was 2100°F.

The cooling air was taken from the 90 psig test stand auxiliary supply line at 80°F to 100°F (See Figure 2). In the control room (Figure 3 and Figure 4) this air was directed through a rotometer for flow measurement. Eight 1/4" hand operated needle valves were used to meter the air to 8 individual lines, one for each of the cooling air passages in the test blades. To reduce the clogging effect of particles on the permeable wall of the test blade, a 5 micron filter was installed in the line. Under actual engine operation conditions the temperature of the coolant air approaches 600°F. To simulate this condition, two Chromalox thermostatically controlled electric preheaters were installed that were capable of heating 400 lb/hr of inlet air at ambient temperature to 600°F.

TEST VEHICLE

The cascade consisted of three blades located in a test section (Figures 5, 6, 7, 8). The hot gas approached the cascade with a uniform temperature distribution, was turned by the blades, and exhausted upwards.

TEST APPARATUS

AIR COOLED POROUS STATOR BLADES

The transpiration cooled test blades used in this investigation (Figures 9, 10) were non twisted, constant section stators with the same profile as the tip section of the J-65 turbine first stage rotor blade with one exception -- the chord was twice size. The assembly consisted of a porous airfoil spot welded to the solid strut (Figure 11). In addition to acting as the load bearing member, the surface of the strut was cast with ribs which, when placed into the airfoil, formed eight distinct passages. Eight individual plenum chambers supplied air to the passages.

The 2.43" chord airfoil was press formed from a wire wound porous tube that was tapered 0.10 inches on the diameter per 12 inches of length. The diameter of the tube was 1.82 inches and the blade length was three inches. The material was AISI310 for both skin and strut. The skin was brazed to the strut as detailed in Reference 11.

WATER COOLED NON POROUS BLADES

Of the three blades used in the cascade, the middle one only was the test piece. The other two were convection, water-cooled workhorse blades. These blades had three straight through passages (See Figure 12, 13) with inlet piping and plenums to accommodate coolant. The water flashed to steam and accumulated in an exit chamber from which exited one "steam out" line. The material used was A.I.S.I. 310 - sheet metal for the airfoils, dividing partitions, plenums, and tubing. So that additional liquid cooling data could be gathered, these blades were fully instrumented as detailed in the following section.

POROUS TUBE AND WEDGE

The porous wedge, (Figure 14, 15) and porous tube (Figure 16) were designed to provide preliminary indications of the properties of porous material while subjected to varied conditions of gas weight flow and temperature. The determination of heat transfer coefficients and permeability was given specific attention so that an optimum material could be selected for the actual tests. From these investigations the desired permeability of the air foils was established.

The four inch long porous tube was instrumented with three coolant static pressure probes, two external hot gas static pressure taps, four coolant temperature thermocouples, and two wall thermocouples.

The wedge test assembly consisted of a 1.00" Dia x .125 wall tube, from which a segment 140° by 1.60 inches was cut. Over this gap in the tubing a 2.00" wide by 1.89" long wedge of porous material .022 thick (wedge angle = 26°) was fitted and spot welded. On the two surfaces of the wedge were placed nine thermocouples and nine static pressure taps to measure surface phenomena. Three additional pressure taps and thermocouples measured the inlet coolant conditions before passing through the porous surface.

The test procedure called for each test apparatus to be rotated in the gas stream so the stagnation temperature could be established at a point where pressure read maximum. For a test point to be set, sufficient cooling air flow would be maintained to keep the stagnation wall temperature low. Then the air flow was decreased until desired temperature was obtained. The difference in surface temperature at the same distance from the wedge apex is an indication of the variation in permeability.

Readings of internal and external pressure, air flow, ambient air temperature and barometer were taken for each point. In calculating the flow area, allowance was made for brazed or weld filled areas in the porous material so the true effusion area could be used in the permeability calculations.

#### POROUS ROTOR BLADE

The final test of this program was conducted on a standard shape J-65 transpiration cooled turbine rotor blade (Figures 17, 18). The porous skin of this blade was made of H.S. 25 wire and the strut cast of H.S. 31 material. This test was conducted to determine the temperatures that would be experienced by the skin (particularly leading edge), and the internal structural member of an actual rotor blade when subjected to hot gas temperatures of over 2000°F. In reality, this blade can be considered as an application of two coolant principles; transpiration cooling, since the skin was made of porous metal, and convection cooling, by virtue of the fact that the tip section was open thus allowing some of the coolant to flow directly spanwise through the blade, without ever penetrating the porous wall. Based on the results of this phase, decisions on the capability of the materials selected would be made prior to the full scale engine test reported in C.W.R. Report No. 300-38.

INSTRUMENTATION

TEST VEHICLE

The duct work upstream and downstream of the cascade section was instrumented so that main gas flow data could be gathered. Approximately 4 feet upstream were four C/A thermocouples, two total pressure probes, and two static pressure probes (Figure 1). This section was in a duct 8 inches in diameter. The thermocouples and total pressure probes were inserted to several depths so a complete picture of the approach profile could be obtained.

At the cascade inlet section (B-B Figure 19) were sixteen static pressure taps and two stagnation type total temperature thermocouples. This instrumentation set up was duplicated at the exit section (D-D). Data accumulated from this instrumentation was used to determine the approach velocity, static pressure, density and viscosity of the gas at ten stations around the periphery of the test blade.

A portable manometer was set up in the test stand so that manual pressure traverses could be taken of the total pressure front in the cascade throat.

Two thermocouples, one upstream of the cooling air rotometer, and one downstream of the electric heaters, were installed to give information on coolant temperature before entering the cascade.

POROUS STATOR BLADES

Ideally a single blade should have been instrumented to provide all of the data sought for in this analysis. Practically, this posed an impossible situation due to the large amount of instrumentation required for the space available. Consideration had to be given to the axiom that the best instrumentation should make its presence unknown; while measuring flow, for example, the flow measuring device must not in anyway alter the magnitude or direction of the measured quantity. To achieve this is an insurmountable problem. Radiation to and from a thermocouple junction is a cause of error. Moreover the brazing of a thermocouple in a porous metal gives rise to a partially clogged area caused by the body of the couple and the flow of the braze material. In this test the Ceramo wire to the thermocouple was placed in machined grooves and cemented over. Thus the only error was caused by the junction and braze. The error in the temperature measured

will be on the high side for the porous metal. When temperature of coolant in a passage is desired the thermocouple will read high due to radiation from the porous metal walls.

It was therefore deemed necessary to divide the required instrumentation over three blades; to perform the test in three segments under identical conditions; to consider the data taken from the three blades at different times to be representative of the data that one blade would yield provided it contained all the instrumentation of the three blades.

Two of the blades were instrumented for temperature data (Figure 20) and the third was instrumented for pressure data (Figure 21). Refer to Figure 22 for the passage numbers referred to in the following tables. The static pressure taps located  $1\frac{1}{2}$ " from the plenum chamber at the midspan location of the blade measured the existing local pressure of the coolant inside the blade in the given passage. The code to the abbreviations used in the instrumentation Tables I (a), I (b) and I (c) are as follows:

- PL. CH. - Plenum chamber for the passage under consideration
- D.E. - dead end. This refers to the end of the coolant passage farthest from the plenum chamber. The passage ends at this position.
- C.L. - Center line of blade (approximately 2" from plenum chamber)
- L.E. - Leading edge of blade (in passage 1)
- T.E. - Trailing edge of blade (in passage 5)

~~CONFIDENTIAL~~

C.W.R. REPORT NO. 300-39

Passage No.	Spanwise Position	Type of Instrumentation
1	Pl. Ch.	Air static pressure
1	Pl. Ch.	Air thermo
1	2" from Pl. Ch.	Skin thermo
1	C.L.	Air thermo
1	D.E.	Air thermo
2	Pl. Ch.	Air static pressure
2	1" from Pl. Ch.	Skin thermo
2	2" from Pl. Ch.	Skin thermo
3	Pl. Ch.	Air static pressure
3	C.L.	Air static pressure
3	2" C.L. Pl. Ch.	Skin thermo
4	Pl. Ch.	Air static pressure
4	C.L.	Strut thermo
4	2" from Pl. Ch.	Skin thermo
5	Pl. Ch.	Air static pressure
5	Pl. Ch.	Air thermo
5	C.L.	Air thermo
5	2" on T.E.	Skin thermo
5	D.E.	Air thermo
6	Pl. Ch.	Air static pressure
6	2" from plen	Skin thermo
7	Pl. Ch.	Air static pressure
7	1" from Plen. Ch.	Skin thermo
7	2" from Plen. Ch.	Skin thermo
8	Pl. Ch.	Air static pressure
8	C.L.	Static pressure
8	2" Pl. Ch.	Skin thermo

INSTRUMENTATION SCHEDULE-TEMPERATURE INSTRUMENTED CASCADE BLADE  
BLADE NO. R110021 N-1  
TABLE I (a)

~~CONFIDENTIAL~~

Passage No.	Spanwise Position	Type of Instrumentation
1	Pl. Ch.	Air thermo
1	Pl. Ch.	Air static pressure
1	Pl. Ch.	Air static pressure
1	C.L.	Air static pressure
1	1" from Pl. Ch. on L.E.	Skin thermo
2	Pl. Ch.	Air static pressure
2	C.L.	Skin thermo
2	D.E.	Air thermo
3	Pl. Ch.	Air thermo
3	Pl. Ch.	Air static pressure
3	1" from Pl. Ch.	Skin thermo
3	C.L.	Air thermo
3	D.E.	Air thermo
4	Pl. Ch.	Air thermo
4	Pl. Ch.	Air static pressure
4	1" from Pl. Ch.	Skin thermo
4	C.L.	Air thermo
4	D.E.	Air thermo
5	Pl. Ch.	Air static pressure
5	1" from Pl. Ch. or T.E.	Skin thermo
5	C.L.	Skin thermo
5	2" from Pl. Ch.	Skin thermo
6	Pl. Ch.	Air static pressure
6	1" from Pl. Ch.	Skin thermo
7	Pl. Ch.	Air static pressure
7	C.L.	Skin thermo
7	D.E.	Air thermo
8	Pl. Ch.	Air static pressure
8	2" from Pl. Ch.	Air static pressure
8	Pl. Ch.	Air thermo
8	1" from Pl. Ch.	Skin thermo
8	C.L.	Air thermo
8	D.E.	Air thermo

INSTRUMENTATION SCHEDULE-TEMPERATURE INSTRUMENTED CASCADE BLADE

BLADE NO. R110021 N-2

TABLE I (b)

Passage No.	Spanwise Position	Type of Instrumentation
1	Pl. Ch.	Air static pressure
1	Pl. Ch.	Air thermo
1	D.E.	Air thermo
1	2 $\frac{1}{2}$ " from plenum	Skin thermo
Land between 1 & 2	C.L.	Gas static pressure
2	Pl. Ch.	Air static pressure
Land between 2 & 3	C.L.	Gas static pressure
3	Pl. Ch.	Air static pressure
3	Pl. Ch.	Air thermo
3	D.E.	Air thermo
Land between 3 & 4	C.L.	Gas static pressure
4	Pl. Ch.	Air static pressure
Land between 4 & 5	C.L.	Gas static pressure
Land between 4 & 5	2 $\frac{1}{4}$ " from Pl. Ch.	Strut thermo
5	D.E.	Air thermo
5	Pl. Ch.	Air static pressure
5	Pl. Ch.	Air thermo
5	C.L. at T.E.	Gas static pressure
Land between 5 & 6	C.L.	Gas static pressure
6	Pl. Ch.	Air static pressure
6	Pl. Ch.	Air thermo
6	Pl. Ch.	Air thermo
Land between 6 & 7	C.L.	Gas static pressure
7	Pl. Ch.	Air static pressure
Land between 7 & 8	C.L.	Gas static pressure
Land between 7 & 8	3/4" from Pl. Ch.	Strut thermo
8	Pl. Ch.	Air static pressure
Land between 8 & 1	C.L.	Gas static pressure

INSTRUMENTATION SCHEDULE--PRESSURE INSTRUMENTED CASCADE BLADE  
 BLADE NO. R110031  
 TABLE I (b)



### WATER COOLED BLADES

The two workhorse blades were identically instrumented as follows: On the skin at the mid-span section were four thermocouples; one each on the leading edge, concave side, trailing edge, and convex side. Temperatures of inlet water, steam in each of the three passages, and steam out were also measured.

The instrumentation set-up used on the porous tube and porous wedge has been outlined under "Apparatus" in the previous section.

### POROUS ROTOR BLADE

The porous engine rotor blade used in the final test was instrumented with a thermocouple on the leading edge at midspan, a thermocouple on the strut near the root section, and a thermocouple in the plenum chamber measuring the inlet air temperature.

### CONTROL ROOM

The control room of the test stand was equipped with ten illuminated banks of 10 tube, 0-60" manometers - 5 mercury filled and 5 water filled (Figure 3). For greater accuracy in reading pressures in the cascade, a typical pressure tap was tagged "reference" and hooked up to a mercury manometer and the reservoirs of two water manometer banks. The readings were then taken in terms of the difference between the water manometers and the "reference". The reference reading was read in mercury and on a W. and T. pressure gage. Of course, the resultant pressure was the sum of the individual water reading, the reference mercury reading, and the barometer.

Main gas flow was taken as the sum of the air flow as determined from the inclinometer and the fuel flow as read on a stand rotometer.

The exhaust pressure and temperature from the cooling air rotometer was measured so the readings could be corrected.

The thermocouples were read on two potentiometers with 40 channels each - one for C/A thermocouples and one for I/C thermocouples.

There were three water rotometers of different sizes to measure the water flow to the workhorse blades.

TEST PROCEDURE

POROUS STATOR BLADES

The test program for each of the transpiration air cooled stator blades in the cascade rig was divided into three phases.

The first phase was essentially a cold flow aerodynamic check-out of the rig proper and adapting ductwork. This phase was necessary to determine if the gas stream approached the test blades with a flat velocity profile. Pressure patterns at the cascade throat showed evidence of free vortex distribution. Inasmuch as this data was taken using a single blade in the cascade, it was anticipated that with the addition of the two water-cooled workhorse blades, there would be more surface presented to deflect the gas stream and a flat approach velocity pattern would be obtained. This premise proved correct.

When each of the cascade blades were installed in the rig, a porosity calibration was run. The reasoning here was to evaluate the consistency of the porous material. At zero main gas flow the air pressure in each plenum chamber was set to 10" water, 4" mercury, and 7" mercury. By recording the barometric pressure and the total coolant flow, the permeability of each blade was established. With no main gas flow the higher pressures were impossible to attain in the large passages (specifically the trailing edge) with their correspondingly large flow area. When there was a main flow, and a pressure pattern existed around the blade periphery, cooling air pressure build-up was possible. This calibration was repeated at main gas approach velocities of 150 FPS, 250 FPS, and 320 FPS. No fuel was added to the main gas stream used in the calibration. Cold flow calibrations introduce a minimum of error inasmuch as the differential expansions caused by a non-linear temperature distribution are absent. After the actual hot testing of each blade this calibration was repeated while the blade was still hot and again after the blade reached ambient temperature. In this way changes in porosity due to exposure to high temperature and possible particle contamination were measured.

By far, the major part of the testing of each blade, was comprised by the third phase. The hot gas test was performed in as close to the same manner as possible for each of the three blades. After starting the Nash pumps and building the air flow up to about 2500 lbs/hr, a bypass valve was partially closed forcing approximately half the air through the rig. The fuel primer supply and ignition system made up of standard J65 igniters and hardware was actuated. A thermocouple at the combustion chamber exit gave immediate indication of light-up at which time the bypass valve was shut completely forcing all the air through the cascade. Simultaneously the main fuel supply was turned on and the Nash pumps accelerated to provide a preselected flow and gas temperature.

~~CONFIDENTIAL~~

G.W.R. REPORT NO. 300-39

Assume that a point was to be set at the following conditions:

Gas temperature - 1800°F  
Wall temperature - 1400°F  
Gas velocity - 550 FPS

To insure that the blade was not damaged by over temperating, the coolant supplies were opened to maximum flow. A series of stand operating curves, (Figure 23) were drawn up on which main gas velocity versus total to static pressure ratio was plotted for gas temperatures of 1500°F, 1800°F, and 2000°F. While the theory behind the plotting of this graph was good, the velocities so set were only approximate because of the inherent inaccuracies of static pressure measurement. As was pointed out in the "instrumentation" section the only total pressure readings were taken upstream of the cascade in the 8 inch duct. During the test it was found that the maximum point of the total pressure profile was constantly shifting due to the influence of the bends in the ductwork in combination with the varied effects on flow caused by the different gas velocities and temperatures. In view of the fact that these readings were not dependable, an iteration process was used to calculate the actual total pressure at the inlet. This process also took into account any friction losses that may have occurred in this system.

Nevertheless, the pressure ratio was taken under running conditions by averaging the 16 static pressures at the inlet and dividing the value thus obtained into the average value of the two upstream total pressures. Reference to the operating curve yielded the approximate velocity of the gas stream. Hence in order to set a given velocity, the necessary pressure ratio was determined from the curve. A trial and error system of varying the main air supply, computing the resulting pressure ratio, and correcting the flow in the proper direction was employed. For the sample point under consideration, at a desired velocity of 550 FPS, the proper curve in Figure 23 yields a pressure ratio of 1.0445. When this ratio was achieved the fuel-air ratio was adjusted to provide the proper gas temperature by varying the fuel only. Addition of the fuel did not materially effect the velocity that had been set. At this point the skin temperatures were read. If the temperature in passage 1. was below the desired 1400°F, the air flow to this passage was reduced. In this manner the temperature at each passage was set. In this series of tests it was calculated that the inlet air would reach a temperature of 350° to 400° by radiation and conduction in the piping, ductwork, and plenums prior to entering the blade passages. Thus, in these cascade tests, the cooling air was not preheated.

The running instructions containing all the "hot" points to be ran for each blade are tabulated in Table II.

Gas Temperature °F			Wall Temperature °F				Gas Velocity (ft/sec)	
1500	1800	2000	1000	1200	1400	1600	450	550
	X				X		X	
	X				X			X
	X		X					X
	X					X	X	
	X			X			X	
X			X					X
X				X			X	
		X			X		X	
		X		X			X	
		X				X		X

TABULATION OF RUNNING TEST SCHEDULE.

TABLE II

The average hot gas mass flow recorded at velocities of 450 FPS and 550 FPS were 1.643 lbs/sec and 2.464 lbs/sec respectively. Several points were run at gas velocities of 250 and 650 FPS. At the lower velocity the combustion chamber was apparently working far below design level. Burning of fuel was taking place downstream of the chamber along the inside walls of the ductwork due probably to the small amount of air needed. The ductwork glowed light red especially at the high temperature-low flow points. On the other hand the very high flow points ( $Mr. >.4$ ) presented a problem of a different nature. The large amount of instrumentation leads necessitated several openings from the blade to the rig exterior. Although clearances were kept to a minimum and packing was used through-out, the hot gas exhausted from all the cracks and damaged the instrumentation. For these reasons, the high and low flow points were not rerun with the second and third blades and were therefore not included in Table II.

#### POROUS ROTOR BLADE

Testing of the J-65 turbine rotor blade proceeded in a manner very similar to that used in the cascade tests. Instead of a separate air supply for each passage, one total supply was hooked up through a rotometer. In this test the heaters were used to supply 600°F coolant to simulate engine conditions. One set of points was, however, run with coolant air at ambient temperature in order to get data for comparison.

An additional test objective was added at this point of the investigation. It was observed that the data taken during the test indicated a marked improvement over existing convection cooled rotor blades. Thought centered on the fact that this blade, being itself cooled partially by convection cooling, could be further improved by capping the tip section and forcing all the air through the wall. Upon completion of the open-tip testing, the tip section was brazed closed, and the blade assembly reinstalled into the cascade rig for retest.

ANALYSIS

REDUCTION OF DATA

Before analysis of the heat transfer parameters could be undertaken, it was necessary to confirm the validity of the aerodynamic data upon which turbine heat transfer calculations depend. Of paramount importance was the accuracy of the total to static pressure ratio of the free stream. For on this quantity depends the Mach number and therefore, the Reynolds number of the gas stream.

Gas mass flows were calculated based on the measured pressure ratio using the relationship:

$$Q = \frac{K P_t A N}{\sqrt{T_t}} \quad (1)$$

The parameter "N" is based upon static to total pressure ratio and the specific heat ratio ( $\gamma$ ).

$$N = \frac{\left[ \left( \frac{P_s}{P_t} \right)^{\frac{2}{\gamma}} - \left( \frac{P_s}{P_t} \right)^{\frac{\gamma+1}{\gamma}} \right]^{\frac{1}{2}}}{\left[ \left( \frac{2}{\gamma+1} \right)^{\frac{2}{\gamma-1}} - \left( \frac{2}{\gamma+1} \right)^{\frac{\gamma+1}{\gamma-1}} \right]}$$

For a given gas at a given pressure, the value of  $\gamma$  decreases with increasing temperature. This value was obtained from a curve of  $\gamma$  versus total temperature plotted for the products of combustion of JP-4 fuel at a pressure of 1.5 atmospheres. For the higher flow rates the value of gas weight flow as calculated from equation (1) were in poor agreement with the value obtained by adding the test air and fuel flows. At the lower flow rates agreement was excellent. Several calibrations of the inclinometer removed any doubt as to its accuracy. The source of error, then, appeared to be one of the components of the pressure ratio. The sixteen static pressure taps located in the cascade section agreed closely. The difference between the high and low values divided by the low value fell within 1%.

$$\frac{\text{Maximum Pressure} - \text{Minimum Pressure}}{\text{Minimum Pressure}} < 1\%$$

It is highly improbable that these values were in error. The fact there was good agreement between calculated and measured weight flows at low flow

and poor agreement at high flow suggests that the gas pressure profile shape changed markedly. Turbulence in the duct work may have caused the two total pressure probes to see a pressure that was not in the path of the maximum velocity head. It is evident that ten or more probes inserted to different depths would have presented a more complete pressure picture. However, to insure that the hot gas approached the cascade with a flat velocity profile, protruding upstream instrumentation was held to a minimum. Moreover, inaccuracies of total pressure readings at the higher flows may have been caused either by improper installation or by bending of the probes under the influence of gas load and temperature causing them to read a value between static and total pressure. Nevertheless, the total pressure test data was deemed inaccurate and a substitute iteration procedure for evaluating the pressure ratio was employed.

Acceptance of the gas weight flow as read by the inclinometer was a pre-requisite to the use of the substitute procedure. On a coordinate system, pressure versus gas weight flow were plotted on Figure 24. A horizontal line representing the inclinometer weight flow was drawn. For each test point several assumptions of  $P_t$  were made. These values divided by the recorded value of  $P_s$  at the given point yielded a ratio from which a corresponding weight flow was calculated and then plotted. If the total pressure was assumed equal to the static pressure, then a ( $P_t/P_s$ ) ratio of 1 would yield a flow of zero. By successively increasing the total pressure assumption, the magnitude of the flow, when plotted, eventually falls above the inclinometer flow line. A smooth curve drawn through the plotted points intersects the inclinometer flow line at that total pressure which will cause the reference weight flow. In this manner the inlet total pressure at each point was read off the iteration curve.

The gas Mach number is obtained by solving the equation:

$$\frac{P_s}{P_t} = \left[ 1 + \left( \frac{\gamma-1}{2} \right) M_n^2 \right]^{-\frac{\gamma}{\gamma-1}} \quad (3)$$

for various trial values of  $M_n$ . When agreement is obtained between both sides of the equation, the static to total temperature ratio is determined:

$$\frac{T_s}{T_t} = \left[ 1 + \left( \frac{\gamma-1}{2} \right) M_n^2 \right]^{-1} \quad (4)$$

of the gas was measured so that  $T_s$  can be evaluated. Equations (3) and (4) are solved for various values of  $\gamma$  in reference (4).

To obtain the acoustic velocity and gas velocity, equations (5) and (6) were solved for each peripheral station.

$$a_g = \sqrt{\gamma R_g T_s} \quad (5)$$

$$v_g = (M_n) (a_g) \quad (6)$$

The gas static pressure was measured at nine peripheral positions on the test blade. Gas velocity and Reynolds number were calculated at each position (Tables IV and V). The Reynolds number was evaluated as:

$$Re_{gx} = \frac{\rho_{gx} v_{gx} x}{\mu_{gx}}$$

using the static conditions that occur at each station.

The porous material specified for the airfoils called for a permeability  $k = 1.215 \times 10^{-10} \text{ cm}^2$  or a  $k/\gamma = 4.6 \times 10^{-10} \text{ ft}^2$ . At the onset of the test, calibrations were performed to check on this value. The total coolant air-flow through the blade was recorded along with the static pressure in the root of each passage. The total flow through the blade is given by

$$Q_a = (\rho_a v_a) A \quad (7)$$

$$\rho_a v_a = \frac{Q_a}{A} \quad (8)$$

From reference (3) the mass velocity ( ) is

$$(\rho_a v_a)_x = C_K (P_{s,a}^2 - P_{s,g}^2)_x^N \quad (9)$$

# CONFIDENTIAL

C.W.R. REPORT NO. 300-39

The value of  $P_{s,a}$  was found by calculating a weighted average internal pressure.

$$P_{s,a} = \sum \frac{P_{s,a,1}A_1 + P_{s,a,2}A_2 + \dots + P_{s,a,8}A_8}{A_{TOTAL}}$$

The value of the exponent  $N$  is determined empirically and is a function of the type of porous material; the value of  $C_K$  is a function of material permeability and thickness, and of cooling air properties based on the porous wall temperature. For the calibration  $P_{s,q,x}$  is taken as the barometric pressure. For several types of porous shell materials equation (9) well approximates the correlation between cooling air mass velocity and the internal and external pressures.

The value obtained for  $C_K$  in equation (9) is now employed to determine an overall value of  $k/\lambda$  in the relationship (10)

$$C_K = 3.050 \left[ \frac{k}{\lambda} \frac{1}{\mu T_w} \right]^{\frac{5}{8}} \quad (10)$$

Upon completion of the calibration, equations 7, 9, and 10 are used to determine the airflows in the individual passages knowing the pressures and permeability.

The entire sequence of operations with resulting values of airflow through all eight passages is shown in Tables III-A and III-B for a typical test point.

The relative effectiveness of dissimilar cooling methods are judged by correlating measured data and comparing it to some datum. Correlation of measured porous-blade temperatures can be achieved by evaluating the temperature difference ratio  $\frac{T_w - T_c}{T_g - T_c}$ ; the greater the effectiveness of the cooling method the lower will be the value of this ratio.

Blade wall temperature data obtained at a constant gas Reynolds number can be correlated by plotting the temperature difference ratio against the mass velocity ratio  $(\rho v)_{a,x} / (\rho v)_{g,x}$  (Reference 1)

In as much as a primary objective of this investigation was a verification of existing theory, a brief outline of the design procedure from a heat transfer standpoint for turbine blading is included here.

Passage Number	$T_{wx}$ °R	$\mu$ $\times 10^{-6}$ Lb/Sec. ft	B $\times 10^{-10}$	$B \frac{5}{8}$ $\times 10^{-5}$	$C_k$ $\times 10^{-5}$
1 Pressure	1590	25.54	34.88	.5173	1.578
1 Suction	1590	25.54	34.88	.5173	1.578
2	1498	24.52	35.66	.5248	1.601
3	1503	24.52	36.54	.5330	1.626
4	1535	25.20	33.82	.5078	1.549
5 Pressure	1499	24.52	35.64	.5245	1.600
5 Suction	1499	24.52	35.64	.5245	1.600
6	1455	24.19	37.22	.5392	1.645
7	1363	23.18	41.55	.5775	1.761
8	1620	25.87	31.26	.4832	1.474

$$B = \left[ \frac{k}{\tau} \frac{1}{\mu T_w} \right]$$

$$C_k = 3.050 [B] \frac{5}{8}$$

$$T_t \text{ gas} = 2362^\circ R$$

$$\frac{k}{\tau} = 1.31 \times 10^{-10} \text{ Ft}$$

$$P_t \text{ gas} = 34.86'' \text{ HG}_{\text{ABS.}}$$

$$\tau = .020'' - .022''$$

$$W_{\text{gas}} = 1.643 \text{ Lb/sec}$$

TRANSPIRATION COOLED TURBINE BLADE.

TABULATION OF COOLANT FLOW PARAMETERS FOR A SAMPLE POINT.

TABLE III A

Passage Number	$P_{sax}$ ( $"HG$ ) <sup>2</sup>	$P_{sgx}$ ( $"HG$ ) <sup>2</sup>	D	$(\dot{m})_{ax}$ $\times 10^{-3}$ Lb/ft <sup>2</sup> sec	A FT <sup>2</sup>	$Q_{acc}$ $\times 10^{-4}$ Lb/sec
1 Pressure	1711.5	1143.2	6765.0	10,675	.00321	3.424
1 Suction	1711.5	1180.6	10,373.0	16,369	.00384	6.284
2	1542.1	1111.5	4417.7	7,073.0	.00584	4.128
3	1605.6	1359.4	6426.7	10,500.0	.00608	6.388
4	1518.7	1349.8	5063.5	7,843.0	.00758	5.942
5 Pressure	1195.1	1133.7	2689.6	4,303.0	.01862	8.014
5 Suction	1195.1	913.2	6970.0	11,152.0	.01867	20.82
6	1483.8	920.5	10,762.0	17,704	.00860	25.22
7	1195.1	929.6	6724.0	11,841	.00823	9.744
8	1629.7	916.3	12,164.0	18,372	.00786	11.144

$$D = \sqrt{\frac{P_{sax}^2 - P_{sgx}^2}{s/s}}$$

$$T_t \text{ gas} = 2362^\circ R$$

$$P_t \text{ gas} = 34.86 \text{ "HG ABS.}$$

$$W_{\text{gas}} = 1.643 \text{ Lb/sec.}$$

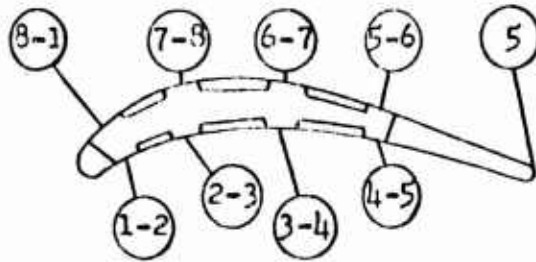
TRANSPIRATION COOLED TURBINE BLADES.

TABULATION OF COOLANT FLOW PARAMETERS FOR A SAMPLE POINT.

TABLE III B

C. W. R. REPORT NO. 300-39

C. W. R. REPORT NO. 300-39



Blade Position	$p_s$ "Hg. abs	$p_s/p_t$	$T_s$ °R	$T_s/T_t$	$M_n$	$a$ Ft/sec	$v$ Ft/sec
1-2	40.39	.9538	2186	9891.5	.2706	2213	598.8
2-3	40.29	.9515	2185	9886	.2774	2213	613.89
3-4	38.39	.9066	2161	9776.3	.3907	2200	859.54
4-5	40.04	.9456	2182	9872	.2942	2211	650.48
5	30.19	.7129	2044	9248	.7359	2140	1574.8
5-6	31.04	.7330	2058	9311	.7023	2147	1507.8
6-7	30.04	.7094	2042	9238	.7114	2139	1586.0
7-8	30.94	.7307	2056	9302	.7075	2146	1518.0
8-1	30.14	.7118	2044	9246	.7375	2140	1578.0

$T_t$  gas = 2210°R

$W_g$  = 2.464 Lb/Sec

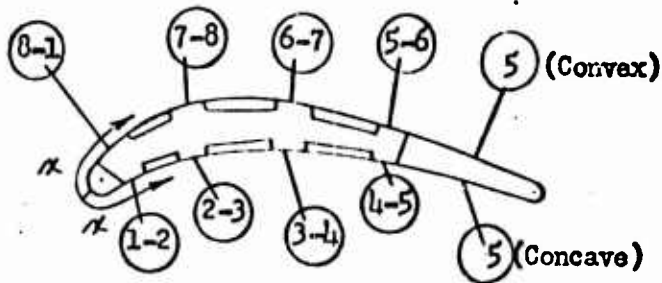
$\gamma$  = 1.3045

$p_t$  gas = 37.26" Hg. abs.

TRANSPIRATION COOLED CASCADE BLADE  
PRESSURE, TEMPERATURE, MACH NUMBERS, ACOUSTIC VELOCITY, AND  
GAS VELOCITY PROFILES TABULATED FOR A SAMPLE RUNNING POINT.

TABLE IV

Page 27



Blade Position	$\rho_{gx}$ Lb/ft <sup>3</sup>	$V_{gx}$ Ft/sec	$\kappa$ Ft	$\mu_{gx}$ Lb/sec ft $\times 10^{-6}$	$Re_{gx}$ $\rho v x / \mu$
1-2	.0245	598.8	.0292	31.6	13,540
2-3	.0244	613.9	.0625	31.6	29,624
3-4	.0236	859.6	.0958	31.6	61,520
4-5	.0243	650.5	.1358	31.6	67,943
5 Concave	.0196	1574.8	.2258	30.6	227,787
5 Convex	.0196	1574.8	.2642	30.6	266,452
5-6	.0200	1507.8	.1750	30.8	171,335
6-7	.0195	1586.0	.1233	30.6	124,646
7-8	.0199	1518.0	.0708	30.8	69,470
8-1	.0195	1578.0	.0233	30.6	23,463

$T_t$  gas = 2210°R       $W_g$  = 2.464 Lb/Sec  
 $\gamma$  = 1.3045           $P_t$  gas = 37.26" Hg. abs.

TRANSPIRATION COOLED CASCADE BLADE  
 TABULATION OF HOT GAS REYNOLDS NUMBERS CALCULATED AROUND THE BLADE PERIPHERY FOR SAMPLE RUNNING POINT.

~~CONFIDENTIAL~~

C.W.R. REPORT NO. 300-39

CASCADE BLADE DESIGN PROCEDURE

Assume that a turbine capable of operation at 2000°F is contemplated. Based largely on experience and on previous design the structural engineer produces a trial section that will have the required strength to operate at 1400°F. This temperature is limited by the properties of the material. Of course, an alloy with sufficient strength to operate at 2000°F would eliminate the need of blade cooling. In actuality, however, the heat transfer engineer must remove that amount of heat which will allow the structural member of the blade to operate within the temperature limit.

At the onset of a specific design the velocity and pressure distribution of the main gas stream chordwise around the blade must be determined. For on these values will depend the coolant to gas pressure ratio, the flow of coolant, and, therefore, the temperature of the blade skin. The aero-dynamic properties of the gas at a point just upstream of the turbine inlet are predicted with good accuracy by the compressor and combustion chamber analysis. From this information the establishment of gas velocity and pressure profiles around the blade can be accomplished by the use of aerodynamic network theory or electrical analog methods (Reference 6).

The static pressure of the coolant flow in the blade at the root section is assumed and the pressure at any spanwise position (y) due to the centrifugal effect is calculated for the blades from the relationship,

$$\left[ 1 - \left( \frac{m}{A} \right)^2 \frac{RT}{P_{s,a}^2} \right] \frac{dP_{s,a}}{dy} = \frac{P_{s,a}}{RT} r \omega^2 \cos. \beta - 2 \frac{RT}{P_{s,a}} \left( \frac{m}{A} \right) \frac{dm}{dy} - \left( \frac{m}{A} \right)^2 \frac{R}{P_{s,a}} \left( \frac{dT}{dy} + \frac{T}{A} \frac{dA}{dy} + \frac{f_t}{2D_h} \right) \quad (11)$$

from Reference 7, using notation of this report. The root pressure can be established by metering orifices in the system. The data taken in this investigation substantiates the supposition that the pressure along the passages of stator blades will remain constant even at relatively high flow rates. Thus, in the design of stator blades, with the effects of centrifugal force removed, equation (11) is greatly simplified.

The maximum allowable temperature (  $T_w$  ) for the blade skin as limited by material properties is used to calculate the cooling air velocity through the porous wall (Equations 9 and 10).

~~CONFIDENTIAL~~

The parameter,  $f_w$ , is calculated using the value of velocity obtained.

$$-f_w = \frac{2}{Eu + 1} \frac{v_g}{Q} \sqrt{Re} \quad (12)$$

$$Eu = \frac{x}{v_{g, B-B}} \frac{\partial v_{g, x}}{\partial x} \quad (13)$$

Thus, the value of  $T_w - T_c / T_{ad} - T_c$  can now be found for both the laminar and the turbulent regions. In the laminar region Figure 4 of Reference 7 gives  $T_w - T_c / T_{ad} - T_c$  at different Euler numbers and coolant flow parameters ( $f_w$ ). For the turbulent region:

$$\frac{T_w - T_c}{T_{ad} - T_c} = \frac{Re^{2.11}}{\exp \left[ \frac{71.3 (\rho v) Pr^{2/3} x}{Re^{0.9} \mu} \right] + \frac{2.11}{Re^{0.1}} - 1}$$

The individual values of  $T_w$  calculated around the blade are now compared with assumed values. If they do not check, the calculation is repeated for a new  $T_w$ . If the value of  $T_w$  that must be assumed for the trial and error procedure is not compatible with design requirements, a new value for the blade root internal coolant pressure ( $P_{s, a, r}$ ) is tried. When a satisfactory skin temperature has been obtained at all locations for which a calculation has been made,  $\rho v$  is determined at each location from equation (9). The coolant requirement for each passage  $Q_{a, 1}; a, 2; \text{ etc.}$  is obtained by summing the product of each  $\rho_a v_a$  and associated skin area over the entire passage. The sum of the  $Q_a$  quantities for all the passages represents the total coolant requirement per blade. Each passage is now equipped with an orifice such that the cooling air pressure available,  $P_{s, b}$  is attenuated to the desired value of  $P_{s, a, r}$ . The diameter of each orifice is calculated from the following equations in the notation of this report (Reference 8).

For subcritical pressure drops,  $\frac{P_{s, a, r}}{P_{s, b}} > 0.528$

$$A_n = \sqrt{\frac{R}{2g}} \frac{Q_a}{C_n} \sqrt{\frac{T_a}{P_{s, a, r} (P_{s, b} - P_{s, a, r})}}$$

For supercritical pressure drops,  $\frac{P_{s,a,r}}{P_{s,b}} \leq 0.528$

$$A_n = 2.067 \sqrt{\frac{R}{2g}} \frac{Q_a}{C_n} \sqrt{\frac{T_a}{P_{s,b}}}$$

The orifice coefficient,  $B$ , is estimated from Figure 5, page 42, Reference 9.

RESULTS

PRESSURE PROFILES AROUND PERMEABLE AIRFOILS

Measured chordwise pressure distribution at the midspan location relative to the gas total pressure is plotted in Figure 25. It is significant that there is a very sharp drop of pressure on the suction surface immediately downstream of the stagnation point. Coolant flow data taken in this investigation has indicated that in a region of rapidly changing outside static pressure, the cooling air will flow mostly to the lower pressure areas. Unless some type of auxiliary compressor is employed to increase the coolant pressure, the placement of a strut fin joined to the inside skin at the stagnation point is perhaps mandatory to prevent the hot gas from entering the blade. To compensate for the lack of coolant exiting at the leading edge, a slightly greater than adequate amount of coolant should be routed through the two passages created by the fin. Thus, the lower skin temperatures immediately downstream of the leading edge will serve as heat sinks for conduction of heat away from the stagnation point. The curves in Figure 25 show that at a given gas flow rate, increase in the gas temperature causes higher velocity (greater specific volume) and therefore, lower static pressure. At nearly equal gas temperature, lower gas flow results in higher static pressure profiles. Inasmuch as flow of coolant depends on the outside static pressure, improved cooling characteristics will result from higher turbine gas velocities.

CORRELATION OF POROUS METAL TEMPERATURE

The method of correlating porous blade wall temperatures, which is described in Reference 1, was utilized in reducing the data presented in this report. By plotting the ratio of coolant weight flow ( $\rho_c v_c$ ) to combustion - gas weight flow ( $\rho_g v_g$ ) against the temperature difference ratio ( $T_{b,x} - T_a$ ) / ( $T_{g,e} - T_a$ ) on semi logarithmic paper, a definite trend towards straight line correlation is achieved for a constant gas weight flow.

In Figure 26 this information is plotted for a gas weight flow of 1.643 lb/sec at two suction side passage positions, one pressure side passage, and at the leading edge. When the gas temperature was varied between 2027°R, 2242°R, and 2379°R, the temperature-difference ratio plot resulted in a straight line at each chordwise station.

In Figure 27 the same curves were plotted for a gas weight flow of 2.464 lb/sec. For these curves data taken at 3 pressure side passage positions and one suction side position at temperatures of 1995°R, 2210°R, and 2480°R plotted fairly well.

It can be shown (Reference 1) that the temperature difference ratio is a function of the gas Reynolds number ( $\rho v x / \mu$ ). This suggests that any data obtained at various gas weight flows and at constant gas temperature would not correlate along a single curve. That this is true is shown in the curves appearing in Figure 28. The temperature at which data was taken was  $2231^{\circ}\text{R}$  and  $2412^{\circ}\text{R}$ . The gas flow rates were 1.693 lb/sec and 2.464 lb/sec.

A measure of the effectiveness with which a surface is cooled is the relative magnitude of the temperature-difference ratio for a given mass velocity ratio. Smaller temperature-difference ratios result when the wall temperature approaches the coolant temperature. Thus, with more B.T.U.'s being given up to the coolant, the numerator of the fraction decreases, thereby decreasing the magnitude of the fraction. Similarly, for a given temperature-difference ratio, the coolant mass velocity required for a given hot gas mass velocity should be minimized. The smaller the value of  $(\rho_c v_c / \rho_g v_g)$  then, the better the cooling efficiency (at  $\frac{T_w - T_c}{T_g - T_c} = \text{constant}$ ).

EXPERIMENTALLY DETERMINED COOLING CHARACTERISTICS OF TRANSPIRATION  
COOLED CASCADE BLADES

Fluids and gases, like electricity, if given the alternative, will choose to flow in the path of least resistance. In almost every turbine application the static pressure level near the trailing edge on the pressure side is 20% greater than the corresponding pressure on the suction side. Inasmuch as the flow through each wall is a function of the difference between the squares of coolant and gas pressures, it is apparent that the suction side will receive more coolant. Justification of this phenomenon is partially attained due to the fact that the gas velocity, and therefore the coefficient of heat transfer from gas to blade is greater on the suction side. In the test being reported, however, there were two instances in which the gas pressure on the pressure side was greater than the static coolant pressure. In these cases it can only be premised that there was flow of hot gas instead of coolant through the wall.

In addition to the obvious problem that arises here is the fact that the deviation angle (the angle between the blade mean camber line and the direction of the gas leaving the blades at the trailing edge) is increased considerably. The power taken by the turbine is a function of the gas turning angle. With a substantial flow of coolant exiting at the convex side, the gases are deflected causing less gas turning (hence, a larger deviation angle).

At first glance it appears that the situation, as regards lack of coolant flow to pressure side, can be corrected by increasing the coolant pressure. This is not the case since the suction side will still take the bulk of the air flow.

The middle set of curves in Figure 29 show the area of negative flow to be between 65% of the chord and the trailing edge. It is seen that by increasing the coolant pressure level and, therefore, the mass flow, the effects are lessened.

For a given coolant pressure increase, the percent increase in flow through the suction side was greater than for the pressure side. Thus, it is seen that merely raising the coolant pressure level does not solve the problem, but does appreciably increase the total coolant flow.

By introducing different amounts of fuel in the combustion chamber, the temperature of a hot gas stream was varied between 1995°R and 2480°R while maintaining the total gas flow constant. Independent control of the coolant pressure level allowed control over the coolant flow rate ( $\rho V_c$ ). Figure 30 shows that at  $T_g = 2210^\circ\text{R}$ , the ( $\rho V_c$ ) term was set at a low value with resulting increase of the temperature difference ratio and the skin temperature. At a gas temperature of 2480°R, the ( $\rho V_c$ ) was increased in each passage. It is observed that the temperature-difference ratio is proportionately lowered as is the skin temperature.

Figure 29 illustrates the effect of increasing the gas weight flow on skin temperature and temperature-difference ratio with the coolant mass velocity as a parameter. Attempt was made to offset the increase in gas mass flow by increasing the coolant velocity ( $\rho V_c$ ). Although the skin temperature was reduced, the proportional increase in ( $\rho V_c$ ) was greater than the gas flow increase. Inasmuch as neither temperature-difference parameter seems to be obviously more advantageous, the benefits that occur from high temperature operation must be equated against the necessary amount of bleed air before any system is adopted.

It has been shown mathematically, in Reference 5, there is practically no difference in temperature between the cooling air and the blade wall at any point within the wall. (Exception to this is experienced in the thin section of wall adjacent to the cooling passage.) This is due to the large area of metal which is in contact with the cooling air in a porous material.

In this investigation, however, there were thermocouples in the passages that measured air temperature. Although the coolant temperature readings were undoubtedly subjected to error by radiation from the passage walls, the temperatures so measured are entirely plausible and present a

more realistic value than can be obtained by measuring the coolant temperature before entry into the blade. Moreover, the temperature of the air before entry into the wall is necessary if the heat transferred to the air is to be found.

Reduction of the amount of cooling air necessary for high temperature turbine operation is of paramount importance. To achieve more efficient cooling, and to increase the power output of the turbine by reducing the deviation angle, the following can be done:

1. Utilize a convection-cooled skin segment on the suction side of the blade near the trailing edge. This would force all the cooling air through the pressure side and convectively cool the suction side. At the solid segment, the advantages of transpiration cooling will not be realized but the deviation angle will be at least as good as with solid blades.
2. Utilize a convection-cooled skin segment on the pressure side of the blade near the trailing edge. This would force all the coolant through the suction side. Inasmuch as there is less static gas pressure on the suction side, a lower coolant pressure level could be used than in case 1. The higher gas velocities prevalent in this area increase the heat transferred to the blade. Thus, the more complete cooling of this area as can be realized by the porous wall is desirable.
3. Partition the trailing edge so that each wall can be supplied with air according to its individual needs.

In lieu of the fact that turbine operating temperatures of 2500°F are contemplated, the use of the more efficient transpiration method of cooling is necessitated throughout. Moreover, the deviation line will be improved by virtue of the fact that there will be no gas passing through the blade trailing edge and the amount of coolant effusing through the skin will be optimized with resulting improvement in the uniformity of the skin temperature around the blade periphery. The adherence to alternative Number 3 is therefore recommended.

#### EFFECTS OF HOT GAS REYNOLDS NUMBER VARIATIONS

The peripheral variation of gas Reynolds number ( $\rho_2 v_2 x / \mu_2$ ) at weight flows of 1.65 lb/sec and 2.46 lb/sec is plotted in Figure 31. The data was taken at four hot gas temperatures ranging from 2027°R to 2480°R.

At a constant temperature the Reynolds number will increase with increasing values of weight flow. The excellent cooling characteristics that have been exhibited in this test can be attributed in part to this phenomenon of increasing Reynolds numbers. Since the coefficient of heat transfer from the gas to the blade varies with the Reynolds number to the .8 power, it can be concluded that less heat was actually transferred to the blade than if the Reynolds number remained constant. Additional data taken for geometrically identical blades cooled by various methods is necessary before a correlation could be made between the Reynolds number and the type of cooling employed. The effects of the coolant exiting through a porous wall on the boundary layer of gas are not exactly known. Because coolant film builds an insulating layer between the blade wall and the hot gas, and because this film is continuously renewed, the blade temperatures will be more uniform along the blade chord than if film cooling or convection cooling were employed. The insulating effect of a gas layer is good because these gases have a lower thermal conductivity than any other known insulating material. The tendency to decrease the transfer of heat from the hot gases to the blade surface is brought about by the continuous slow movement of the coolant away from the blade surface. New coolant, being continuously forced through the pores, maintains this flow. A counter flow is created between the heat flowing from the hot gases towards the blade surface and the cooling air flowing away. By continuously carrying away heat from the blade surface through convection, the cooling air decreases the over-all heat transfer to the surface.

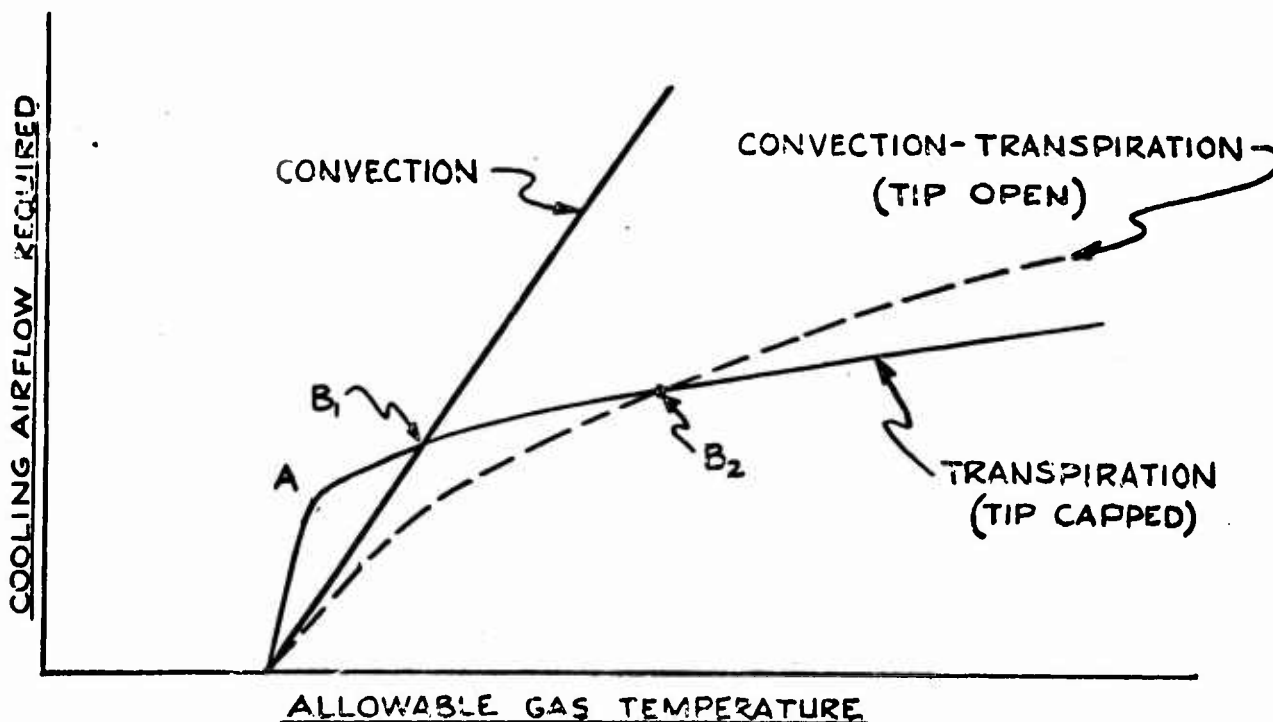
#### TRANSPIRATION-COOLED ROTOR BLADE

The transpiration-cooled rotor blade was tested in the hot gas cascade at gas temperatures up to 2510°R. The total time of 14 hours, 45 minutes was divided almost equally into two phases; first with the blade tip open; then, sealed. Upon completion of the test careful inspection revealed the blade was in perfect condition.

One of the important criterions by which cooling configurations are evaluated is the coolant flow required to achieve adequate heat removal relative to some datum. In engine tests, this datum is the total air flow delivered by the compressor, and the bleed is expressed as a percentage of this flow. As more bleed is demanded, total engine performance decreases. The benefits derived from high temperature operation are equated against the decrease in performance so that an optimum bleed can be chosen for maximum engine performance.

The cooling effectiveness in the cascade could be measured in two ways. Using the gas flow that is attained in a test engine as the datum by

which the cascade coolant flow is divided is an indication of the temperature which will exist in the engine (at the same per cent bleed and gas stream temperature). Since the strut is not affected by such gas flow parameters as Reynolds number, an idea of the amount of heat that can be removed from the strut by the coolant can be obtained. The variation of strut temperature with per cent coolant relative to engine gas flow (taken at 124 lb/sec) is shown in Figure 32 with gas temperature as a parameter. The flattening of the curves suggests that beyond a certain point additional cooling air does not appreciably lower the temperature of the strut. Since the rate of conduction of heat from the skin to the strut is a function of the difference in these temperatures, the cooler the strut, the more effective it is as a heat sink. Thus, as its temperature approaches that of the coolant, it gets exceedingly difficult to cool it further without excessive coolant flow. Figure 32 is plotted for the condition where the tip of the blade is uncapped. In addition to passing through the porous walls, air was permitted to exit axially at the blade tip. Following this test, the tip section was brazed forcing all the air through the porous walls. The philosophy here was to experimentally establish the temperature range in which transpiration cooling transcends convection cooling as the best available method. It is believed that below some temperature, and therefore, some coolant flow rate, convection cooling is more effective than transpiration cooling. Above this point there may be a transition range in which either method used separately is not as effective as both used simultaneously. At low coolant flows there may not be a sufficient air film on the blade surface to afford the full potential of transpiration cooling. The accompanying sketch shows that in order to run



at a given gas temperature, the flow required for adequate cooling is higher for transpiration cooled than it is for convection cooled configurations up to a break-even point. The point "A" shows the point at which the coolant flow has built up to that level which could sustain an insulating film. For higher temperatures comparatively small addition of coolant would be required. At steady state conditions the amount of heat removed in the purely convection cooled configuration is a direct function of the temperature difference between the metal and the coolant. Thus, at increased gas temperatures the heat removed increases proportionately. The break-even point in gas temperature above which it is more beneficial to use transpiration cooling techniques is at "B". For the condition in which the tip of the blade was open, the data taken shows better cooling effectiveness than for the capped configuration as evident by the curves in Figures 34 and 35.

The dotted line in the sketch, previous page, describes a condition which is believed to exist in a still unattainable temperature region.

It is thought that a porous-walled open-tipped blade would perform better than one of solid wall construction. This can be caused by the greater surface area and roughness in the porous-walled passage. Added to this is any small advantage that may occur due to the building up of the air film. At the flow which supports this "buffer" film, cooling characteristics will improve (dotted line). It is unlikely that such a blade will be effective at very high temperatures because there is not the complete washing of all the pores in the skin as occurs in the fully transpiration cooled blade. The data taken suggests that gas temperatures of 1600°F to 2050°F fall to the left of the second break-even point B<sub>2</sub>. In this area it is apparent that the combination of both methods is most efficient.

Transpiration cooling promises to be a very effective method of cooling objects in contact with high-temperature high-velocity gas streams. The cascade investigation reported herein confirms this. Comparison of the results of this analysis with that of a convection cooled configuration demonstrates the possibilities offered by transpiration cooling. Reference 10 reports the results of a full scale engine test in which strut supported impermeable airfoils were employed. At a gas temperature of 1650°F and 2% coolant flow, the skin temperature was 1250°F and the strut temperature was 990°F. For the rotor blade placed in the cascade of 2050°F gas temperature, 2% air flow cooled the skin to 800°F and the strut to 600°F. Although no justifiable conclusion can be deduced in the comparison of an engine test to a cascade test operating at far less weight flow, the potential of the cooling method is clearly seen. Figure 33 graphically illustrates the comparison. Here, again, there is an asymptotic approach of the metal temperature to the coolant temperature with increasing air flows. The engine test coolant flow demand is in terms of engine bleed percentage. Because the

heat transfer characteristics of the porous airfoil is affected by the magnitude of the gas mass flow, the cascade coolant demand is given relative to total cascade gas mass flow. The data for this figure was taken for a capped blade.

The leading edge skin temperatures at various gas temperatures are plotted in Figure 34. Coolant bleeds of 2% and 3.6% of engine total flow were used for both the capped and uncapped conditions. The steeper slope of the 3.6% line supports the existence of an optimum bleed. At this bleed it is seen that as high gas temperatures are reached there is only modest increase of leading edge metal temperature. At 2000°F gas temperature, the leading edge metal temperature was 50°F lower for the open tip than for the capped tip blade. To correlate the data in which the open tip configuration seemingly performed better than the capped tip, the curves in Figure 35 were plotted. As is expected, increase in the ratio of coolant to gas flow decreases the strut to gas temperature ratio. Again, with the addition of coolant, the rate of decrease of metal temperature tapers off to the extent that there is small advantage derived from additional bleed. The two curves plotted for 2005°F gas temperature seem to approach each other. This can be interpreted as evidence in support of the theory that the fully transpiration cooled blade will be more effective at the higher temperatures.

#### PERMEABILITY

Before and after the hot testing of each blade, a porosity calibration was performed so that any change in the permeability during a given hot test cycle could be measured. Because of the direct dependence of the air flow on permeability, the extent of variation of permeability with temperature was desired. Figure 36 is a plot of the total coolant flow versus plenum chamber pressure for two blades of slightly different permeabilities. Data, taken before and after the test, with the skin hot, and at room temperature, shows there is no appreciable change in the permeability during 9 hours and 35 minutes ( $\frac{k}{\mu} = 1.51 \times 10^{-10}$  ft.) and 4 hours and 35 minutes ( $\frac{k}{\mu} = 1.31 \times 10^{-10}$  ft.) of high temperature testing. Moreover, the permeability, and therefore, the average effusion rate, was not affected by the change in the skin temperature from 70°F to approximately 600°F. The five micron filter placed in the coolant supply line appears to have performed satisfactorily.

It should be pointed out that the coolant flow rate necessary to maintain a predetermined wall temperature is a function of gas Reynolds number, the gas temperature, and the coolant temperature. It is not directly dependent upon the wall permeability. However, once the coolant supply pressure is established, the coolant flow is metered by the effective orifice

offered by the permeable wall.

Close control and inspection of the permeability of porous material is necessary. This is illustrated by the fact the calculated values of  $k/\lambda$  are less by factor of  $2\frac{1}{2}$  -  $3\frac{1}{2}$  than those specified for the fabrication of the cascade blades (  $k/\lambda = 4.6 \times 10^{-10} \text{ft.}$  ).

#### COMPARISON OF CALCULATED AND MEASURED GAS TEMPERATURES

Upon completion of the report outlining the design procedure (Curtiss-Wright Research Division Report No. 300-37) it was decided to utilize the IBM 704 computer to calculate the wall temperatures that would result at a given set of gas temperature, coolant flow, and gas mass flow conditions. The actual input values were taken from three points run on the cascade. Comparison of the wall temperatures measured in the cascade with the temperatures predicted by the computer was made. The cascade running points selected were at measured gas temperatures of 2210°R, 2027°R, and 2362°R. The skin temperatures at these points varied between 1350°R and 1950°R. At the 2362°R point the gas flow was 2.46 lb/sec; flow at the other two points was 1.64 lb/sec.

In a check out procedure such as this it is desirable for the mathematical method to be entirely and independently hypothetical and for the experimental phase to be comprised of physical data. However, a departure from the rigid comparison was necessary because heat transfer characteristics depend on boundary conditions and assumption of these boundary conditions in the theoretical approach could be very inaccurate. Therefore, a verification of the solutions obtained from the design method based upon the static pressure profiles measured in the cascade section was attempted. Any inaccuracy in the static pressure measuring taps and total pressure probes would throw the calculations off. Errors in flow measurement devices were no doubt present in the experimental method. The solutions for turbulent boundary-layer heat transfer equations are not exact; consequently, some of the assumptions under which the equations were derived may not be completely valid. Another factor is the accuracy with which the local cooling air flow rates could be determined. These may be slightly inaccurate because the local static pressure around the outside of the blade was obtained by a tap brazed to the wall from the inside. This immediate vicinity, therefore, was impermeable. Notwithstanding these very plausible reasons for deviation of results between the two approaches, the temperatures of the wall as calculated, fall on the average within 15% of the measured temperatures.

The blade wall temperatures were measured at eight chordwise positions, three spanwise positions, three different gas temperatures, and two gas flows. The comparison of a portion of this varied sampling of data with the calculated values is shown in Figure 37. A 45° line has been drawn on the figure. If the temperature points fall on this line, perfect agreement between calculated and measured values is indicated. In the curve there appears to be no correlation between the gas temperature and the agreement obtained. There exists a 15% tolerance on both sides of the line of perfect agreement along the entire range of test temperatures.

In the process of determining the blade wall temperatures, there are other check points that are available. Agreement of the gas Reynolds numbers and coolant flow per passage between the calculated and measured values was good. It cannot be over emphasized that the calculation method will give dependable data provided the aerodynamic engine data that is predicted will actually prevail.

#### TURBINE PERFORMANCE

The final measure of the effectiveness of turbine cooling is the performance of the engine in which it is utilized. Utilization of the best available heat-transfer data for the outside and the inside of the cooled blade should be made. The coolant flow requirements for the anticipated range of operating conditions imposed on the turbine are then determined. These operating conditions are functions of the turbine configuration, turbine inlet temperature, turbine speed, compressor pressure ratio, flight Mach number, and altitude. The last factor must be considered because of the significant effect it has on coolant requirements and losses. The principal factors to be considered are the thermodynamic effects of heat loss, friction, the internal pumping in the flow passages, the external pumping before bleed off, the decrease in mass flow through the turbine, and the mixing of the coolant with the working fluid. The summation of these effects in a turbojet engine is a decrease in jet nozzle inlet temperature and pressure, which adversely effects performance of the engine.

The results of this cascade test indicate that for the very high gas temperature contemplated, transpiration cooling techniques shall appreciably further the state of jet engine technology.

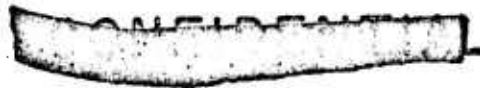
APPENDIX

NOMENCLATURE

The following nomenclature is used in this report:

A	Flow area, sq. ft.
a	Acoustic velocity, ft/sec.
B	$\left(\frac{k}{\lambda}\right) \frac{1}{\mu T_w}$
C <sub>K</sub>	Quantity containing permeability coefficient, $\frac{Lb(ft^4)^n}{Sec(ft^2)(Lb^2)^n}$
C <sub>n</sub>	Orifice flow coefficient
C <sub>p</sub>	Specific heat at constant pressure, BTU/lb <sup>o</sup> F
C <sub>v</sub>	Specific heat at constant volume, BTU/lb <sup>o</sup> F
D <sub>h</sub>	Hydraulic diameter of coolant passage, ft.
E <sub>u</sub>	Euler number of gas flow over blade, $\frac{x}{v_g} \frac{dv_g}{dx}$
f	Cooling passage friction factor
f <sub>w</sub>	Coolant flow parameter for laminar flow region
g	Gravitational constant, ft/sec <sup>2</sup>
K	Constant based upon units used
k	Permeability coefficient, sq. ft.
m	Mass coolant flow, lb/sec.
M <sub>n</sub>	Mach number
N	$\left[ \frac{\left(\frac{P_s}{P_t}\right)^{\frac{\gamma}{\delta}} - \left(\frac{P_s}{P_t}\right)^{\frac{\gamma+1}{\delta}}}{\left(\frac{2}{\gamma+1}\right)^{\frac{\gamma}{\delta-1}} - \left(\frac{2}{\gamma+1}\right)^{\frac{\gamma+1}{\delta-1}}} \right]^{\frac{1}{2}}$
Pr	Prandtl number
P <sub>s</sub>	Static pressure, lb/sq. ft. abs. except when noted otherwise

$P_t$	Total pressure, lb/sq. ft. abs. except when noted otherwise
$Q$	Weight flow rate, lb/sec. or as noted
$R$	Gas constant, ft-lb/lb <sup>o</sup> F
$Re$	Reynolds Number based on combustion gas properties, $\frac{\rho v x}{\mu}$
$r$	Radius, ft.
$T_{ad}$	Adiabatic gas temperature, <sup>o</sup> R
$T_s$	Static temperature, <sup>o</sup> F or <sup>o</sup> R as noted
$T_t$	Total temperature, <sup>o</sup> F or <sup>o</sup> R as noted
$v$	Velocity, ft/sec.
$x$	Peripheral distance along blade surface from leading edge to particular station being investigated, ft.
$\beta$	Angle between blade axis and rotor radius sector
$\gamma$	Specific heat ratio, $\frac{C_p}{C_v}$
$\mu$	Absolute viscosity, lb/sec. ft.
$\rho$	Density, lb/cu. ft.
$\omega$	Angular velocity, sec <sup>-1</sup>
$\delta$	Thickness of porous material, ft.



C.W.R. REPORT NO. 300-39

SUBSCRIPTS

- a Denotes cooling air while inside blade passage
- b Compressor bleed air upstream of turbine blade
- c Denotes cooling air while in skin pores
- g Combustion gas
- B-B Indicates section just upstream of cascade blades
- D-D Indicates section just downstream of cascade blades
- n Orifice
- r Turbine Blade Root
- w Porous blade wall
- x Local (Refers to condition at distance x from leading edge in direction of gas flow)
- y Spanwise distance in coolant passage from blade root, ft.
- 1,2,3,.....8 Specific stations around blade periphery



REFERENCES

1. Schafer, Louis J., Bartoo, Edward R., and Richards, Hadley T.: Experimental Investigation of the Heat-Transfer Characteristics of an Air-Cooled Sintered Porous Turbine Blade. NACA RM E51K08, 1952.
2. Donoughe, Patrick L., and McKinnon, Roy A.: Experimental Investigation of Air-Flow Uniformity and Pressure Level On Wire Cloth For Transpiration-Cooling Applications. NACA TN 3652, 1956.
3. Salamone, J. J.: Design Procedure for Transpiration - Cooled Strut Supported Turbine Rotor Blades. Curtiss-Wright Research Division Report No. 1, Project XC-788, 1956.
4. Lewis Laboratory Computing Staff: Tables of Various Mach Number Functions for Specific Heat Ratios from 1.28 to 1.38. NACA TN 3981, April, 1957.
5. Weinbaum, S., and Wheeler, H. L., Jr.: Heat Transfer in Sweat Cooled Porous Metals. Progress Report No. 1-58, Air Laboratory, Project No. MX121, Jet Propulsion Laboratory, C.I.T., April 8, 1947. (AMC Contract No. W-535-ac-20260, Ordinance Department Contract No. W-04-200-ORD-455).
6. Lang, Ronald, and Petrick, Ernest: Application of Electrical Analog Theory in the Preliminary Analysis of Air-Cooled Turbines - Proposed ASME Paper, Unreleased.
7. Lang, Ronald, and Lloyd, Wallis A.: Design Procedure for Transpiration-Cooled Gas Turbine Blades. Curtiss-Wright Research Division No. 300-37.
8. Prasse, Ernest I., and Livingood, John N.B.: Design Procedure for Transpiration-Cooled Strut-Supported Turbine Rotor Blades. NACA RM E55J21 December 19, 1955.
9. Esgar, Jack B., and Richards, Hadley T.: Evaluation of Effects of Random Permeability Variations on Transpiration-Cooled Surfaces. NACA RM E53G16 November 30, 1953.
10. Lauziere, N.: Final Report - Cooled Turbine Blades, Curtiss-Wright Corporation, Wright Aeronautical Division Serial Report No. 1958, Contract No. AF 33(600)-22759, January 10, 1955.
11. Lauziere, N., and Kump, D.J.: Final Report - Transpiration-Cooled Turbine Blades, Curtiss-Wright Research Report No. 300-38, December 1958.

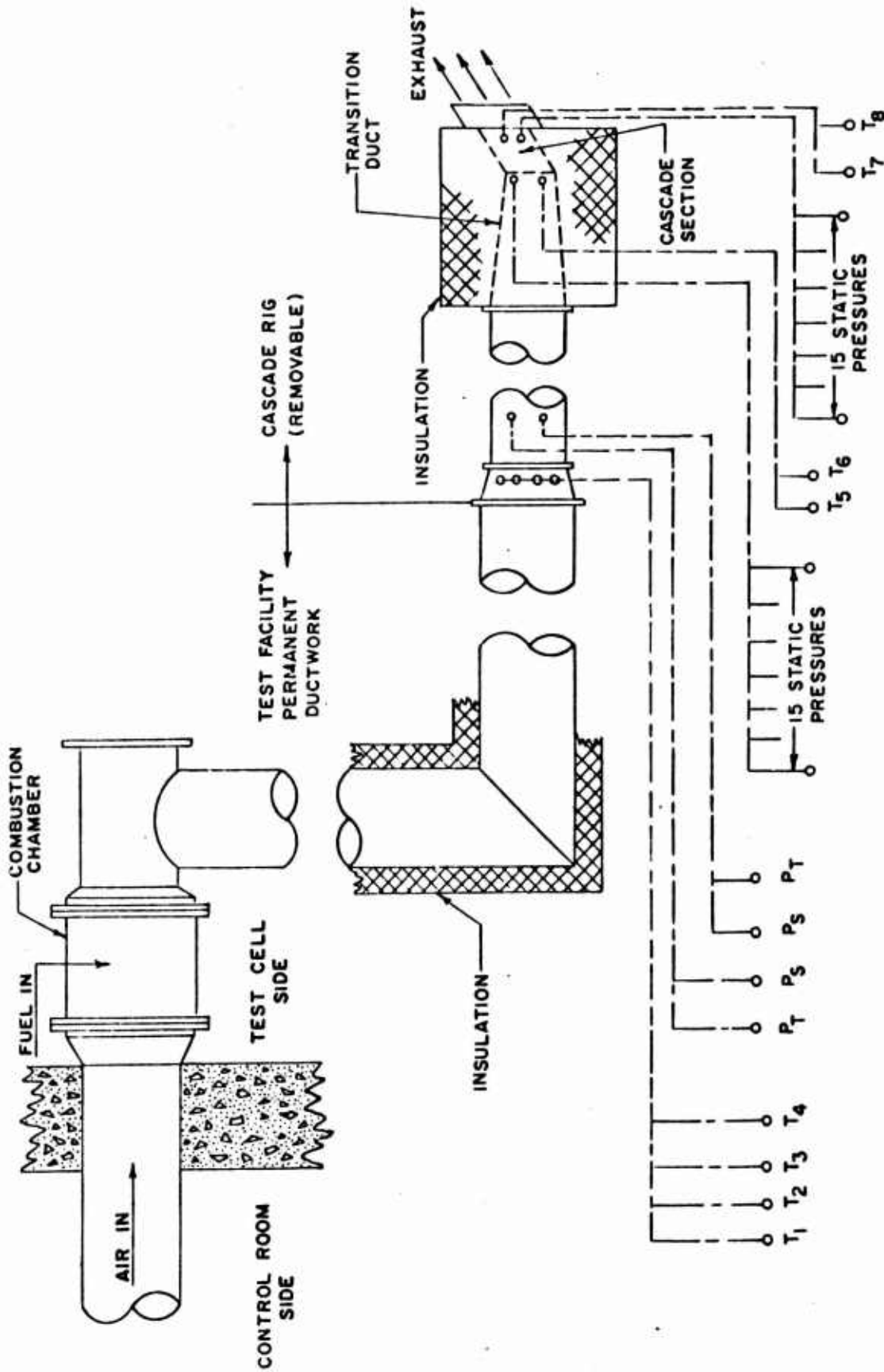


Figure 1. ELEVATION SCHEMATIC  
CASCADE RIG INSTALLED ON TEST FACILITY

~~CONFIDENTIAL~~

C.W.R. REPORT NO. 300-39

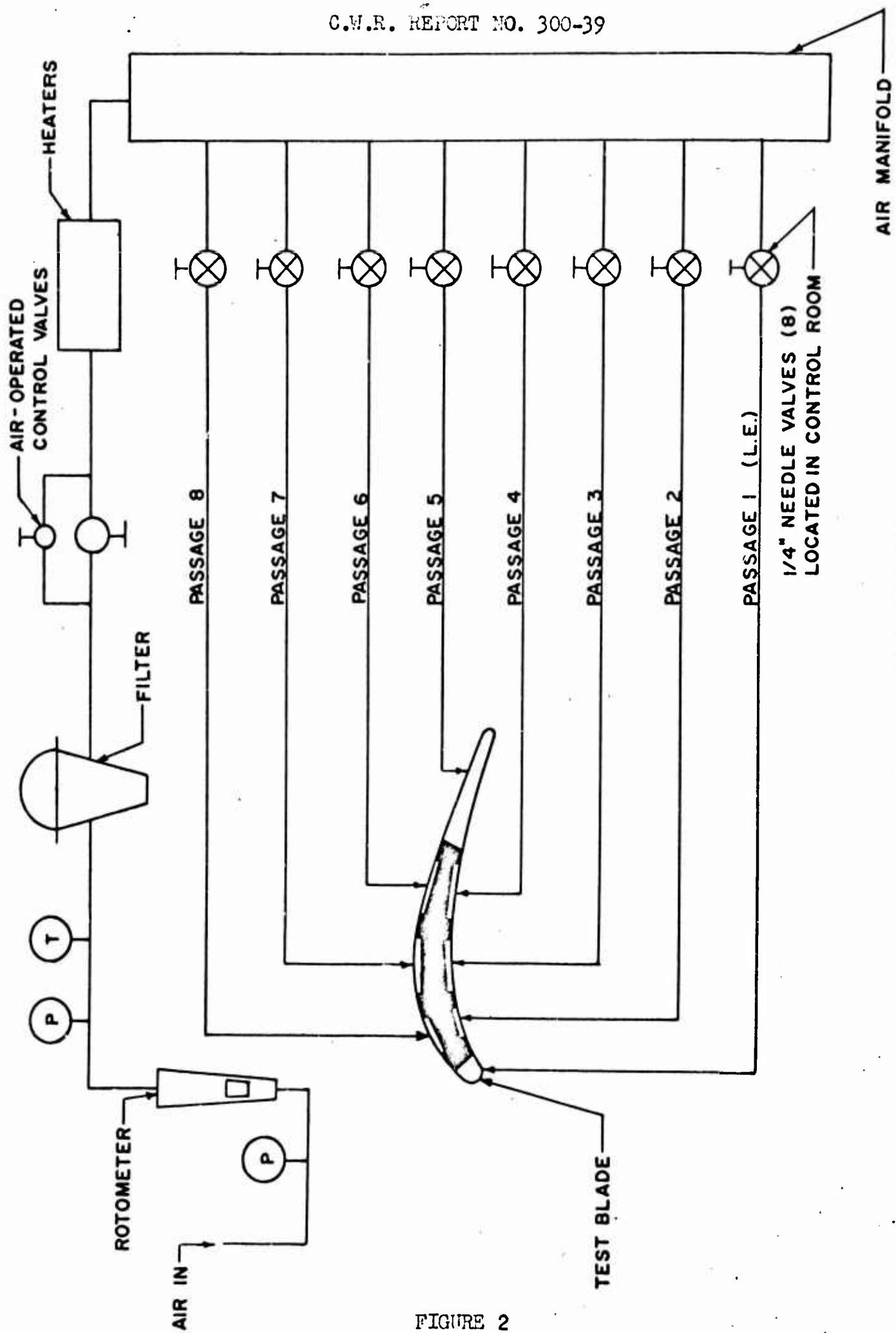


FIGURE 2

~~CONFIDENTIAL~~

FIG. 16 AIR SUPPLY  
FLOW DIAGRAM

**CONFIDENTIAL**

C.W.R. REPORT NO. 300-39

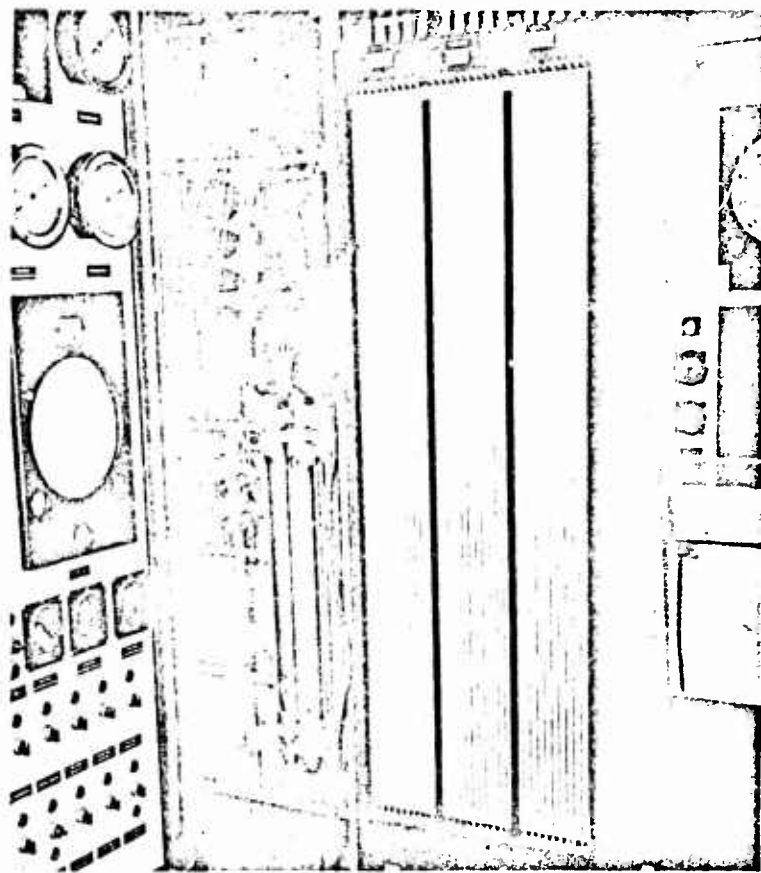


FIG. 3

VIEW OF THE 8 COOLANT CONTROL VALVES AND 3 BANKS OF MERCURY MANOMETERS WHICH MEASURED STATIC PRESSURE.

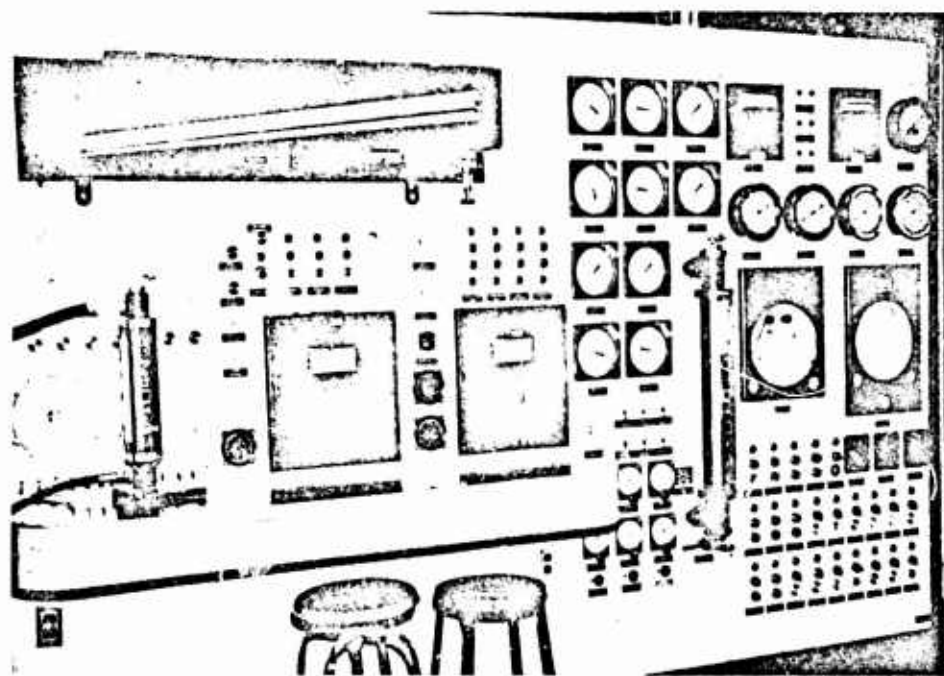


FIG. 4 VIEW OF CONTROL ROOM

AT LEFT ON DESK IS COOLING AIR ROTOMETER. AT EXTREME RIGHT IS 100 INCH MANOMETER USED AS A CHECK ON ROTOMETER. UPPER LEFT - INCLINOMETER FOR MAIN FLOW MEASUREMENT. ROTOMETER TO RIGHT OF DESK MEASURED FUEL FLOW. TWO BLACK PANELS ABOVE DESK ARE THE C/A AND I/C BROWN POTENTIOMETERS.

**CONFIDENTIAL**

~~CONFIDENTIAL~~

C.W.R. REPORT NO. 300-39

FLANGE CONNECTING TO B DUCT

SECTIONAL VIEW OF TRANSPIRATION COOLED CASCADE RIG

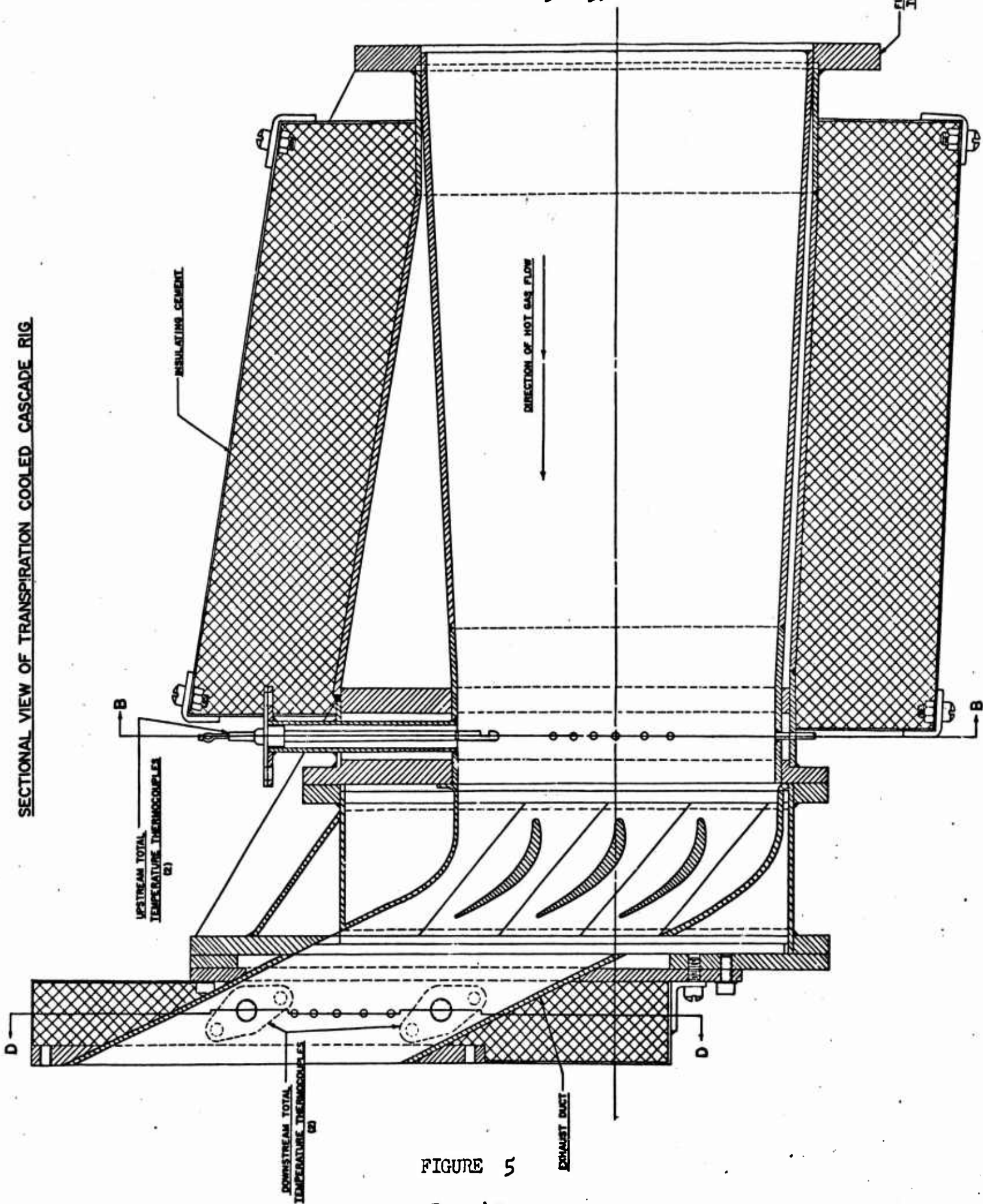


FIGURE 5

~~CONFIDENTIAL~~

PITCH	$\frac{1.883''}{1.743''}$
CHORD	2.43''
SOLIDITY	1.34
ANGLE OF INCIDENCE	0°

64° 24'

64° 24'

GAS FLOW

41° 12'

6.71''

POROUS TEST BLADE

WATER COOLED  
WORKHORSE BLADES (2)

FIGURE 6  
CASCADE GEOMETRY

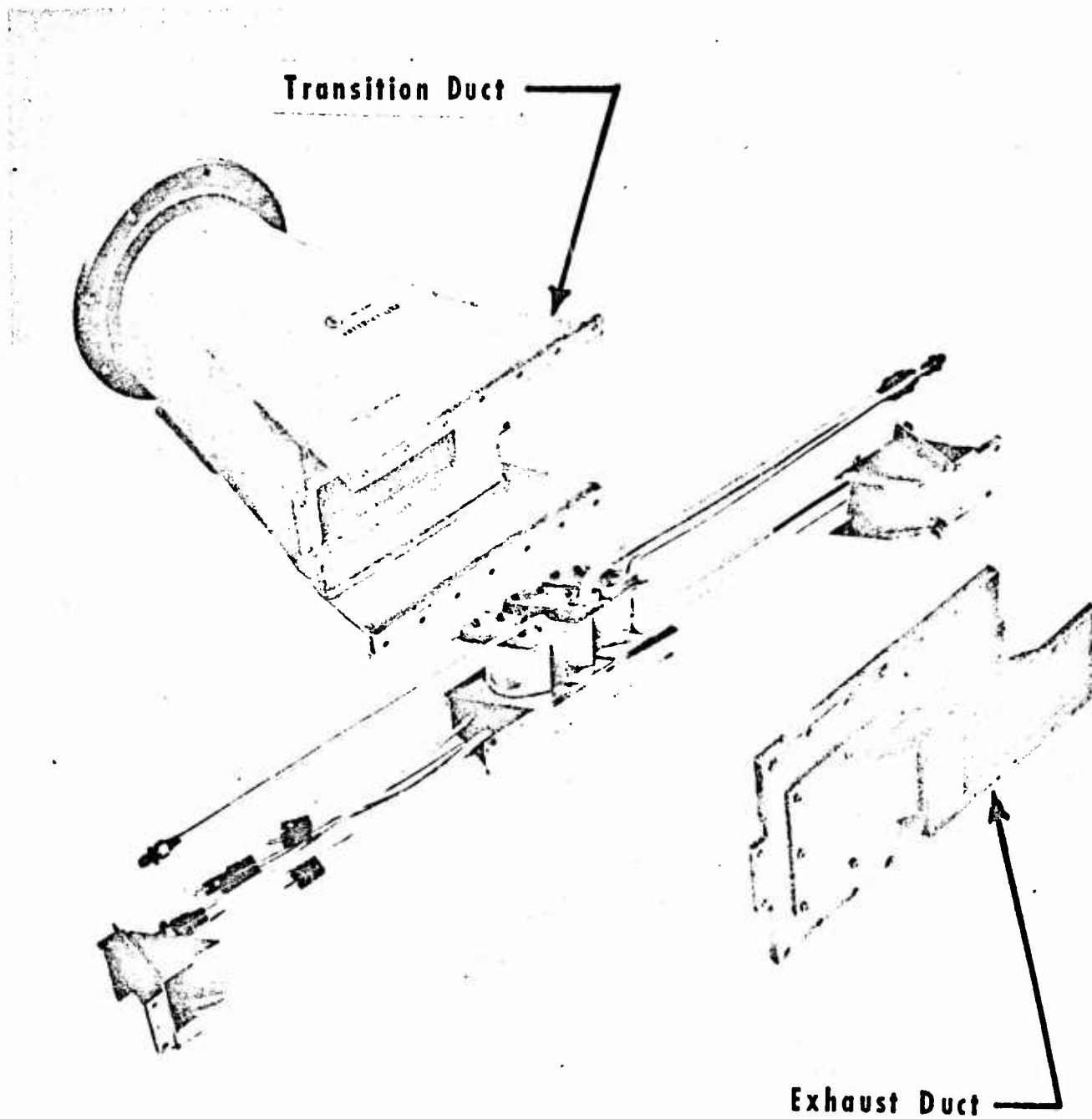


FIG. 7 EXPLODED VIEW OF CASCADE RIG ADAPTING PARTS.  
INSULATION ON TRANSITION DUCT NOT SHOWN.

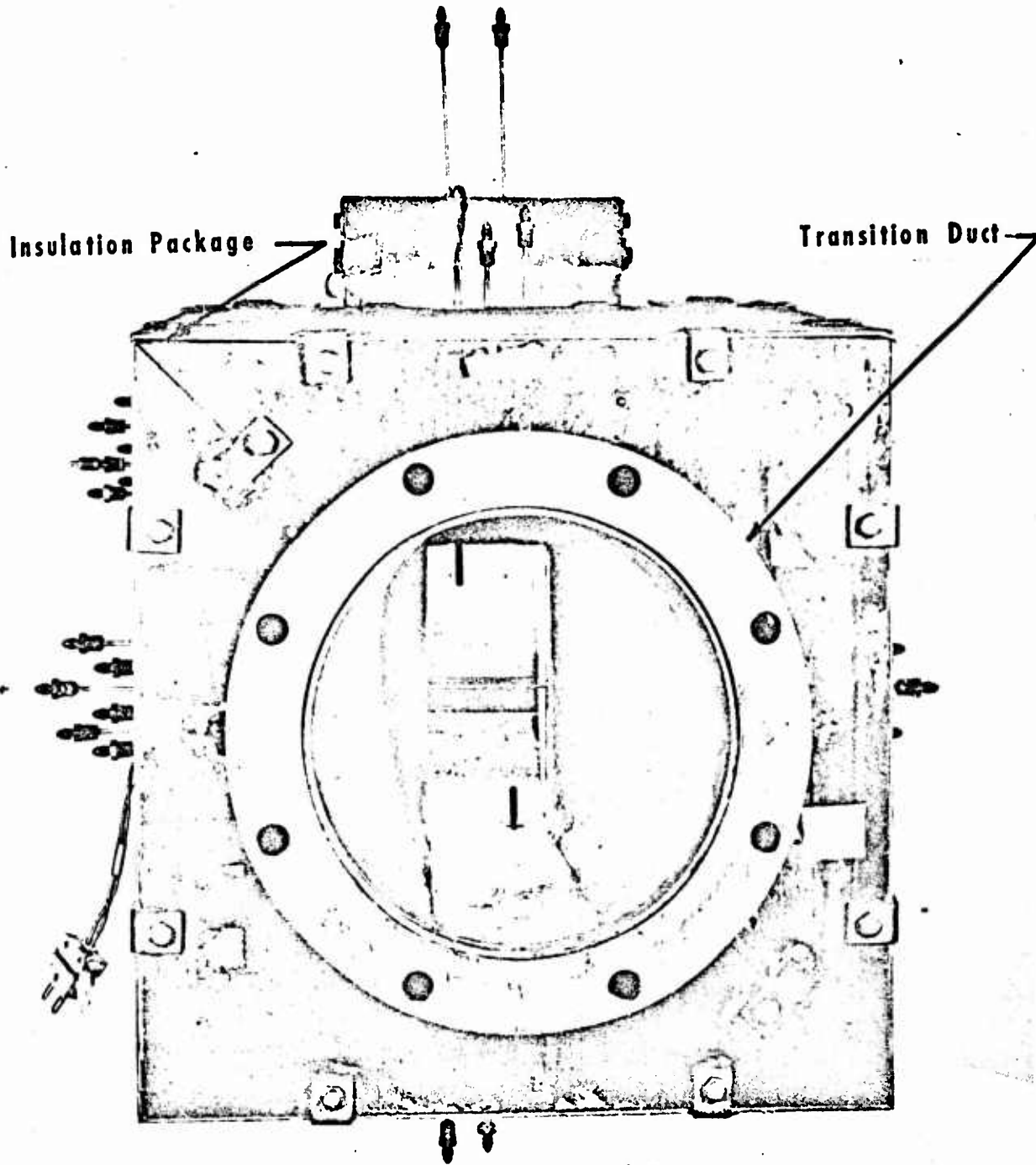
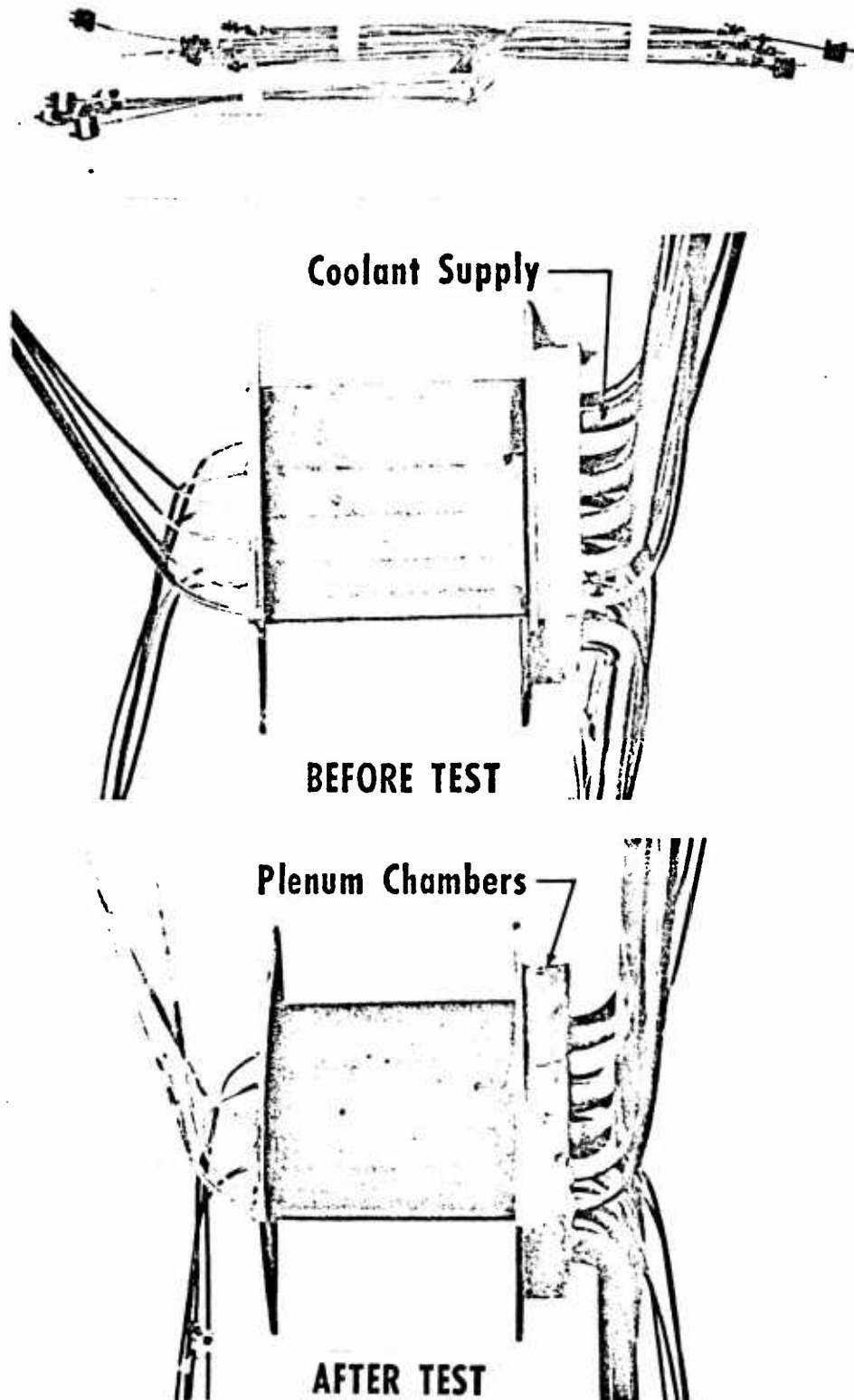


FIG. 8 VIEW LOOKING DOWNSTREAM INTO CASCADE HOUSING.

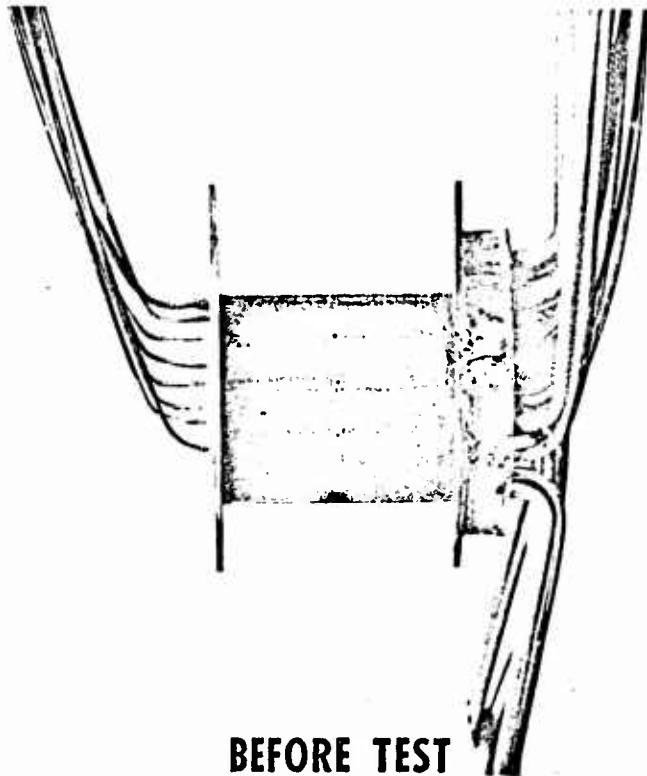
BLADES ARE NOT INSTALLED.



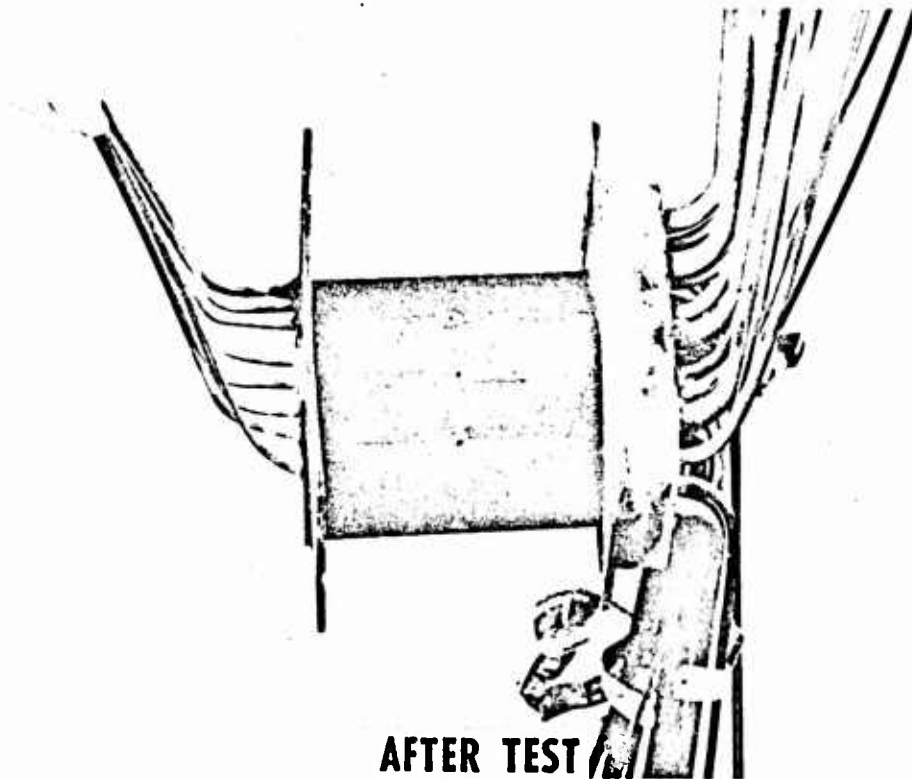
**FIG. 9**  
**TOP; OVERALL VIEW OF TEMPERATURE INSTRUMENTED BLADE**  
**PART NUMBER R11002IN-1. CENTER AND BOTTOM; BEFORE AND**  
**AFTER VIEWS OF CONCAVE SIDE. IN BOTTOM PHOTO NOTE HOLE**  
**FROM WHICH THERMOCOUPLE JUNCTION WAS BLOWN OUT.**

~~CONFIDENTIAL~~

C.W.R. REPORT NO. 300-39



BEFORE TEST



AFTER TEST

**FIG. 10**  
**CONVEX SIDE OF PRESSURE-INSTRUMENTED TEST CASCADE BLADE**  
**PART NUMBER R110031 SHOWN BEFORE AND AFTER TEST. NOTE**  
**STATIC PRESSURE TAPS AT MIDSPAN. LONGITUDENAL BEADS**  
**RESULTED FROM THE TRAVERSE OF THE RESISTANCE WELDING HEAD.**

~~CONFIDENTIAL~~

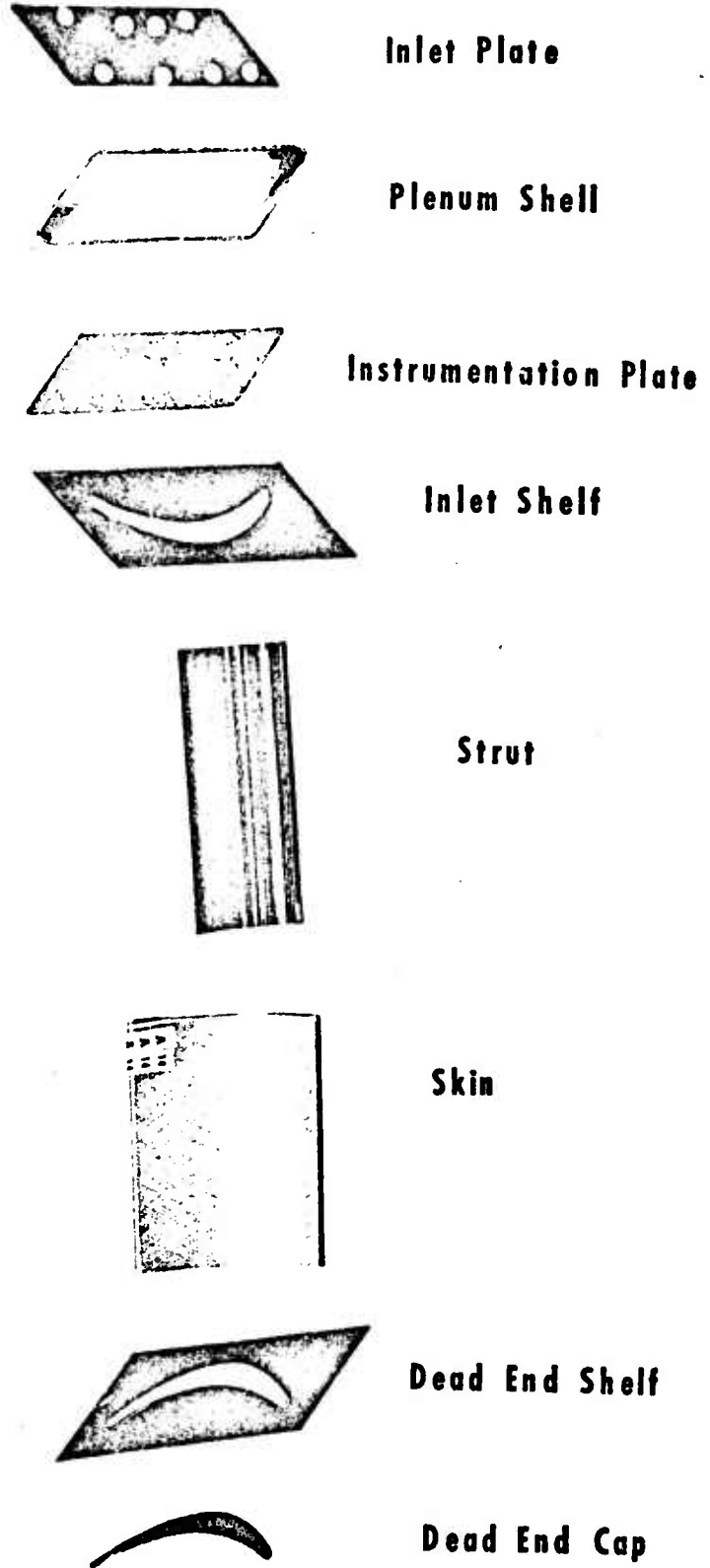
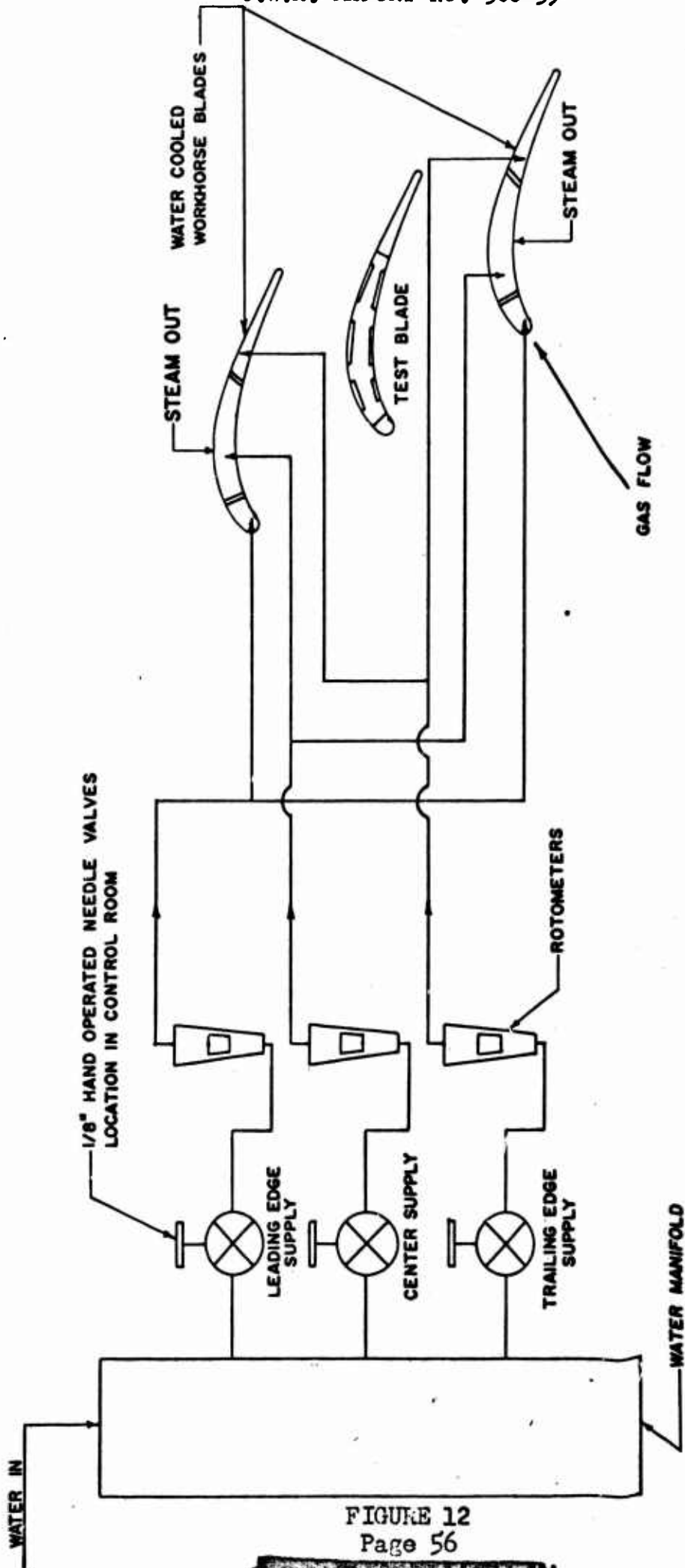


FIG. 11 EXPLODED VIEW OF A CASCADE BLADE ASSEMBLY

~~CONFIDENTIAL~~

C.W.R. REPORT NO. 300-39



COOLING WATER SUPPLY  
FLOW DIAGRAM

FIGURE 12  
Page 56

~~CONFIDENTIAL~~

~~CONFIDENTIAL~~

C.W.R. REPORT NO. 300-39

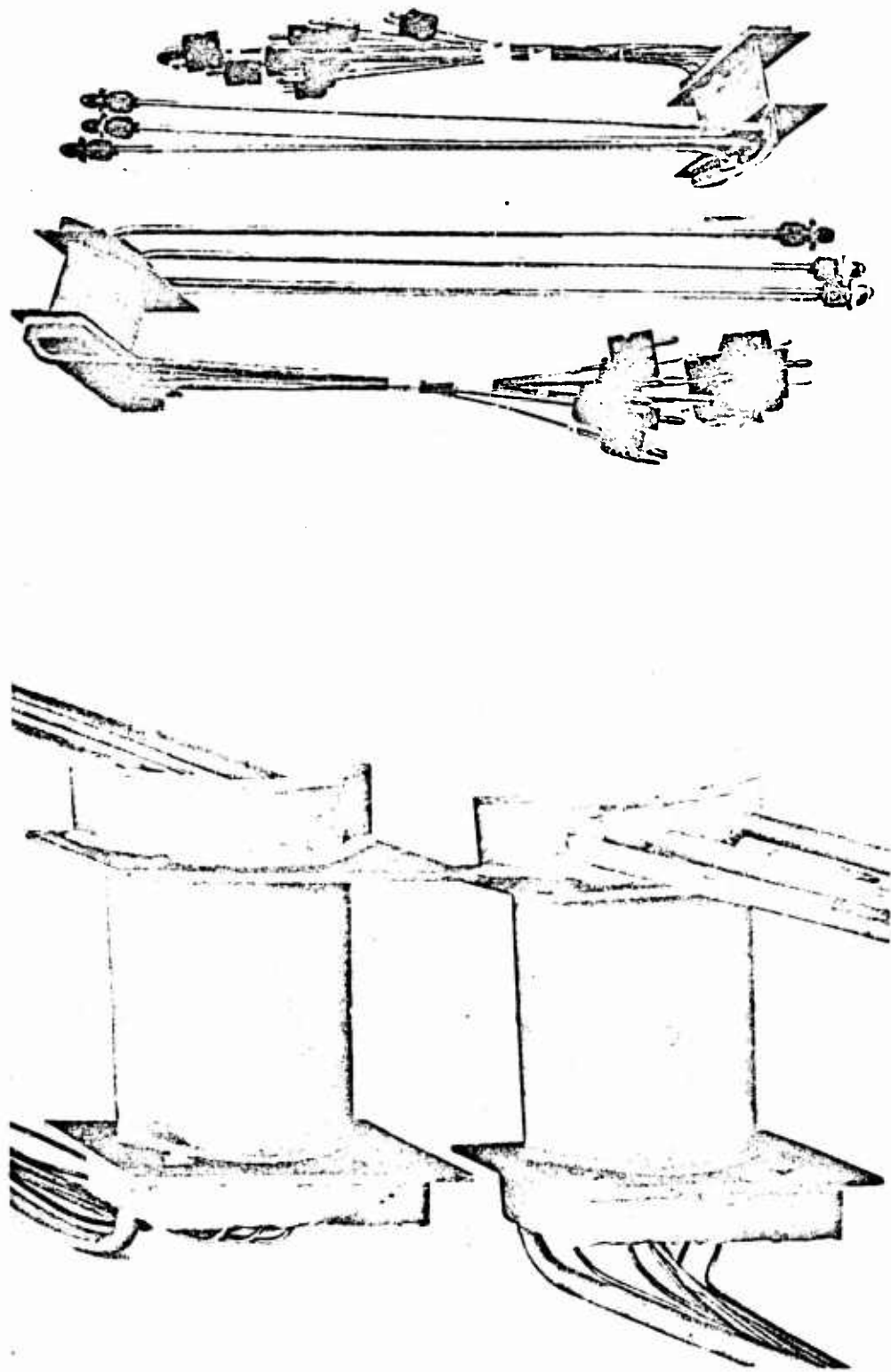


FIG. 13 WATER-COOLED WORKHORSE CASCADE BLADES

~~CONFIDENTIAL~~

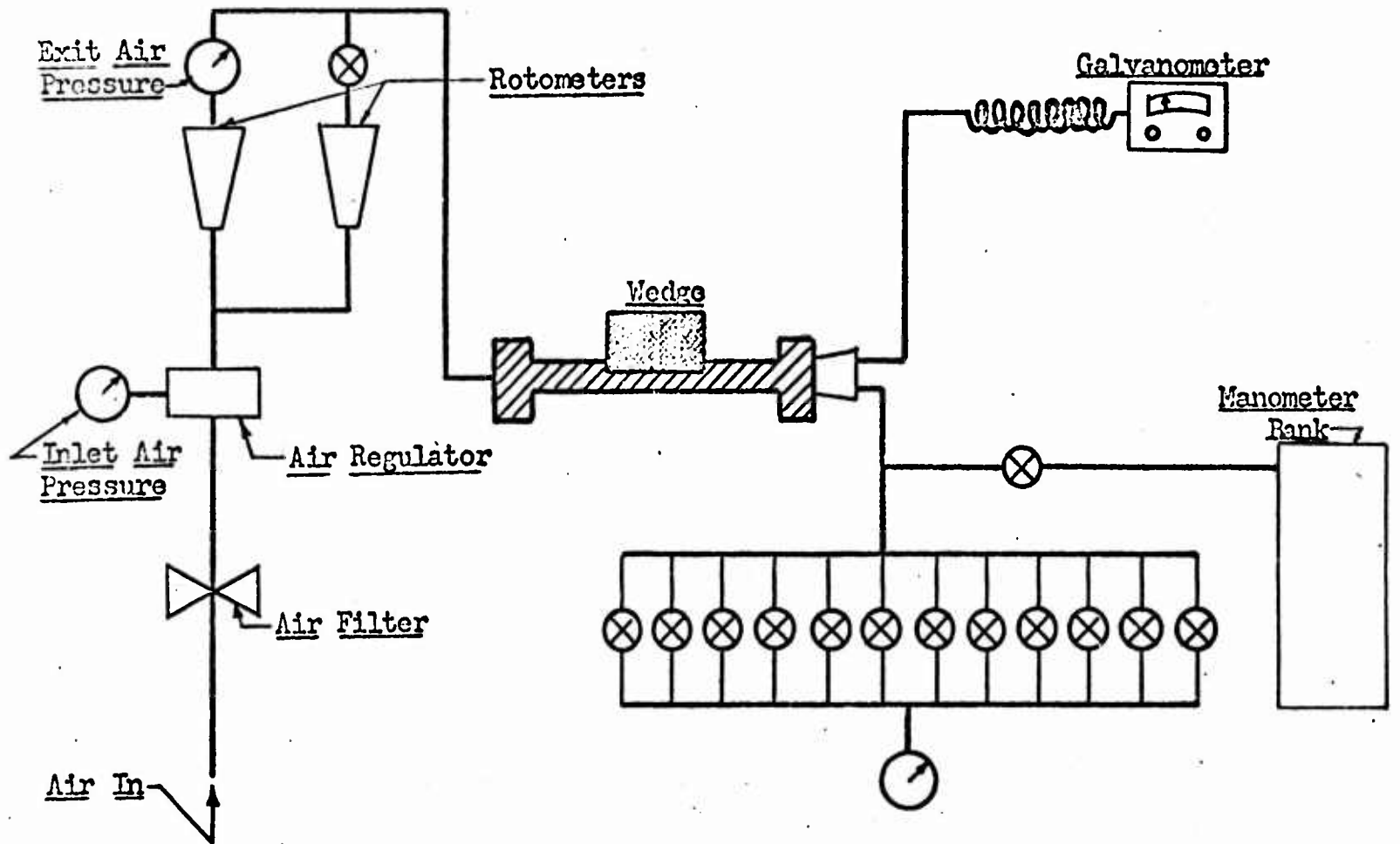


Fig. 14 FLOW DIAGRAM OF POROUS WEDGE TEST SET-UP

~~CONFIDENTIAL~~

C.W.R. REPORT NO. 300-39

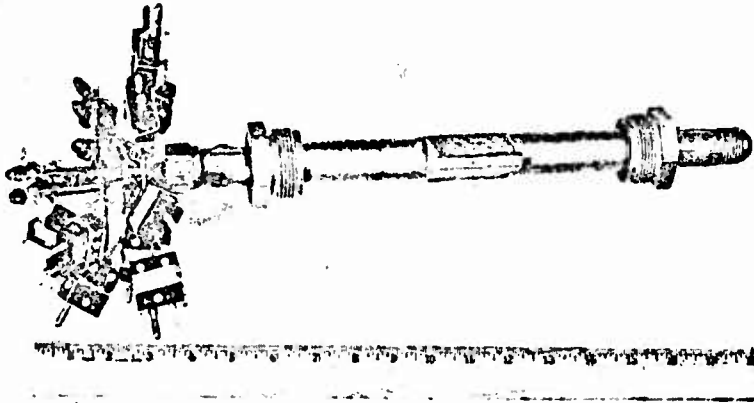


FIG. 15      POROUS WEDGE ASSEMBLY

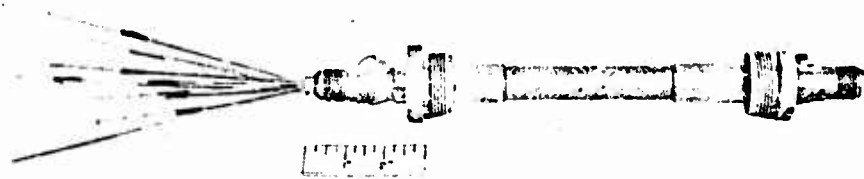
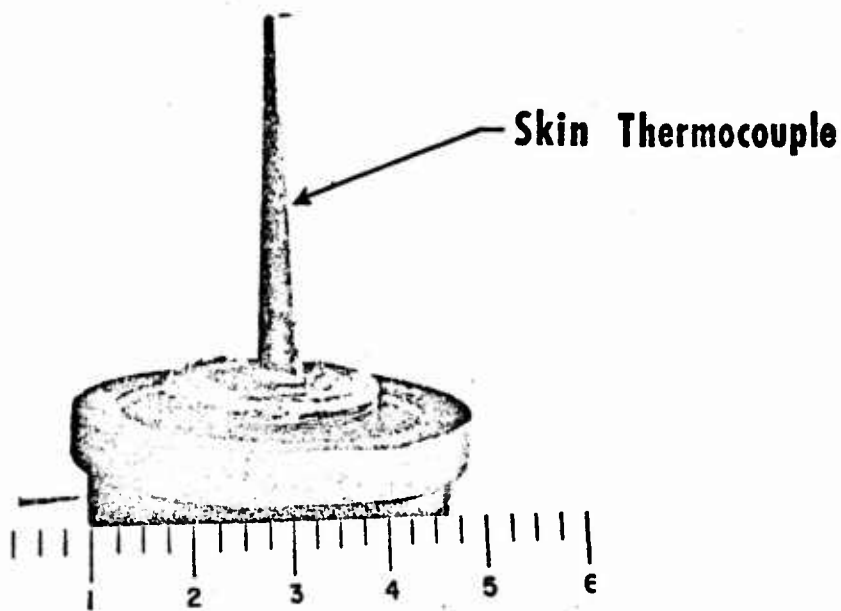
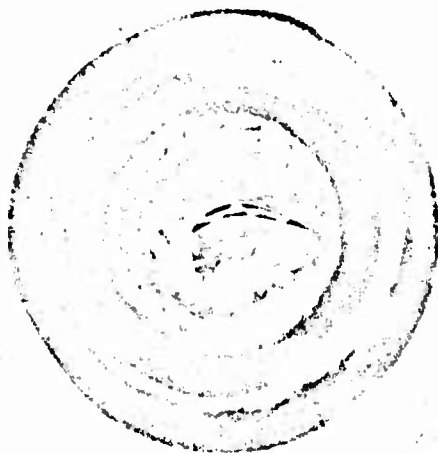


FIG. 16      POROUS TUBE ASSEMBLY

~~CONFIDENTIAL~~

~~CONFIDENTIAL~~

C.W.R. REPORT NO. 300-39



Skin Thermocouple

FIG. 17

OVER-ALL TEST ASSEMBLY, CLOSE-UP OF OPEN TIP SECTION, & FRONT VIEW OF TRANSPIRATION COOLED J-65 TURBINE ROTOR BLADE, BEFORE TEST.

~~CONFIDENTIAL~~

~~CONFIDENTIAL~~

C.W.R. REPORT NO. 300-39

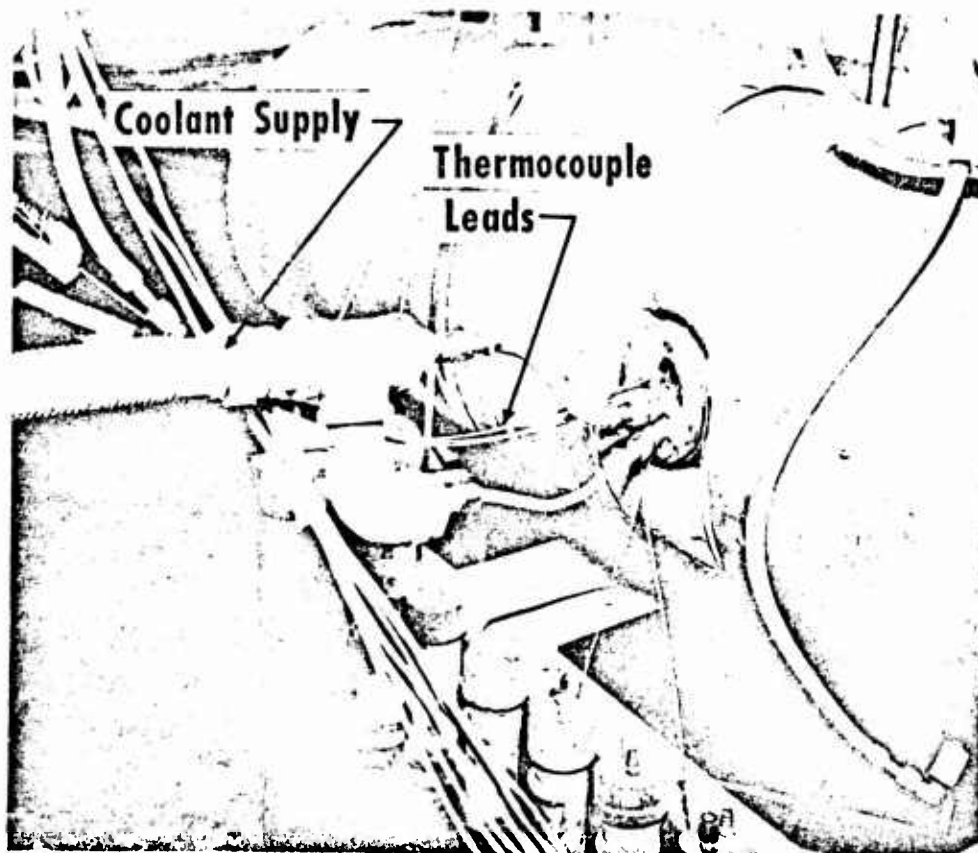
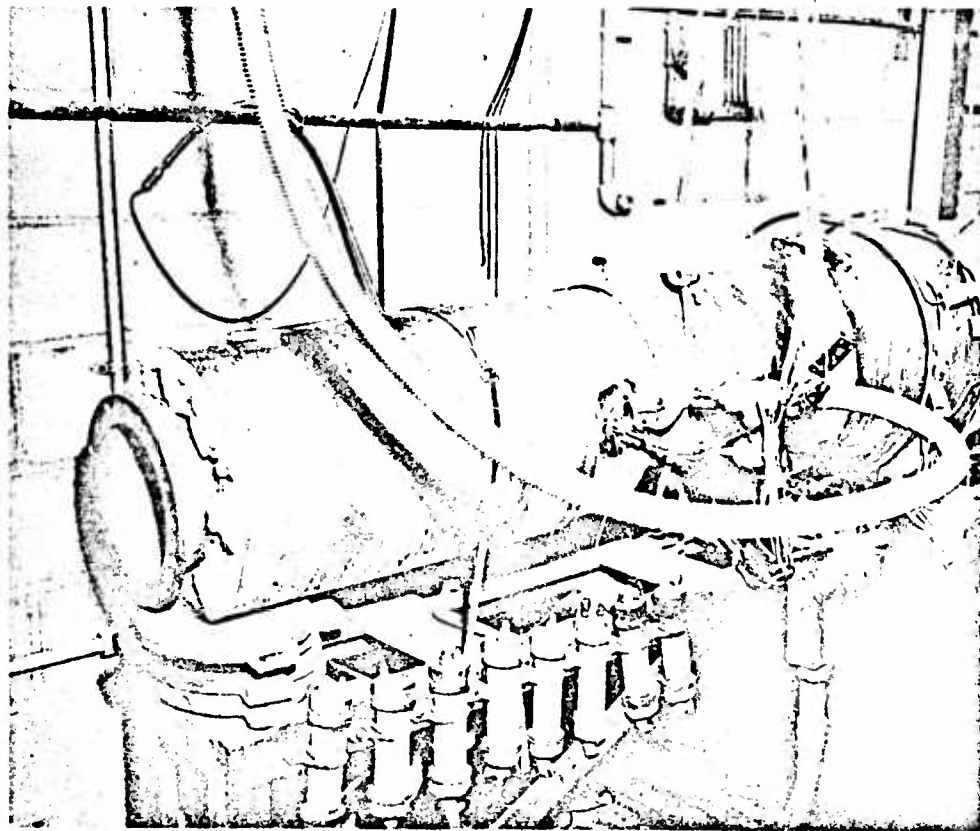


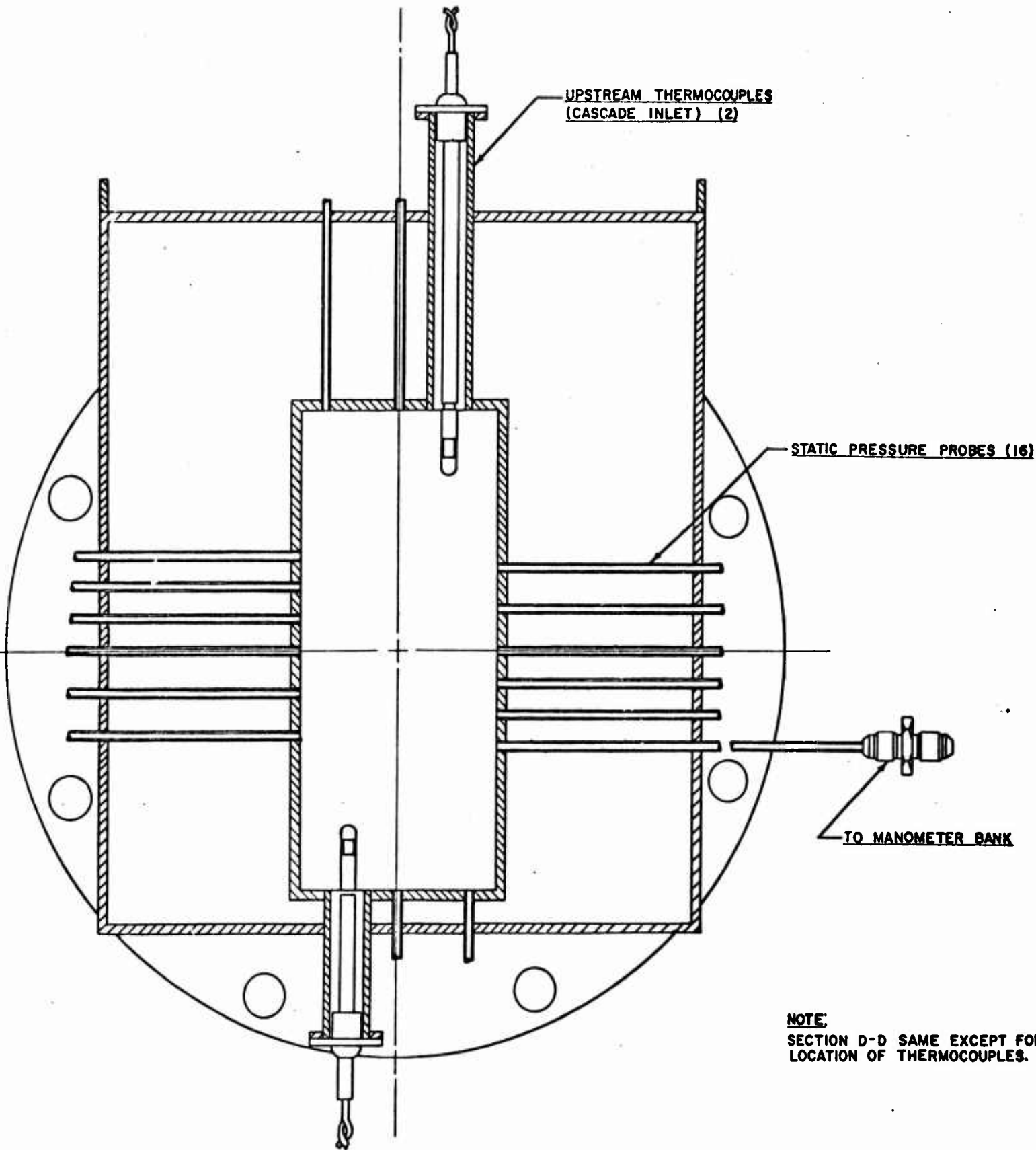
FIG. 18 TWO VIEWS OF TRANSPIRATION COOLED ROTOR BLADE INSTALLED IN RIG.

~~CONFIDENTIAL~~

~~CONFIDENTIAL~~

C.W.R. REPORT NO. 300-39

SECTION SHOWING INSTRUMENTATION SET-UP AT CASCADE INLET



SECTION B-B

FIGURE 19

~~CONFIDENTIAL~~

**CONFIDENTIAL**

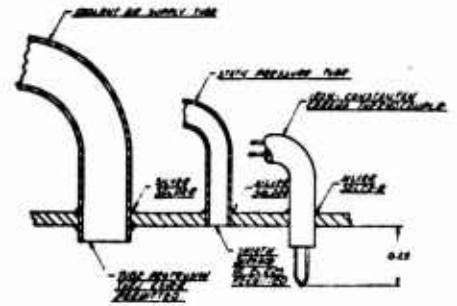
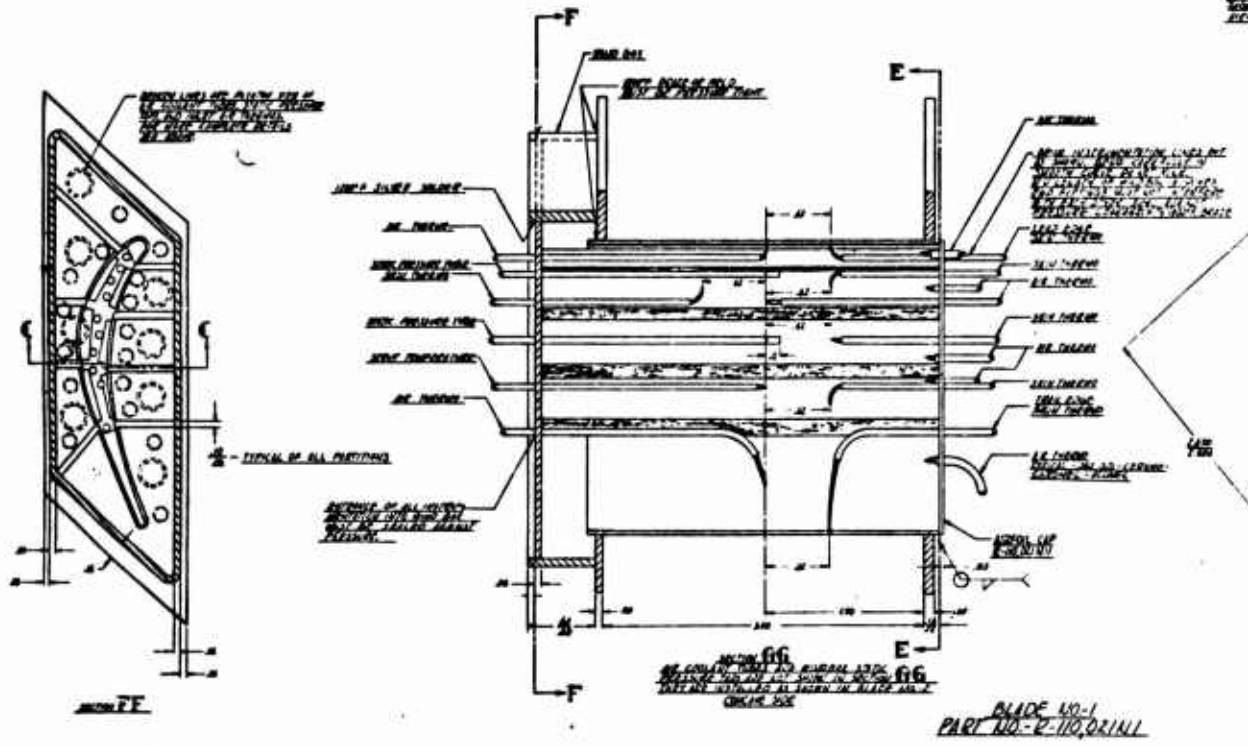
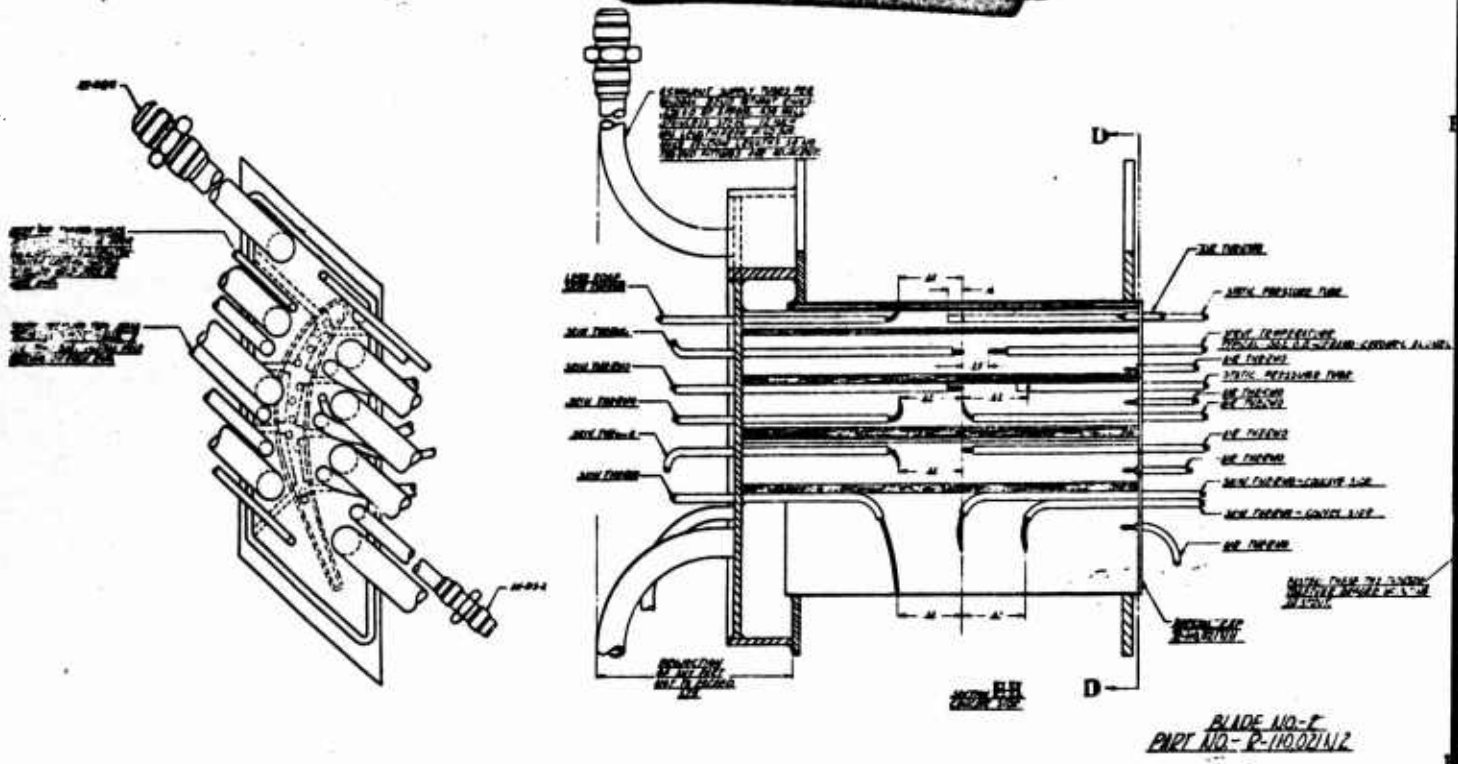
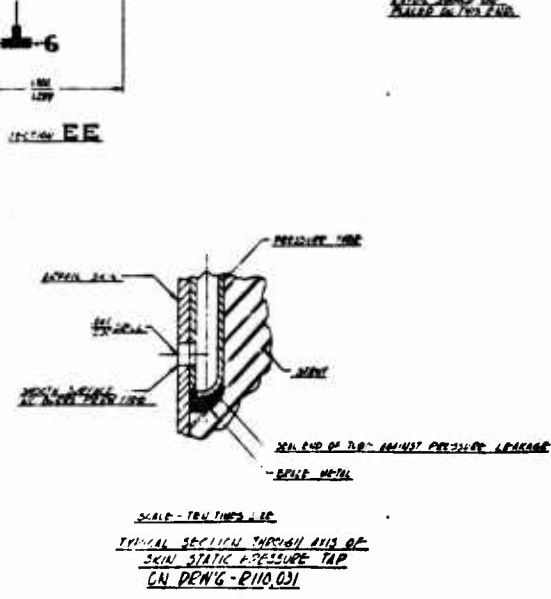
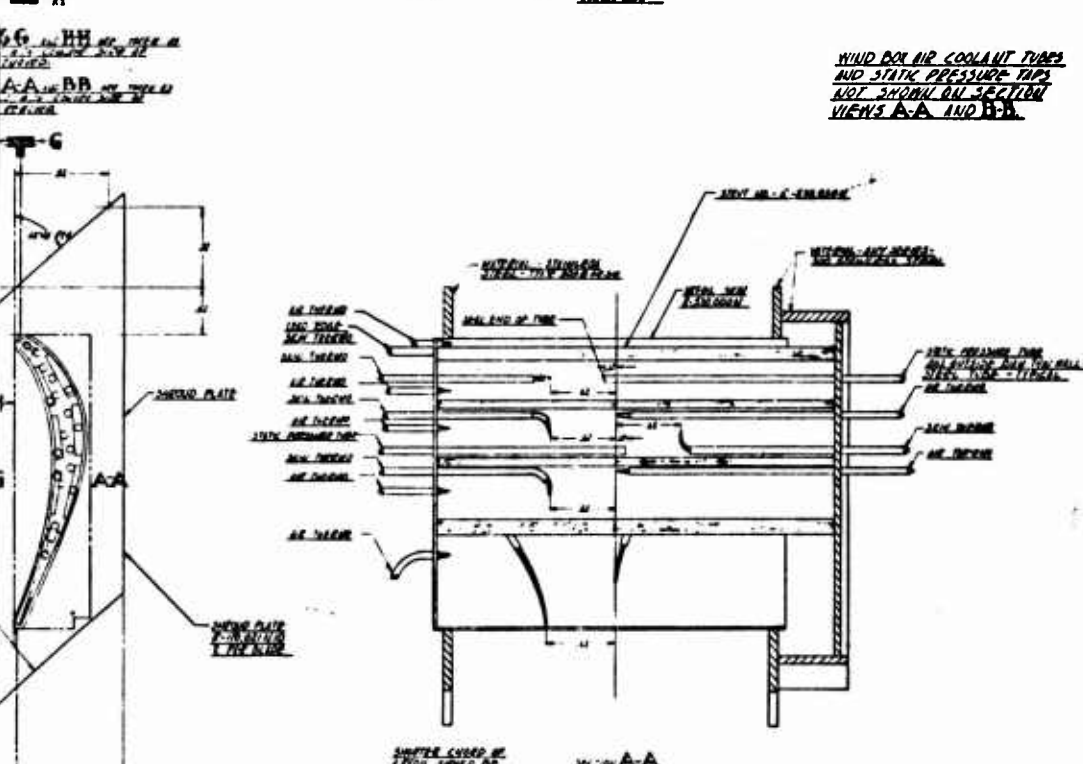
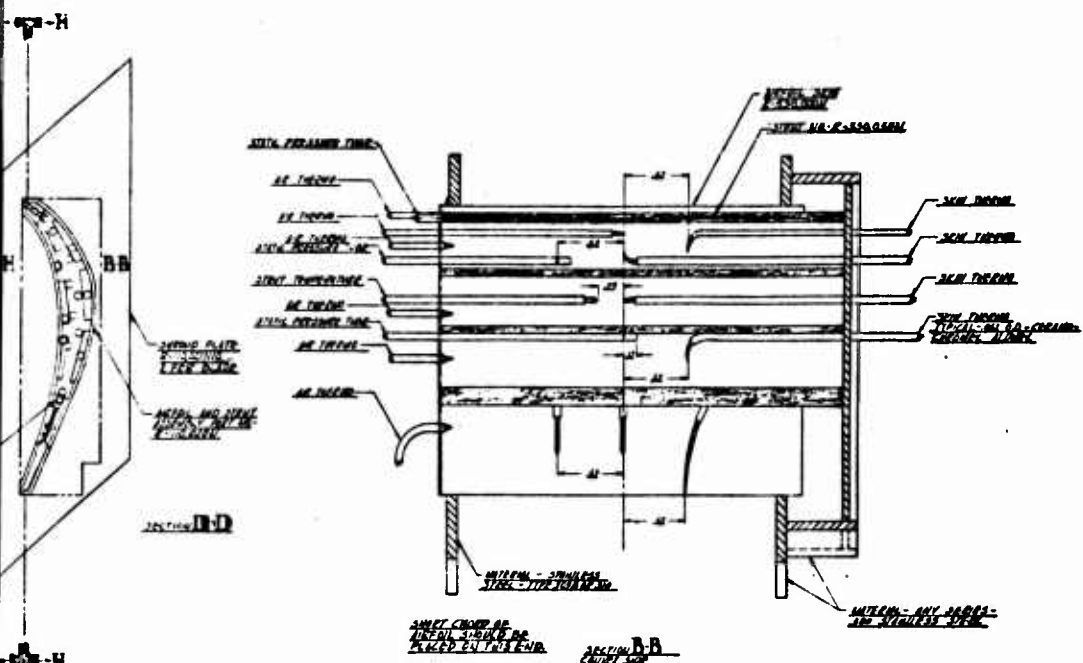
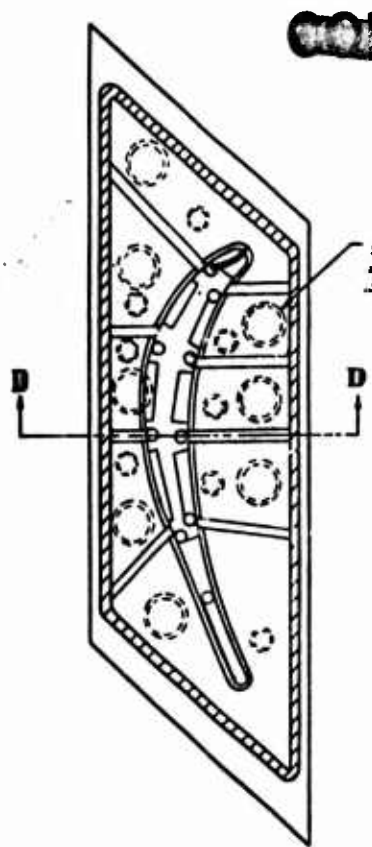


FIGURE 20 TEMPERATURE INSTRUMENTED POROUS BLADE ASSEMBLY

**CONFIDENTIAL**

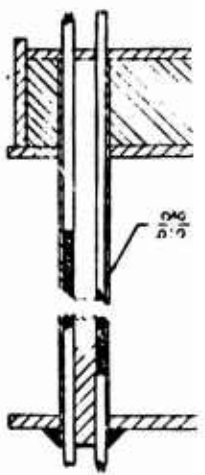


DRAWING NO. R-110,031  
 TITLE: SKIN STATIC PRESSURE TAP  
 DATE: 8/22/55  
 DESIGNED BY: [Name]  
 CHECKED BY: [Name]  
 APPROVED BY: [Name]  
 MATERIAL: [Material]  
 FINISH: [Finish]  
 QUANTITY: [Quantity]  
 UNIT WEIGHT: [Weight]  
 WEIGHT: [Weight]  
 PART NO. [Part No.]  
 PART NAME [Part Name]  
 PART SPEC. [Part Spec.]  
 PART DIMS. [Part Dims.]  
 PART MFG. [Part Mfg.]  
 PART ASSEMBLY [Part Assembly]  
 PART INSPECTION [Part Inspection]  
 PART STORAGE [Part Storage]

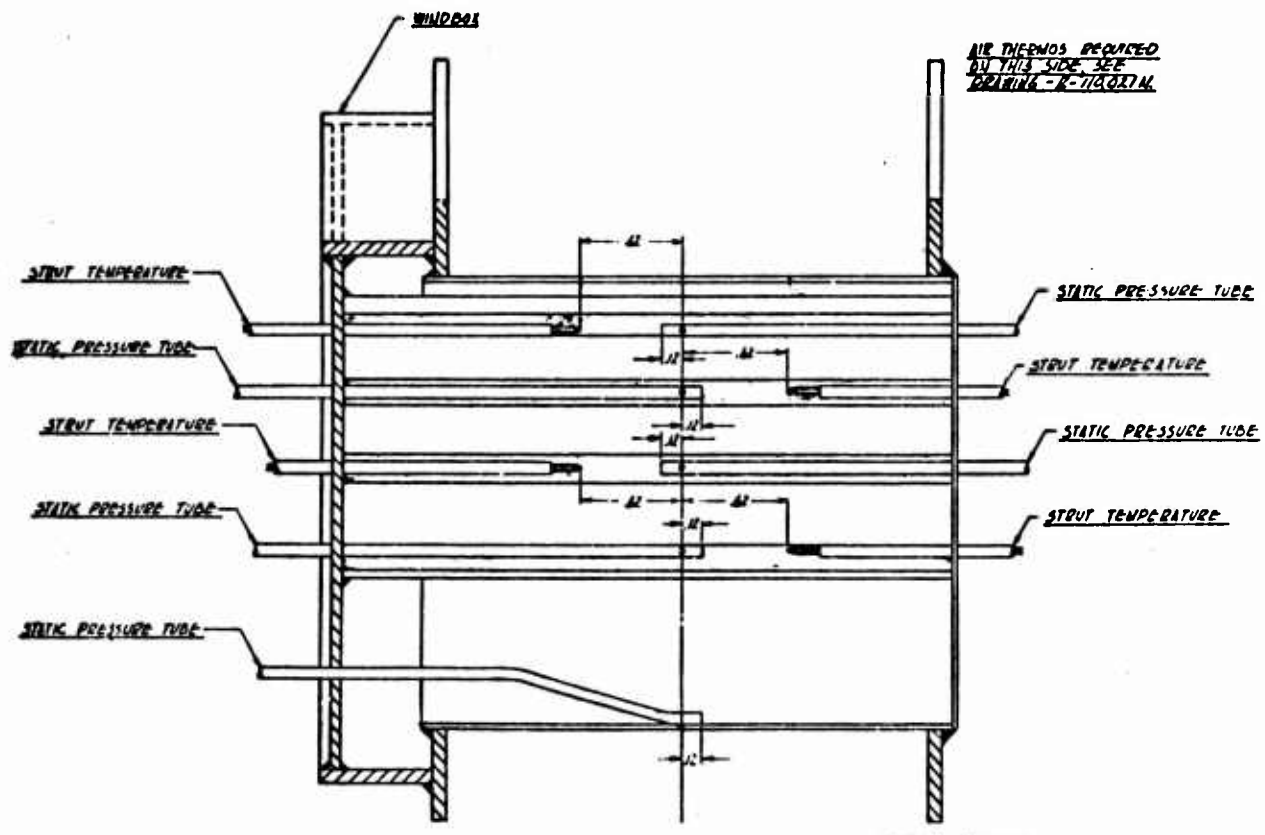


COOLANT AIR TUBES AND INSTRUMENTATION ARE SAME AS SHOWN IN DRAWING R-110.021M ALL ARE NOT SHOWN IN VIEWS BELOW.

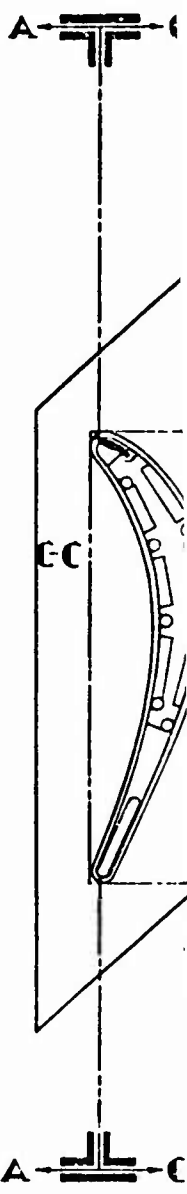
SECTION EE



SECTION DD  
WINDBOX PARTITIONS MUST BE FASTENED WITH 1100°F SILL



SECTION CC  
CONCAVE SIDE



SECTION BB



~~CONFIDENTIAL~~

C.W.R. REPORT NO. 300-39

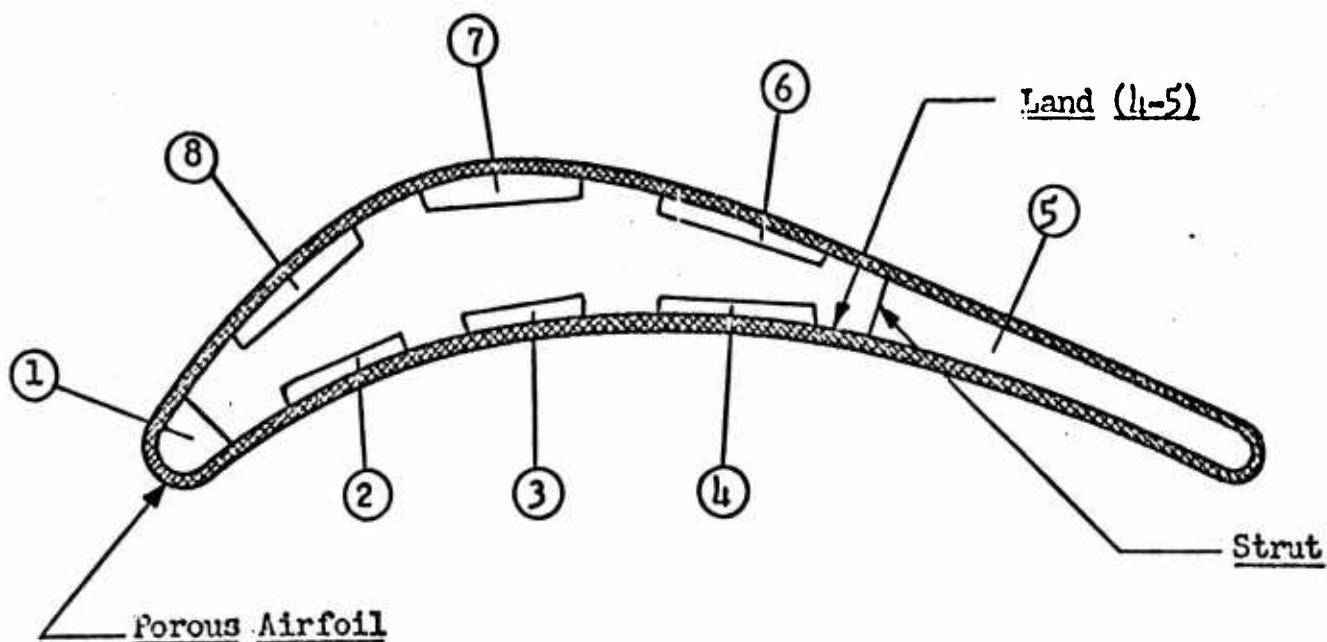


Figure 29. GROSS - SECTION OF CONSTANT SECTION CASCADE BLADE SHOWING PASSAGE DESIGNATIONS

~~CONFIDENTIAL~~

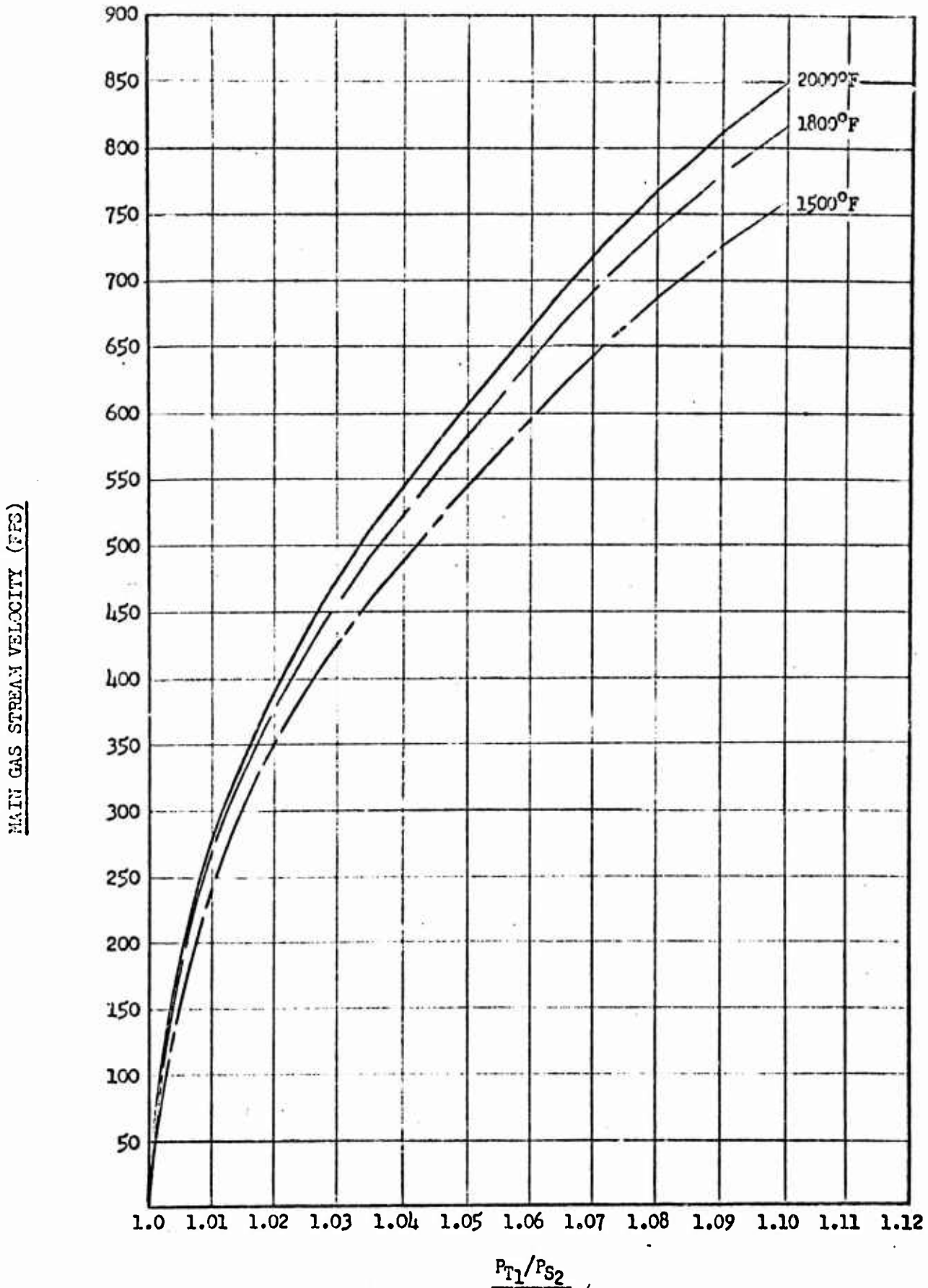


Figure 23. GAS VELOCITY VERSUS TOTAL TO STATIC PRESSURE RATIO  
TEST STAND RUNNING CURVES USED FOR APPROX. SETTING OF GAS VELOCITY

~~CONFIDENTIAL~~

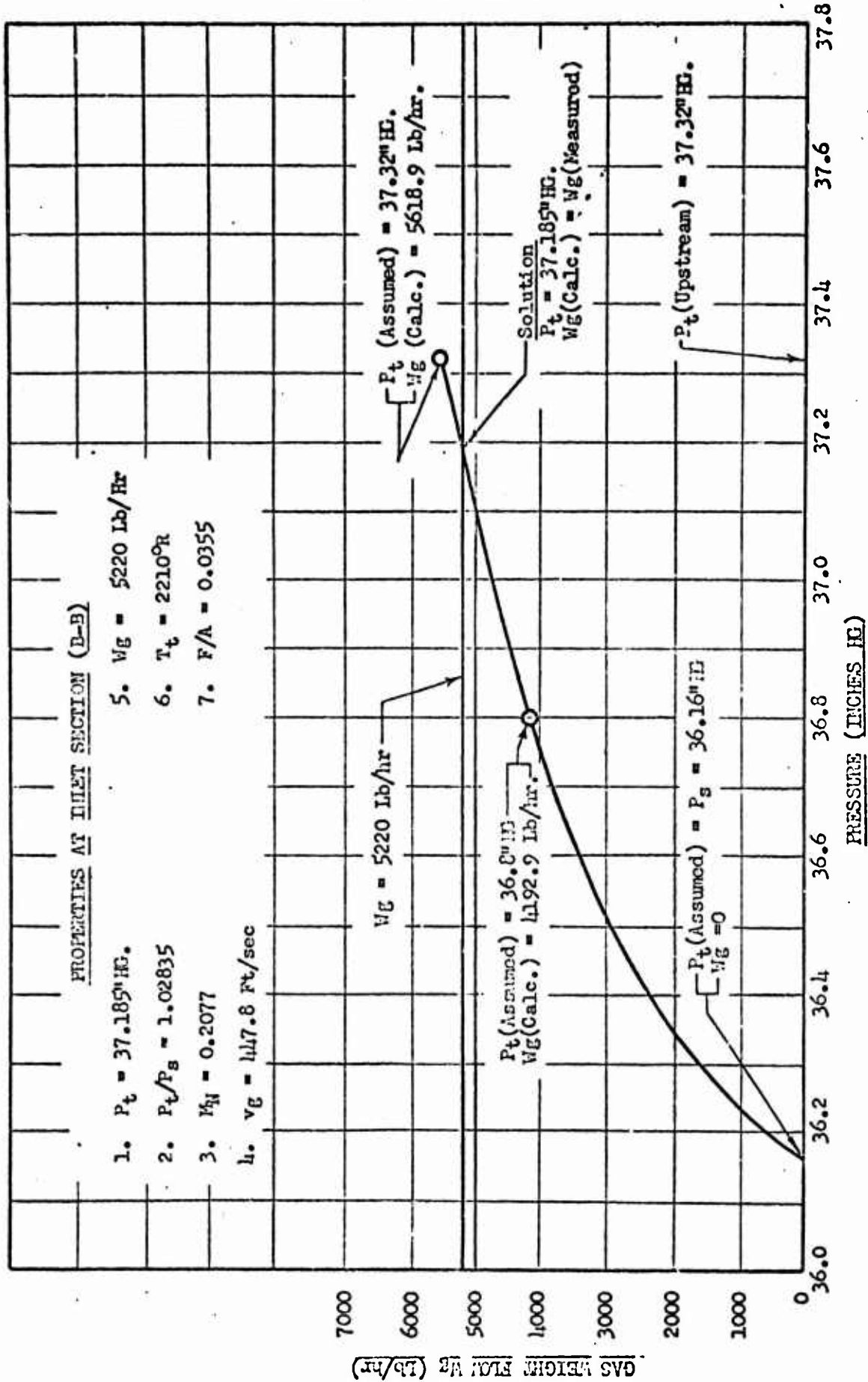


FIGURE 4 GRAPHIC DETERMINATION OF TOTAL PRESSURE AT CASCADE INLET BY ITERATION

~~CONFIDENTIAL~~

G.W.R. REPORT NO. 100-39

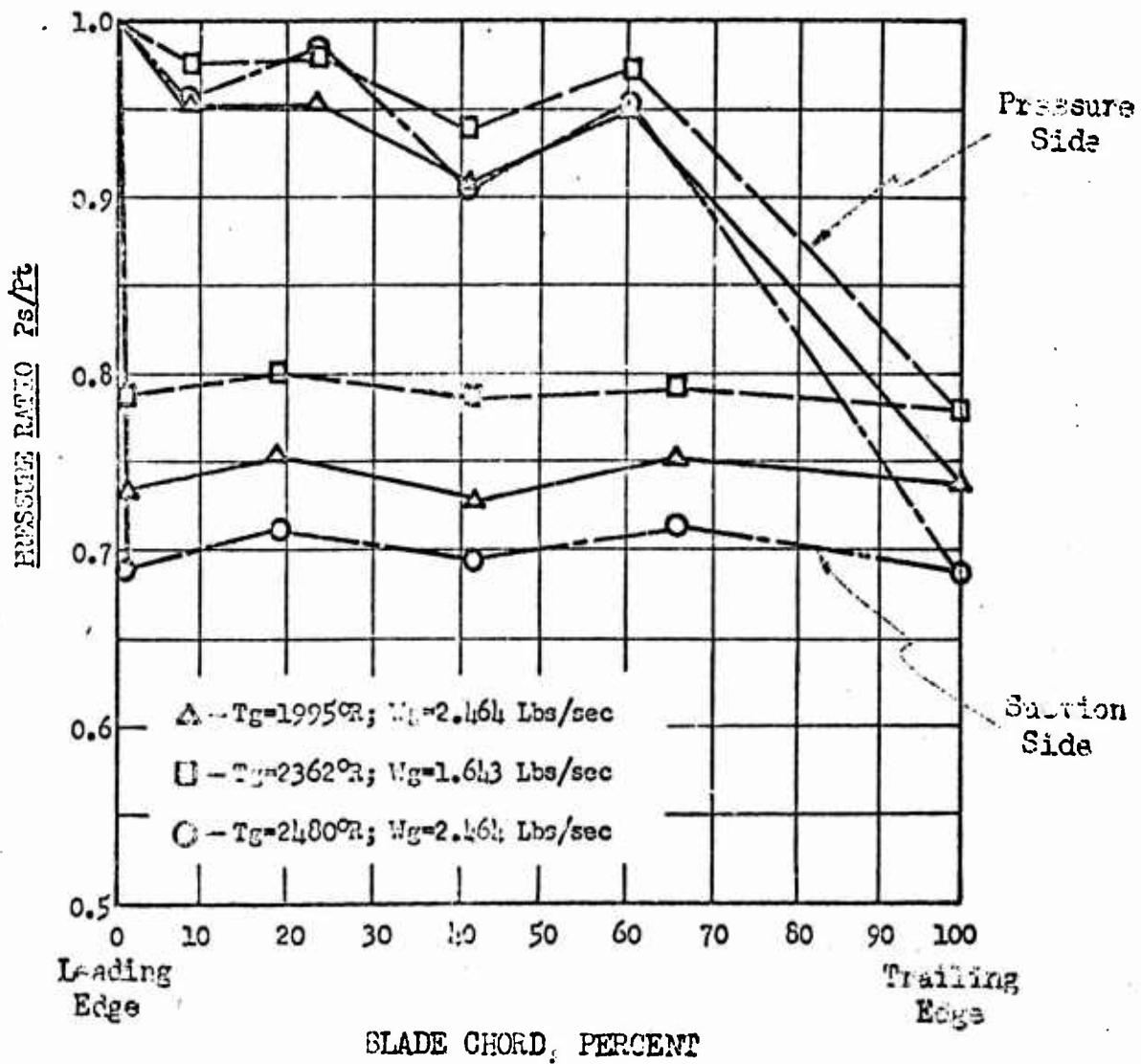
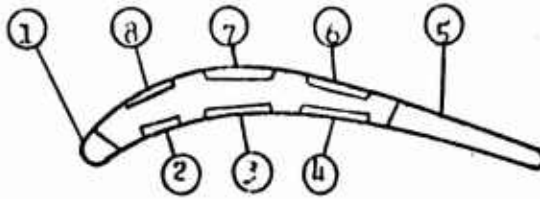
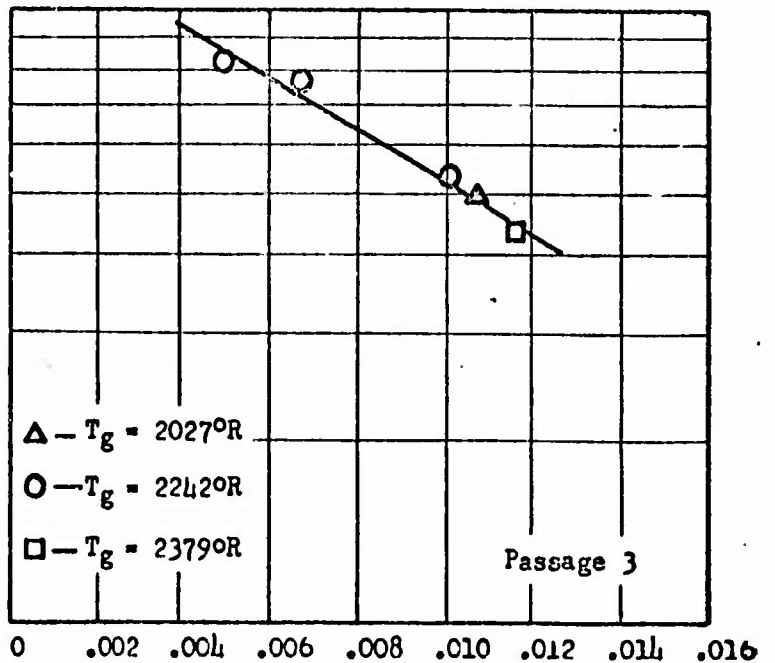
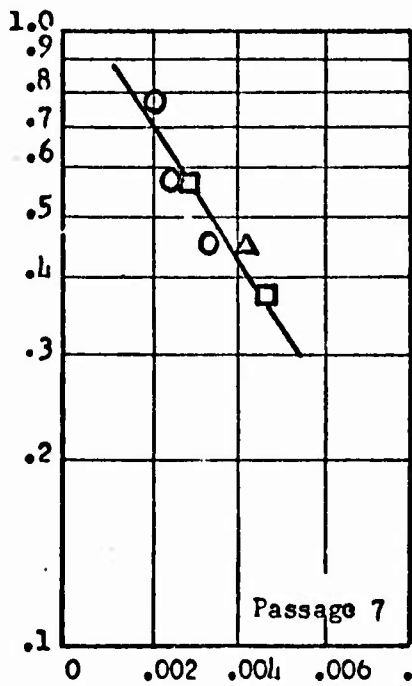
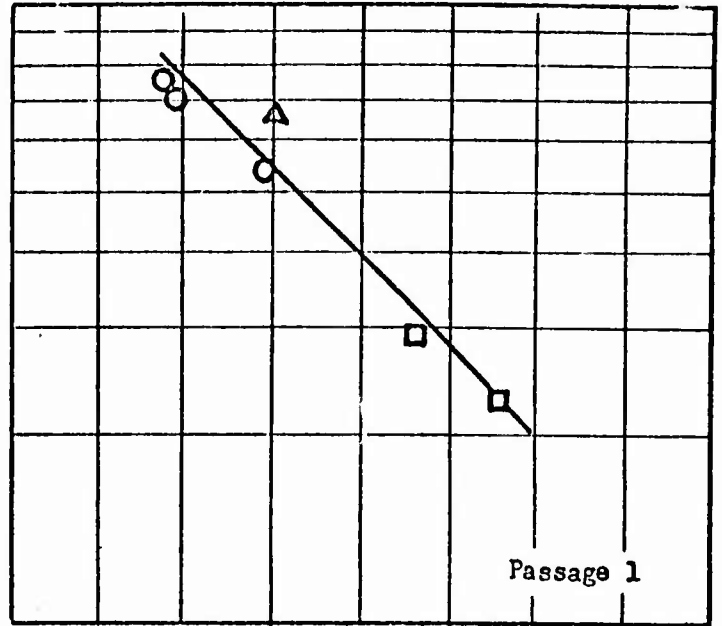
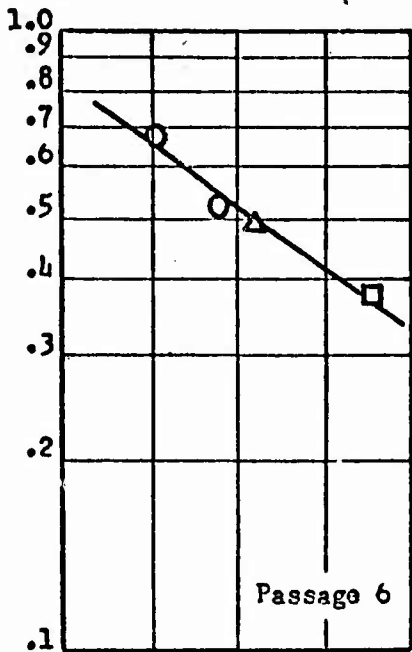


Figure 1. PRESSURE DISTRIBUTION AROUND TRANSPIRATION COOLED CASCADE STATOR BLADES AT VARIOUS GAS TEMPERATURES AND FLOW RATES

~~CONFIDENTIAL~~

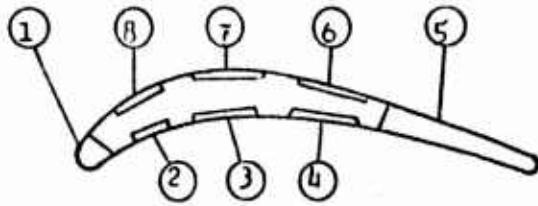


TEMPERATURE DIFFERENCE RATIO,  $\frac{T_w - T_c}{T_g - T_c}$

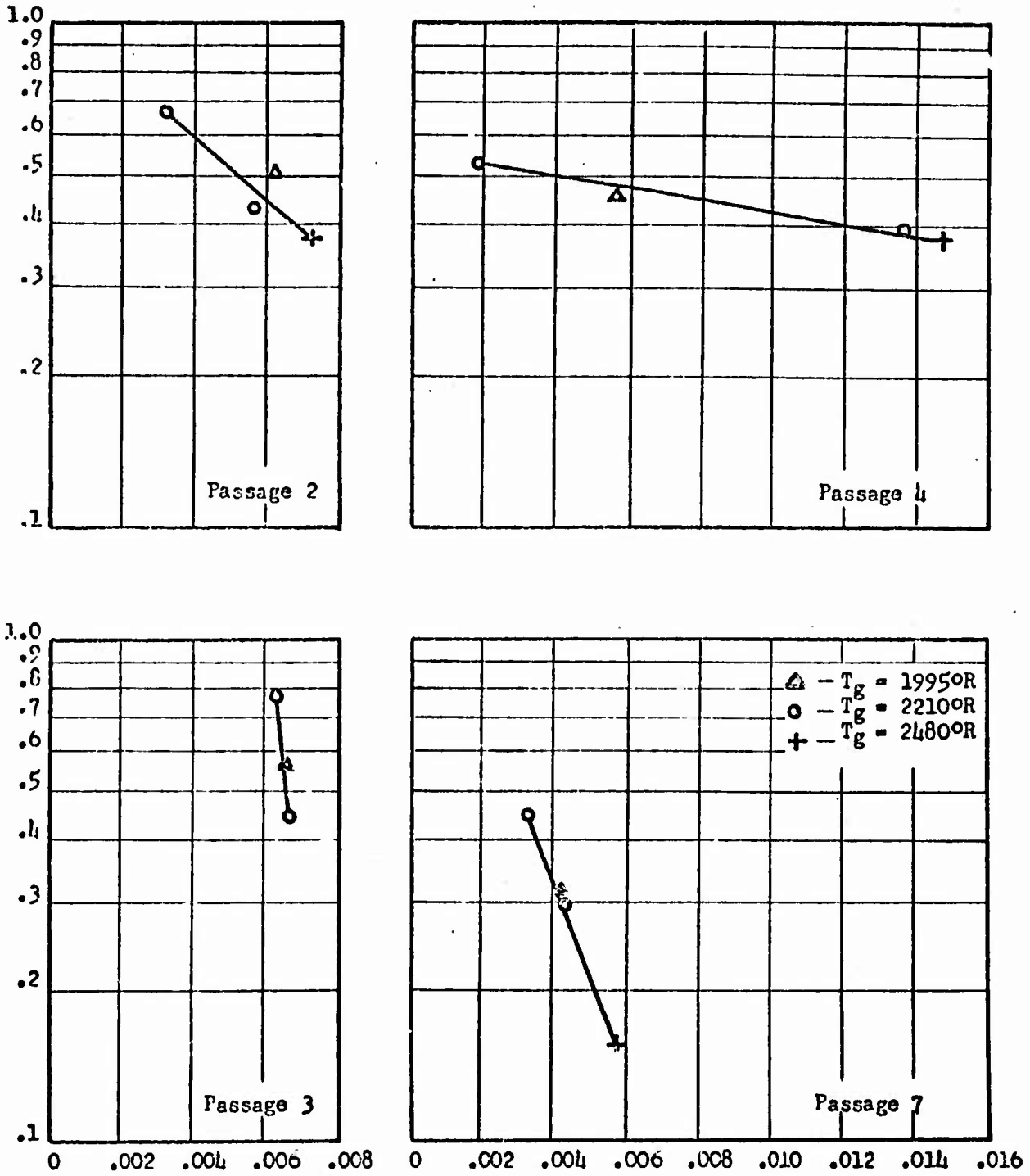


COOLING AIR TO COMBUSTION GAS MASS VELOCITY RATIO,  $\rho v_c / \rho v_g$

Figure 10. TEMPERATURE DIFFERENCE RATIO VERSUS MASS VELOCITY RATIO FOR VARIOUS GAS TEMPERATURES AND CHORDWISE STATIONS. GAS WEIGHT FLOW, 1.643 LBS/SEC.



TEMPERATURE DIFFERENCE RATIO,  $\frac{T_w - T_c}{T_g - T_c}$



COOLING AIR TO COMBUSTION GAS MASS VELOCITY RATIO,  $\rho v_c / \rho v_g$

Figure 27. TEMPERATURE DIFFERENCE RATIO VERSUS MASS VELOCITY RATIO FOR VARIOUS GAS TEMPERATURES AND CHORDWISE STATIONS. GAS WEIGHT FLOW, 2.164 LBS/SEC.

~~CONFIDENTIAL~~

C.W.R. REPORT NO. 300-19

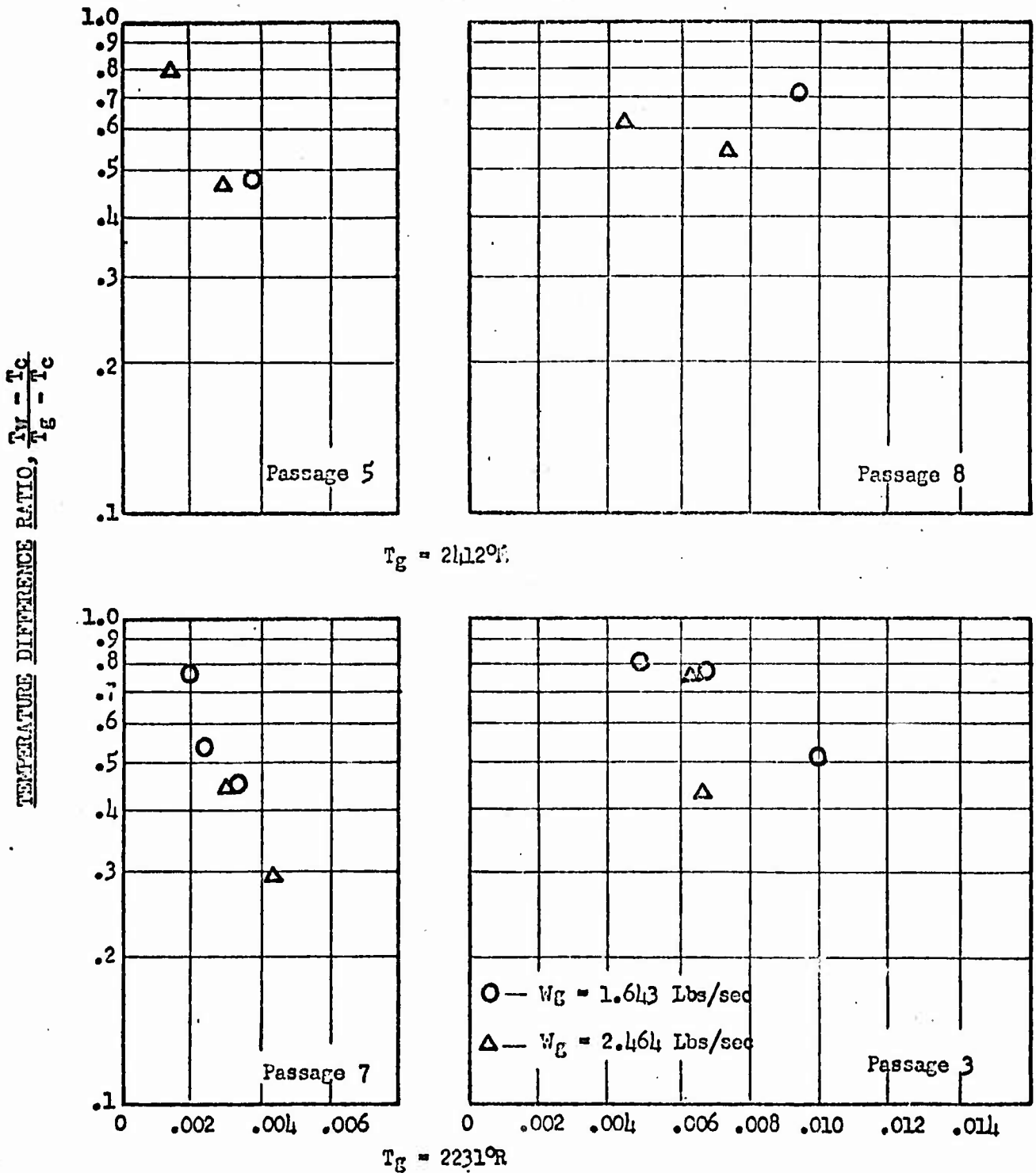
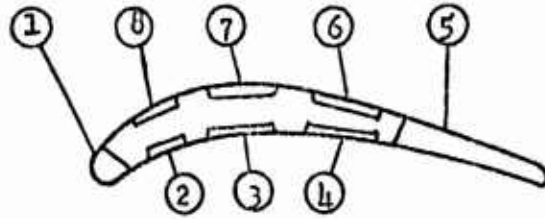


Figure 10. TEMPERATURE DIFFERENCE RATIO VERSUS MASS VELOCITY RATIO FOR VARIOUS GAS WEIGHT FLOWS & CHORDWISE STATIONS. ABOVE: EFFECTIVE GAS TEMP. =  $2412^\circ R$ ; BELOW: EFFECTIVE GAS TEMP. =  $2231^\circ R$ .

~~CONFIDENTIAL~~

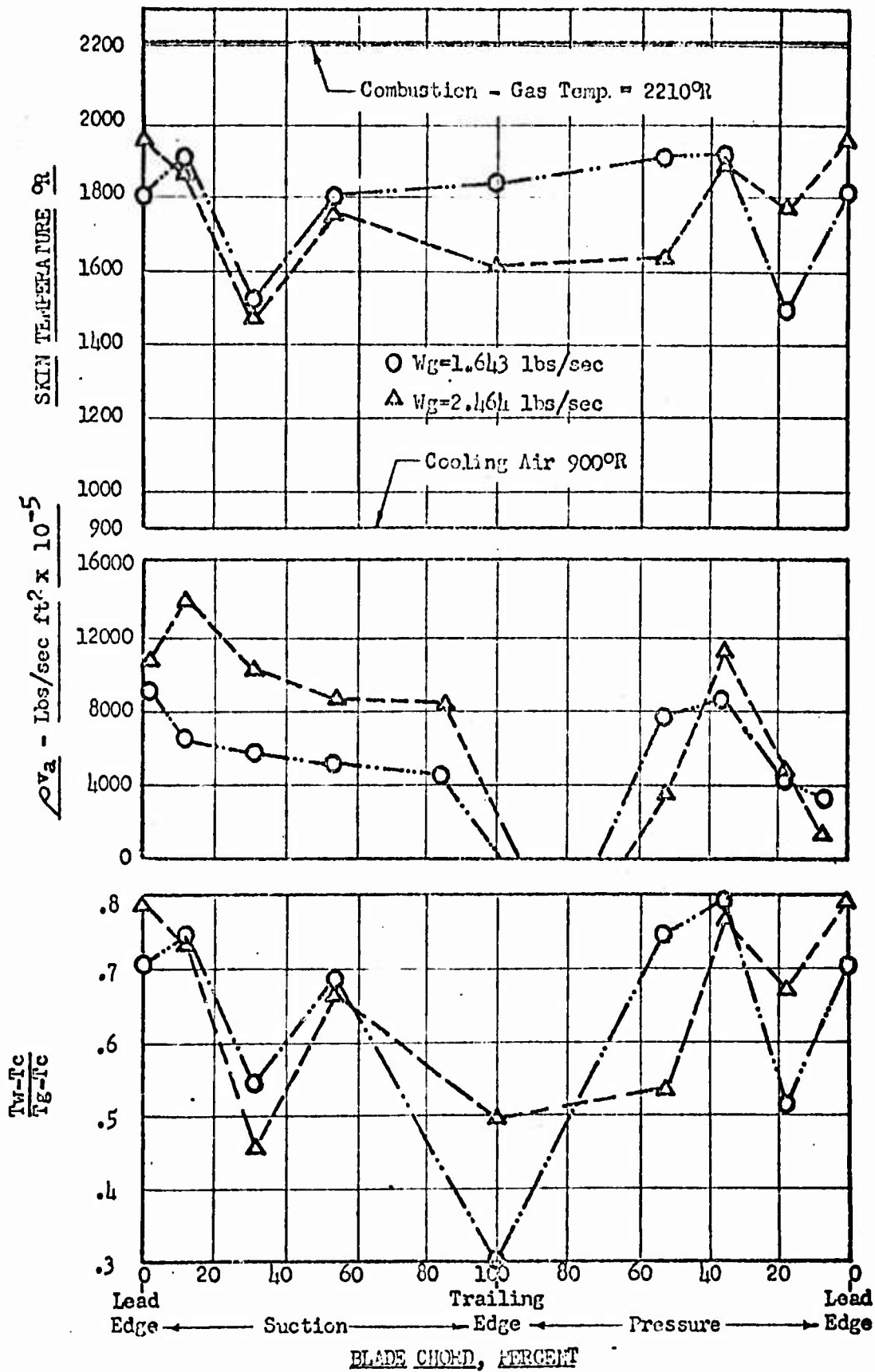


Figure . Peripheral cooling air flows, temperature difference ratios, & absolute temperature distributions on a transpiration cooled cascade blade at two gas weight flows. Gas temperature, 2210°R.

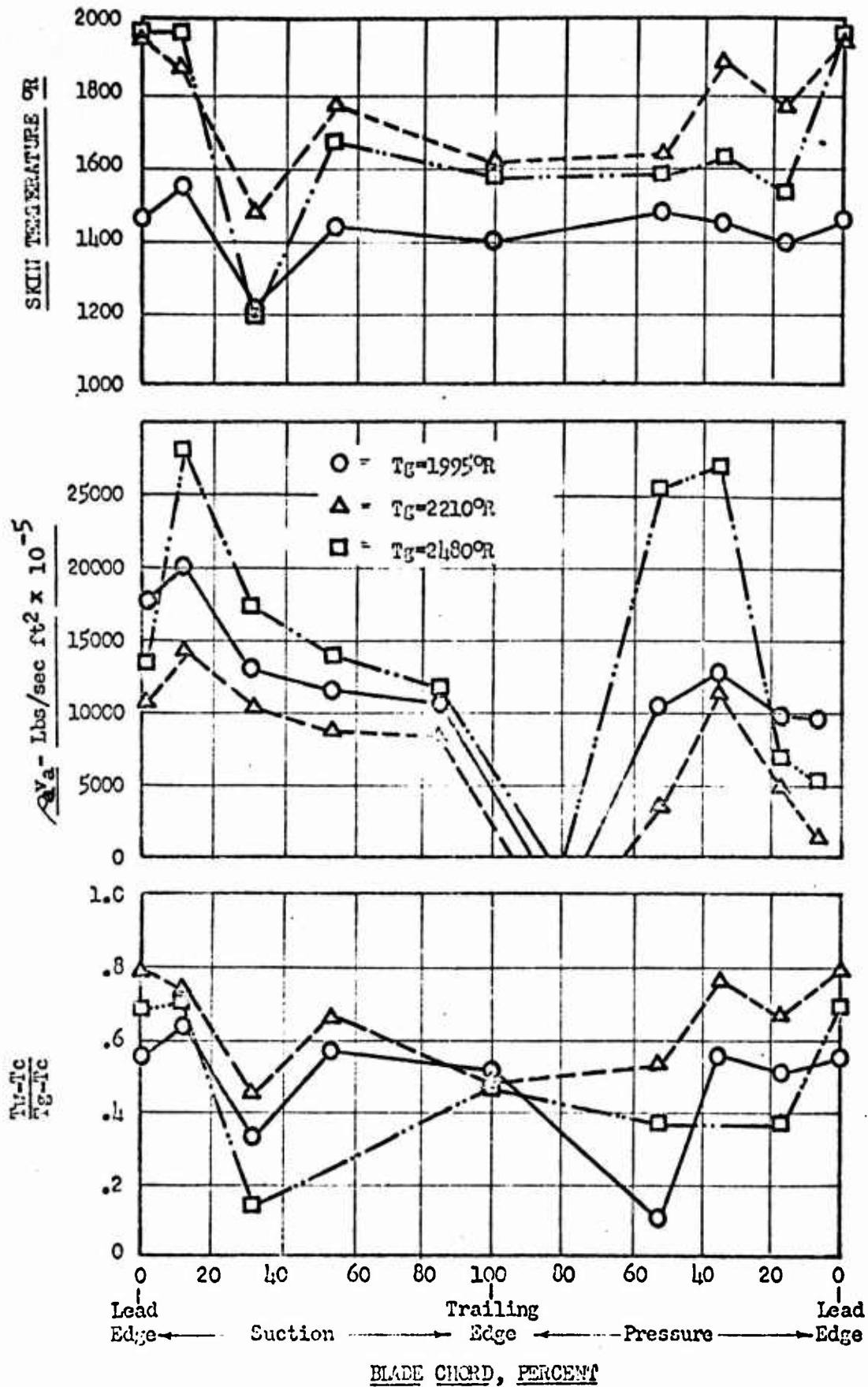
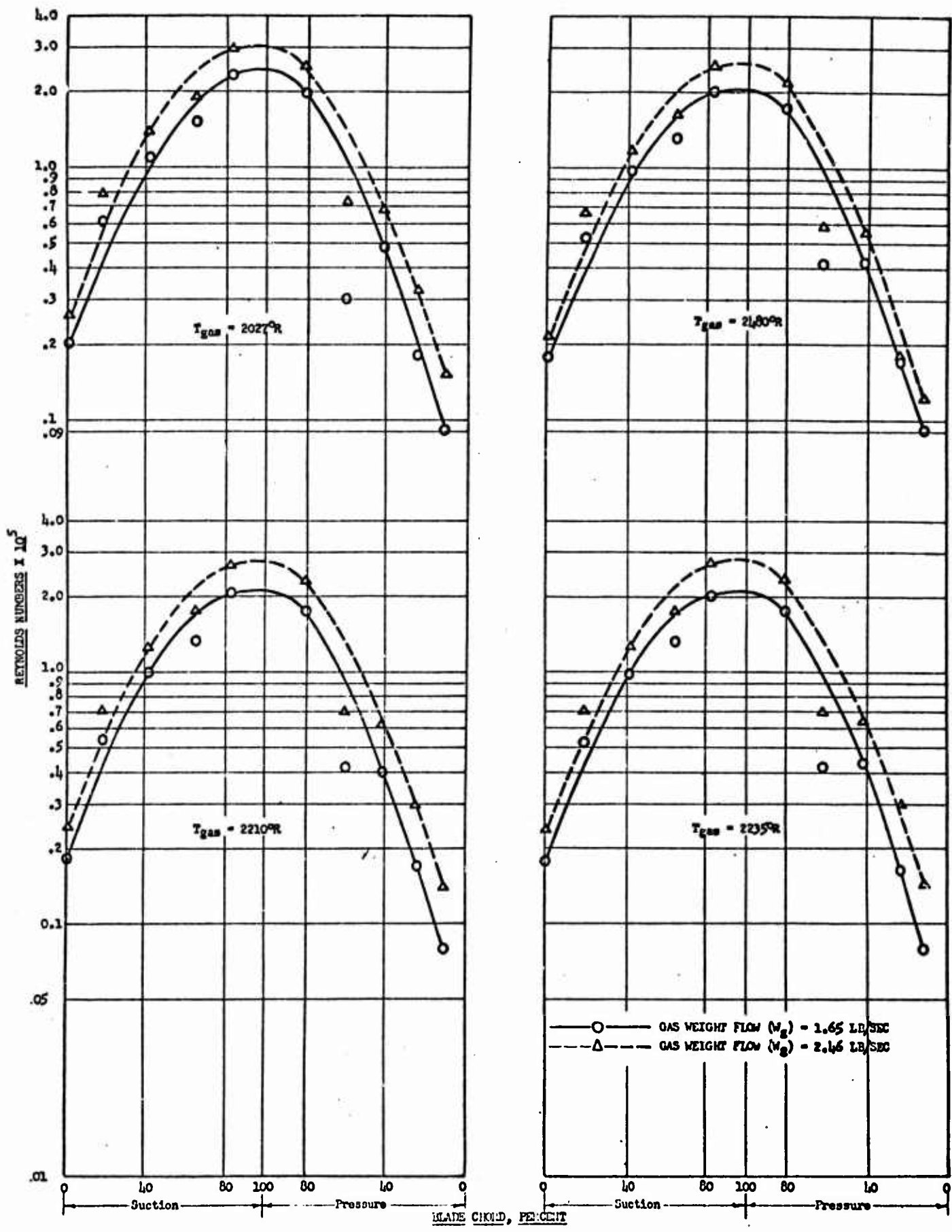


Figure 30. Peripheral cooling air flows, temperature difference ratios, and absolute temperature distributions on a transpiration cooled cascade blade at three gas temperatures. Gas weight flow; 2.464 Lbs/sec.

~~CONFIDENTIAL~~

## C.W.R. REPORT NO. 300-39



PERIMETRAL VARIATION OF HOT GAS REYNOLDS NUMBER AT SEVERAL GAS WEIGHT FLOWS AND INLET GAS TEMPERATURES

Figure 31

~~CONFIDENTIAL~~

C.W.R. REPORT NO. 300-39

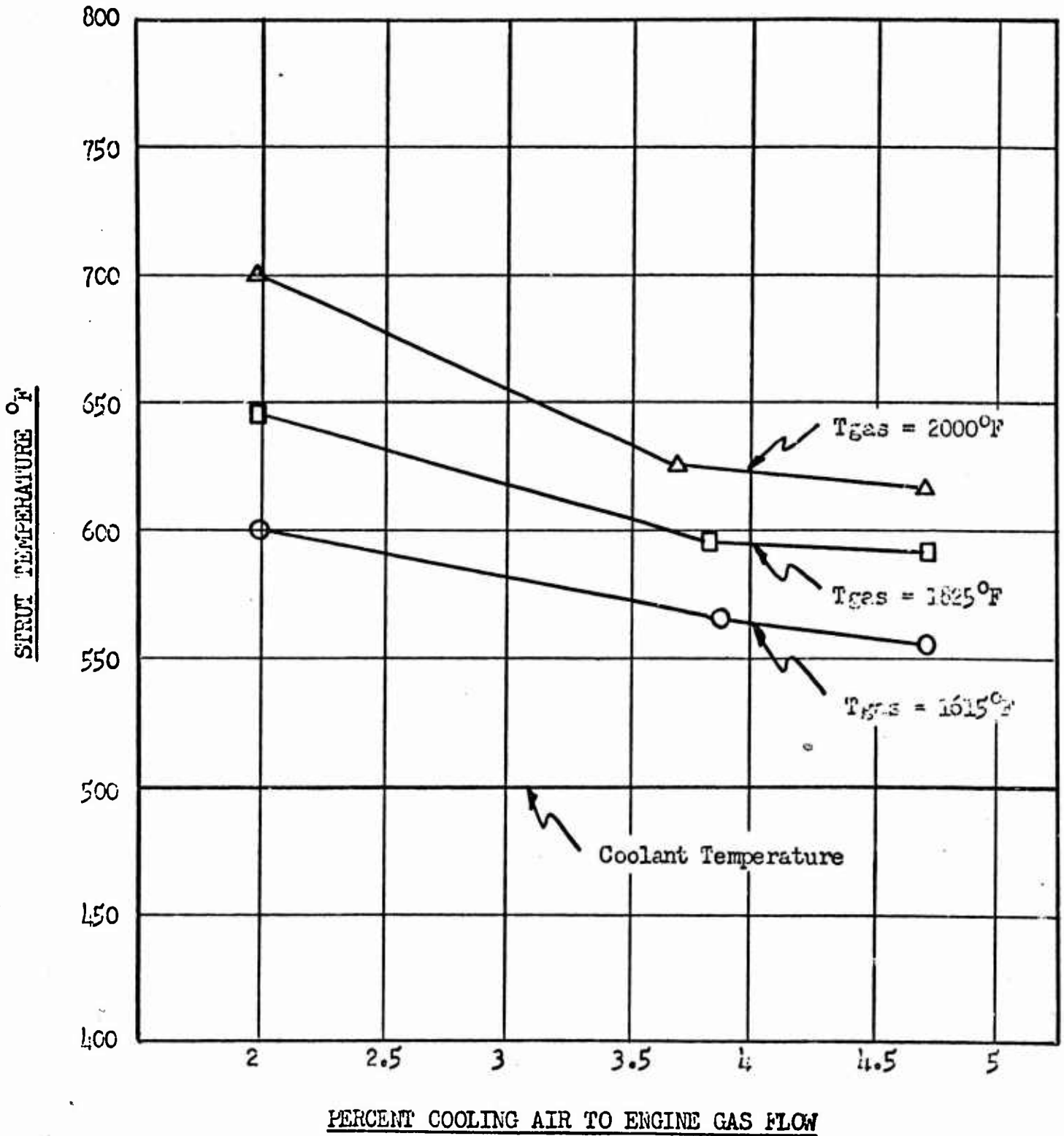


Figure 32. TRANSPIRATION COOLED ROTOR BLADE: VARIATION OF STRUT TEMPERATURE WITH COOLANT FLOW AND GAS TEMPERATURE. DATA TAKEN WITH TIP UN-CAPPED.

~~CONFIDENTIAL~~

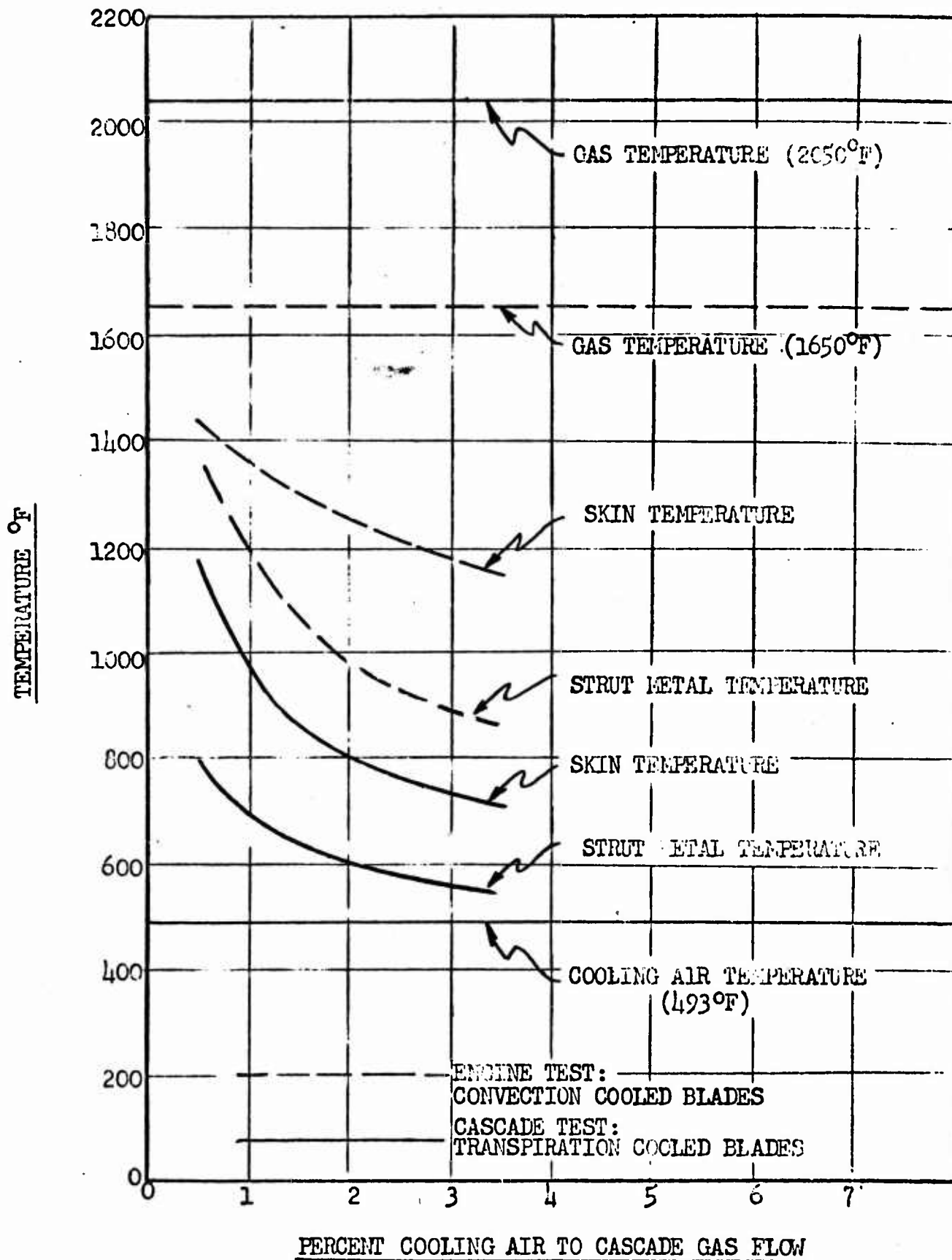


Fig 33 COMPARISON OF TRANSPIRATION-COOLED TURBINE ROTOR BLADE CASCADE DATA WITH CONVECTION COOLING DATA TAKEN IN FULL SCALE ENGINE TEST. VARIATION OF COOLANT BLEED AND RESULTING EFFECTS ON STRUT ROOT SECTION AND AIRFOIL LEADING EDGE TEMPERATURES ARE SHOWN. CASCADE DATA TAKEN WITH BLADE TIP CAPPED.

~~CONFIDENTIAL~~

C.W.R. REPORT NO. 300-39

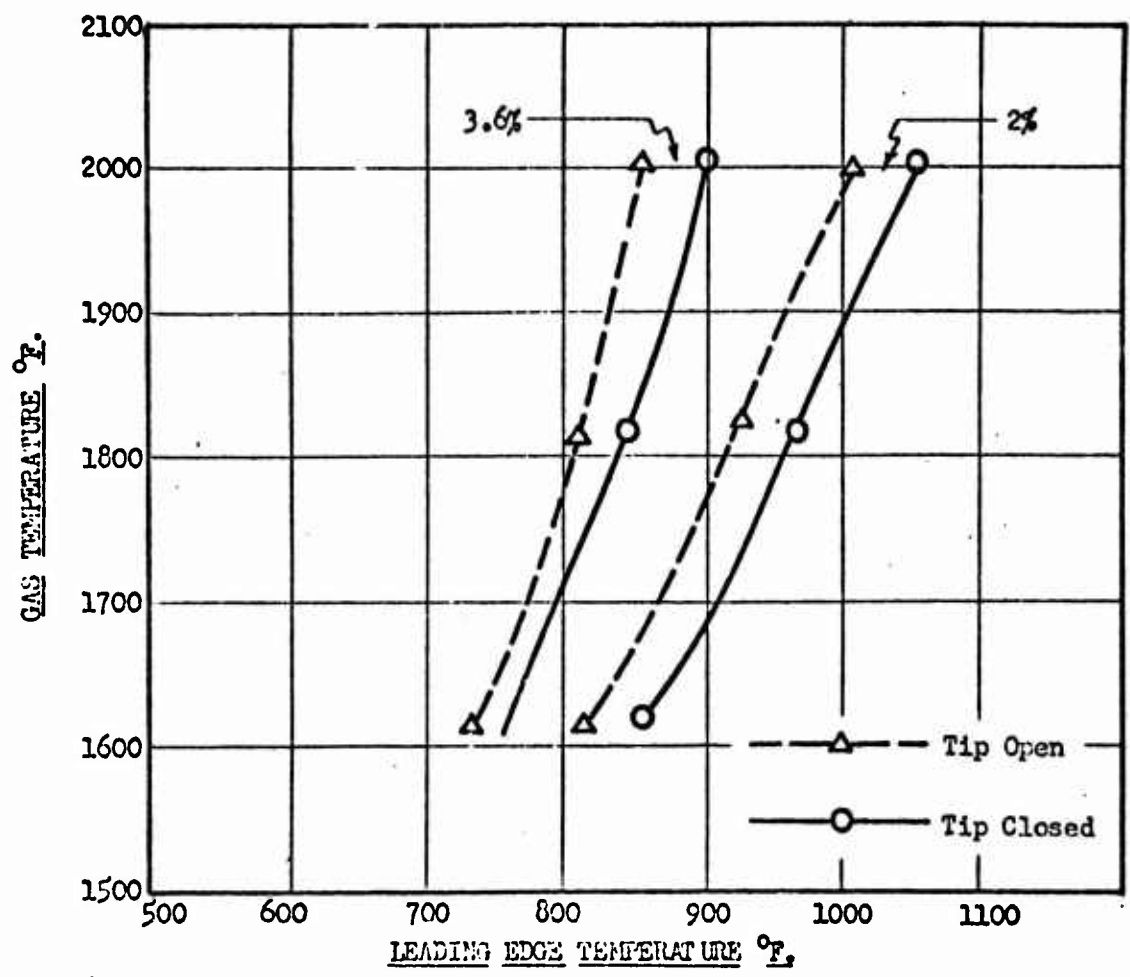


Figure 34. TRANSPIRATION-COOLED TURBINE ROTOR BLADE-HOT GAS CASCADE. COMPARISON OF DATA WITH BLADE TIP OPEN AND CLOSED. VARIATION OF LEADING EDGE TEMPERATURE FOR VARIOUS GAS TEMPERATURES & COOLANT MASS FLOWS. COOLING AIR TEMPERATURE = 500°F.

~~CONFIDENTIAL~~

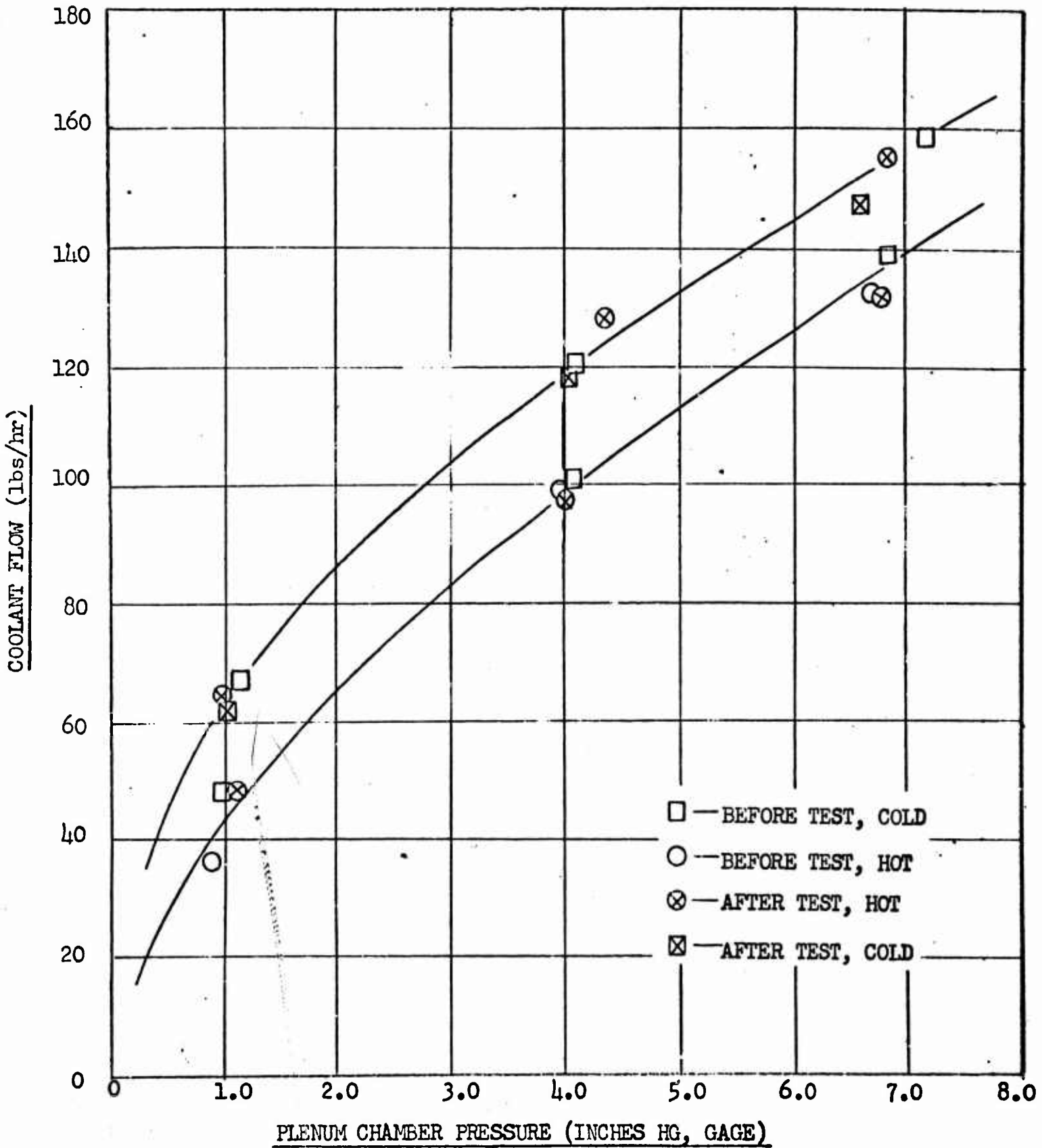


Fig. 36. COMPARISON OF SKIN PERMEABILITY OF TWO BLADES BEFORE AND AFTER TEST WITH DATA TAKEN AT ROOM TEMPERATURE AND AT 600°F.

~~CONFIDENTIAL~~

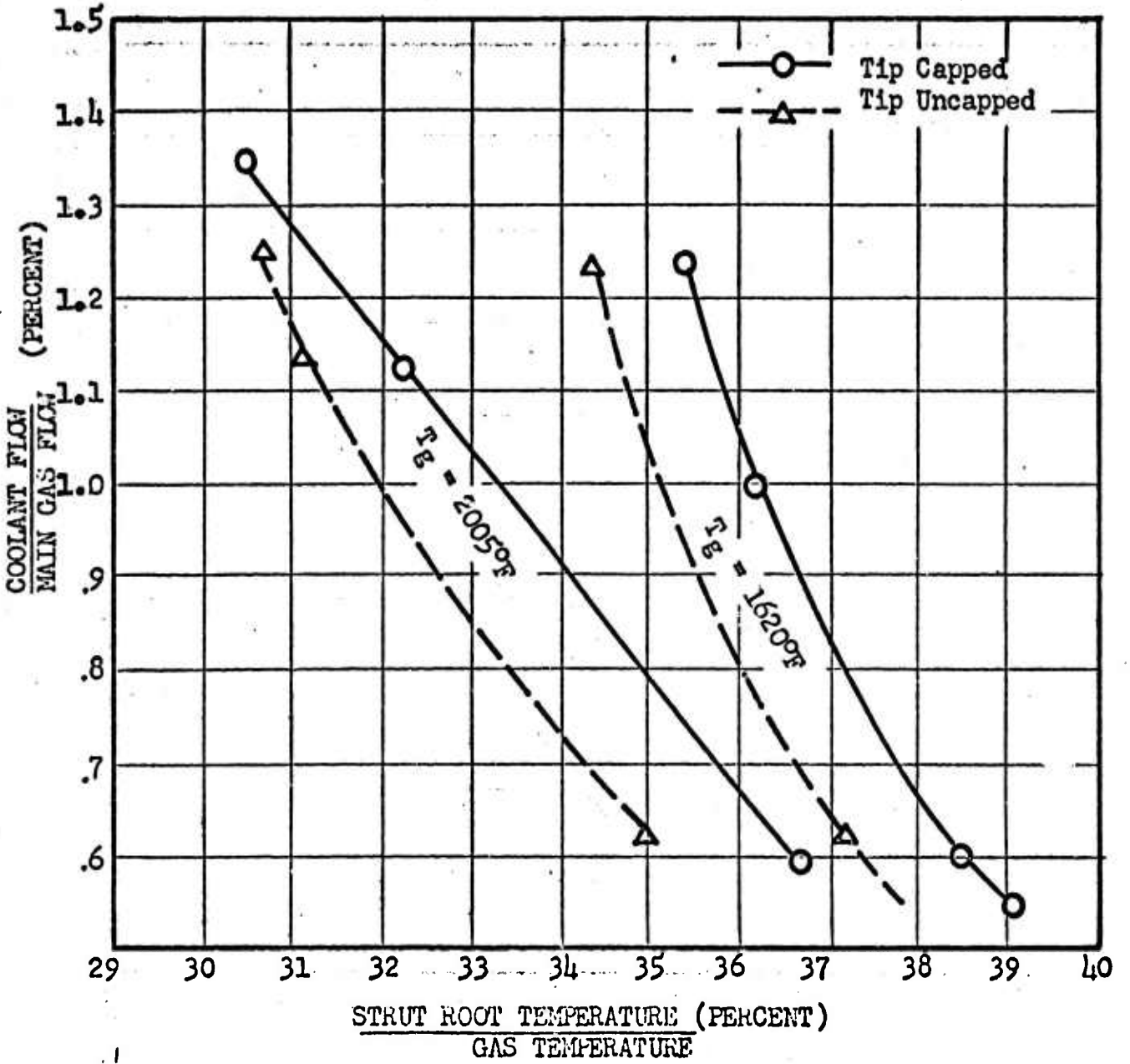


Figure 35. CORRELATION CURVE-COMPARISON OF TRANSPIRATION COOLED TURBINE ROTOR BLADE WITH BLADE TIP OPEN AND BLADE TIP CLOSED AT TWO GAS TEMPERATURES AND VARIOUS COOLANT AIR FLOWS.

~~CONFIDENTIAL~~

~~CONFIDENTIAL~~

C.W.R. REPORT NO. 300-39

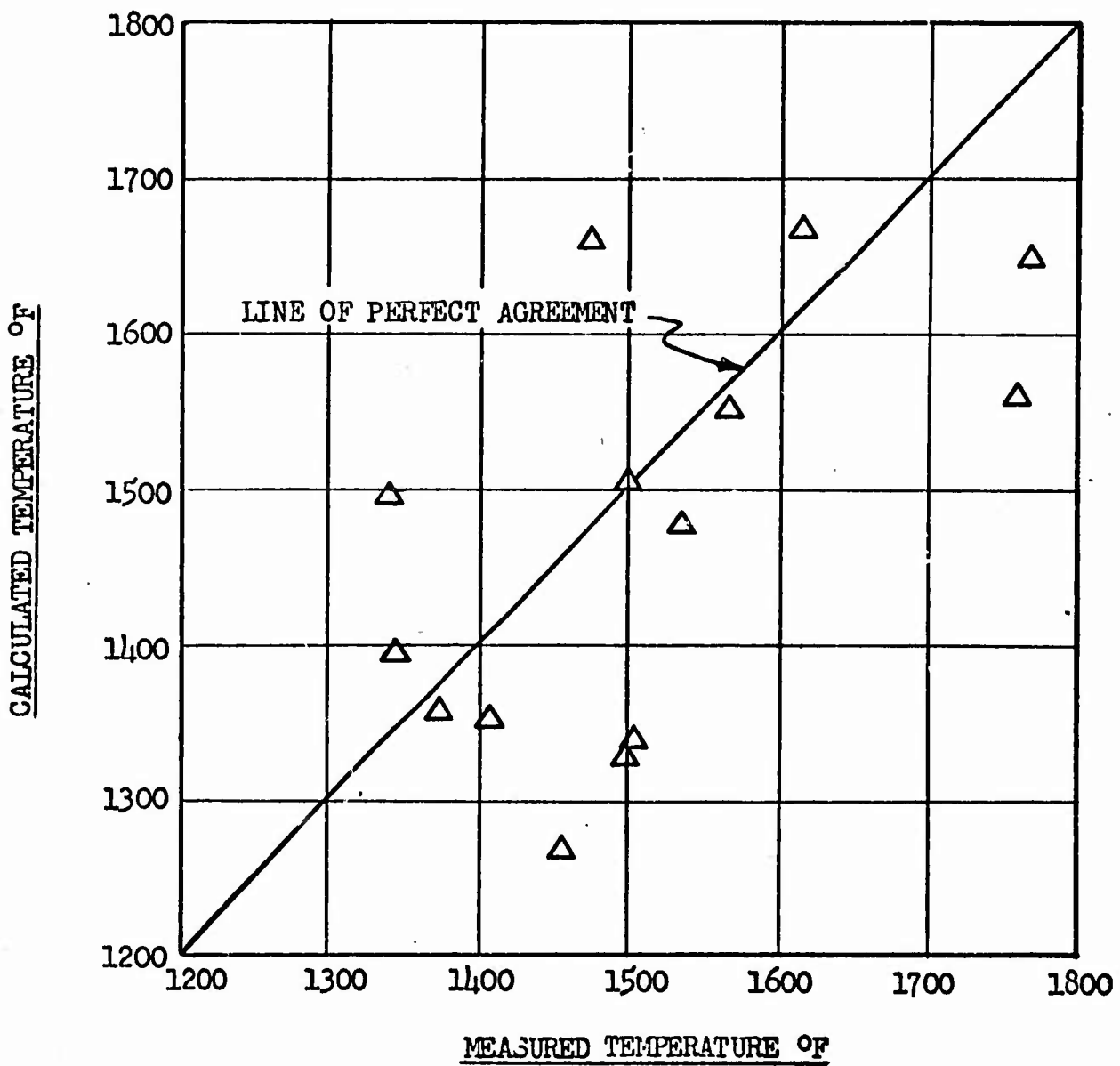


Figure 37. COMPARISON OF TEMPERATURES MEASURED IN CASCADE RIG WITH TEMPERATURES PREDICTED BY CALCULATION PROCEDURE.

~~CONFIDENTIAL~~